Report No.385

epa Research

Air Pollution Sources in Ireland

Authors: Jurgita Ovadnevaite, Chunshui Lin, Matteo Rinaldi, Darius Ceburnis, Paul Buckley, Liz Coleman, Maria Cristina Facchini, John Wenger and Colin O'Dowd

www.epa.ie

Rialtas na hÉireann
Government of Ireland

ENVIRONMENTAL PROTECTION AGENCY

The Environmental Protection Agency (EPA) is responsible for protecting and improving the environment as a valuable asset for the people of Ireland. We are committed to protecting people and the environment from the harmful effects of radiation and pollution.

The work of the EPA can be divided into three main areas:

Regulation: *We implement effective regulation and environmental compliance systems to deliver good environmental outcomes and target those who don't comply.*

Knowledge: *We provide high quality, targeted and timely environmental data, information and assessment to inform decision making at all levels.*

Advocacy: *We work with others to advocate for a clean, productive and well protected environment and for sustainable environmental behaviour.*

Our Responsibilities

Licensing

We regulate the following activities so that they do not endanger human health or harm the environment:

- waste facilities *(e.g. landfills, incinerators, waste transfer stations)*;
- large scale industrial activities (*e.g. pharmaceutical, cement manufacturing, power plants)*;
- intensive agriculture *(e.g. pigs, poultry)*;
- the contained use and controlled release of Genetically Modified Organisms *(GMOs)*;
- sources of ionising radiation *(e.g. x-ray and radiotherapy equipment, industrial sources)*;
- large petrol storage facilities;
- waste water discharges;
- dumping at sea activities.

National Environmental Enforcement

- Conducting an annual programme of audits and inspections of EPA licensed facilities.
- Overseeing local authorities' environmental protection responsibilities.
- Supervising the supply of drinking water by public water suppliers.
- Working with local authorities and other agencies to tackle environmental crime by co-ordinating a national enforcement network, targeting offenders and overseeing remediation.
- Enforcing Regulations such as Waste Electrical and Electronic Equipment (WEEE), Restriction of Hazardous Substances (RoHS) and substances that deplete the ozone layer.
- Prosecuting those who flout environmental law and damage the environment.

Water Management

- Monitoring and reporting on the quality of rivers, lakes, transitional and coastal waters of Ireland and groundwaters; measuring water levels and river flows.
- National coordination and oversight of the Water Framework Directive.
- Monitoring and reporting on Bathing Water Quality.

Monitoring, Analysing and Reporting on the Environment

- Monitoring air quality and implementing the EU Clean Air for Europe (CAFÉ) Directive.
- Independent reporting to inform decision making by national and local government *(e.g. periodic reporting on the State of Ireland's Environment and Indicator Reports)*.

Regulating Ireland's Greenhouse Gas Emissions

- Preparing Ireland's greenhouse gas inventories and projections.
- Implementing the Emissions Trading Directive, for over 100 of the largest producers of carbon dioxide in Ireland.

Environmental Research and Development

- Funding environmental research to identify pressures, inform policy and provide solutions in the areas of climate, water and sustainability.

Strategic Environmental Assessment

- Assessing the impact of proposed plans and programmes on the Irish environment *(e.g. major development plans)*.

Radiological Protection

- Monitoring radiation levels, assessing exposure of people in Ireland to ionising radiation.
- Assisting in developing national plans for emergencies arising from nuclear accidents.
- Monitoring developments abroad relating to nuclear installations and radiological safety.
- Providing, or overseeing the provision of, specialist radiation protection services.

Guidance, Accessible Information and Education

- Providing advice and guidance to industry and the public on environmental and radiological protection topics.
- Providing timely and easily accessible environmental information to encourage public participation in environmental decision-making *(e.g. My Local Environment, Radon Maps)*.
- Advising Government on matters relating to radiological safety and emergency response.
- Developing a National Hazardous Waste Management Plan to prevent and manage hazardous waste.

Awareness Raising and Behavioural Change

- Generating greater environmental awareness and influencing positive behavioural change by supporting businesses, communities and householders to become more resource efficient.
- Promoting radon testing in homes and workplaces and encouraging remediation where necessary.

Management and structure of the EPA

The EPA is managed by a full time Board, consisting of a Director General and five Directors. The work is carried out across five Offices:

- Office of Environmental Sustainability
- Office of Environmental Enforcement
- Office of Evidence and Assessment
- Office of Radiation Protection and Environmental Monitoring
- Office of Communications and Corporate Services

The EPA is assisted by an Advisory Committee of twelve members who meet regularly to discuss issues of concern and provide advice to the Board.

EPA RESEARCH PROGRAMME 2021–2030

Air Pollution Sources in Ireland

(2016-CCRP-MS.31)

EPA Research Report

Prepared for the Environmental Protection Agency

by

National University of Ireland Galway, Istituto di Scienze dell'Atmosfera e del Clima and University College Cork

Authors:

Jurgita Ovadnevaite, Chunshui Lin, Matteo Rinaldi, Darius Ceburnis, Paul Buckley, Liz Coleman, Maria Cristina Facchini, John Wenger and Colin O'Dowd

ENVIRONMENTAL PROTECTION AGENCY
An Ghníomhaireacht um Chaomhnú Comhshaoil
PO Box 3000, Johnstown Castle, Co. Wexford, Ireland

Telephone: +353 53 916 0600 Fax: +353 53 916 0699
Email: info@epa.ie Website: www.epa.ie

ACKNOWLEDGEMENTS

This report is published as part of the EPA Research Programme 2021–2030. The EPA Research Programme is a Government of Ireland initiative funded by the Department of the Environment, Climate and Communications. It is administered by the Environmental Protection Agency, which has the statutory function of co-ordinating and promoting environmental research.

This work was also supported by the following projects: MaREI, the SFI Research Centre for Energy, Climate, and Marine (Grant No. 12/RC/2302_P2), the European Commission, the National Natural Science Foundation of China (NSFC) (grant No. 91644219), the China Scholarship Council (CSC) (grant No. 201506310020) and the Irish Research Council (GOIPG/2015/3051). We acknowledge Met Éireann and the European Centre for Medium-Range Weather Forecasts (ECMWF) for providing meteorological data.

The authors would like to thank the members of the project steering committee, namely John McEntagart (EPA), Patrick Kenny (EPA) and David Dodd (Dublin Metropolitan Climate Action Regional Office – CARO), for their time and advice on the project; and Oonagh Monahan (Research Project Manager on behalf of the EPA) for her continuous support throughout the project. Thank you also to Gary Fuller (Imperial College London) and Markus Kalberer (University of Basel) for taking the time to review the final report.

DISCLAIMER

This report is based on research carried out/data from 4 January 2016 to 3 January 2019. More recent data may have become available since the research was completed.

The EPA Research Programme addresses the need for research in Ireland to inform policymakers and other stakeholders on a range of questions in relation to environmental protection. These reports are intended as contributions to the necessary debate on the protection of the environment.

EPA RESEARCH PROGRAMME 2021–2030
Published by the Environmental Protection Agency, Ireland

ISBN: 978-1-80009-007-1 July 2021

Price: Free Online version

Project Partners

Professor Colin O'Dowd (MAE, MRIA, DSc, FInsP, FRMetS)
School of Physics
The Ryan Institute's Centre for Climate and Air Pollution Studies
National University of Ireland Galway
Galway
Ireland
Tel.: +353 9 149 3306
Email: colin.odowd@nuigalway.ie

Dr Jurgita Ovadnevaite
School of Physics
The Ryan Institute's Centre for Climate and Air Pollution Studies
National University of Ireland Galway
Galway
Ireland
Tel.: +353 9 149 2496
Email: jurgita.ovadnevaite@nuigalway.ie

Dr Maria Cristina Facchini
Istituto di Scienze dell'Atmosfera e del Clima (ISAC)
Consiglio Nazionale delle Ricerche (CNR)
Bologna
Italy
Tel.: +39 051 639 9618/9626
Email: mc.facchini@isac.cnr.it

Professor John Wenger
School of Chemistry and Environmental Research Institute
University College Cork
Cork
Ireland
Tel.: +353 21 490 2454
Email: j.wenger@ucc.ie

Contents

List of Figures

List of Tables

Executive Summary

Atmospheric aerosol particles (also known as particulate matter or PM) are central to the cause of the two greatest threats to human security: air pollution (with ~5 million premature deaths per year) and climate change (with ~0.5 million per year). Addressing these threats requires an understanding of the PM sources responsible for both extreme air pollution immediately affecting human health and less extreme levels affecting climate over longer time and larger spatial scales. The goal of this project was to deploy a state-of-the-art PM characterisation technique, namely aerosol mass spectrometry, in conjunction with source apportionment and meso-scale modelling analysis, to elucidate and quantify the most important air pollution sources affecting air quality in Ireland.

The National Transboundary Air Pollution Network was augmented with three sophisticated aerosol mass spectrometer nodes, delivering real-time PM concentration and composition data and enabling the application of subsequent source apportionment, leading to the first next-generation national air quality monitoring network. This pilot network, AEROSOURCE, is regarded as a next-generation network, as, for the first time, it provides real-time quantification and speciation of organic matter, the dominant pollutant species in PM, and source apportionment capabilities.

The network, operated continuously for a 3-year period, revealed that, under polluted conditions, carbonaceous chemical species (e.g. organic matter and black carbon) prevail over historically dominant inorganic chemical species (e.g. sulfur and nitrogen), with carbonaceous species contributing from 60% to 90% of PM_1 (the mass of all particles ≤ 1 µm in aerodynamic diameter). Carbonaceous compounds are diverse in source and nature, resulting in quite complex challenges, in terms of both measuring their contribution to PM in regulatory air quality networks and determining their sources; however, such information is essential to the development of effective pollution control strategies. AEROSOURCE provides the solution to both challenges, and the success and power of this next-generation aerosol mass spectrometry network immediately became evident after identification, in real time, of the magnitude and composition of frequent extreme pollution events in south Dublin. These events, occurring during cold, stagnant conditions, led to PM_1 mass concentrations reaching 300 µg m^{-3}, of which 70% was from organic matter sources, increasing to approximately 90% when considering total carbonaceous PM_1.

These events, during which the concentration of $PM_{2.5}$ (the mass of PM with a diameter of less than 2.5 µm) exceeded daily recommendations of 25 µg m^{-3} (World Health Organization guidelines), occurred on one in five winter days (Lin *et al*., 2018). Using sophisticated fingerprinting techniques, we found that consumption of peat and wood, although contributing only a minor part of the city's energy budget, accounted for up to 70% of PM_1 during exceedance events. The network approach revealed similar patterns in other locations in Ireland (Carnsore Point, Galway and Mace Head), where peat and wood contributed >50% of PM_1 during cold stagnant conditions, pointing to a nationwide problem.

Analysis of seasonality revealed that emissions from peat and wood burning contributed 43% of total organic aerosol (OA) mass in winter, with the absolute concentration being approximately seven times higher than in autumn or spring; OA levels from peat and wood burning were below the detection limit in summer. Likewise, coal emissions were higher in winter (contributing 11% of total OA) than in autumn or spring (less than 5% of total OA). The contribution from traffic was comparable over all seasons and constituted ~8–15% of total OA.

On average, organic matter dominated PM_1 concentrations in the residential Dublin area (>60%), while black carbon was the major compound (>50%) at Dublin's kerbside location. However, carbonaceous PM was the leading contributor in both locations and contributed ~80% at the residential background site and ~90% at the kerbside location.

AEROSOURCE also elucidated distinct potential health effects arising from different sources of organic matter based on toxicity, and found that solid fuel burning had large potential for adverse health impacts.

Our approach to determine toxicity focused on only soluble organic matter and hence is likely to give a conservative estimate, as toxicity from insoluble materials (e.g. coming from traffic) is also known to make a large contribution to PM effects. Nevertheless, it provides valuable insights into the toxicity of emissions from solid fuel burning and highlights detrimental effects arising from organic matter as opposed to major inorganic compounds (sulfate and nitrate).

In summary, the results from this approach can better inform emission reduction policies and help to ensure that the most appropriate air pollution sources are targeted.

1 Introduction

Airborne aerosol particles adversely affect human health (Pope *et al*., 2002, 2009). Globally, millions of premature deaths per year have been estimated to be associated with outdoor air pollution caused by fine particulate matter (PM) with a particle diameter of less than 2.5 µm ($PM_{2.5}$) (Lelieveld *et al*., 2015). Even short-term exposure to outdoor $PM_{2.5}$ is associated with an increased risk of mortality and morbidity, and an increase in emergency admissions to hospital (Atkinson *et al*., 2014). The World Health Organization (WHO) recommends a 24-hour average concentration of 25 µg m^{-3} as the short-term guideline limit value for $PM_{2.5}$ and urges countries not meeting these values to undertake immediate actions. As for the long-term guideline value for $PM_{2.5}$, an annual average of no more than 10 µg m^{-3} is recommended. However, mass concentration alone is not enough to evaluate the health effects of $PM_{2.5}$, as certain chemical components and sources are more harmful than others. Specific sources such as traffic emissions and emissions from fuel oil combustion and biomass burning have been shown to be more closely associated with mortality and adverse health effects than other sources (Uski *et al*., 2014; Zanobetti *et al*., 2014).

Aerosol particles also affect climate directly by scattering or absorbing solar radiation and indirectly by acting as cloud-condensation nuclei (O'Dowd *et al*., 2004). The effects of aerosol particles on climate depend on their composition and sources. Moreover, uncertainties in regard to aerosol–cloud–climate interactions cause the highest errors in global aerosol forcing estimations and, thus, climate projections.

Some airborne aerosol particles, such as dust, pollen, sea salt and volcano ash, are naturally occurring, while others can come from anthropogenic sources. Generally, airborne aerosols are divided into two types, primary and secondary (Hallquist *et al*., 2009). Primary aerosols are directly emitted or injected into the atmosphere in the particle phase, while secondary aerosols are formed by the nucleation/oxidation/ condensation of precursor gases. Human activities such as driving, cooking and solid fuel burning emit both primary aerosols, e.g. black carbon (BC) and organic matter (OM), and secondary aerosol precursor gases, such as sulfur dioxide, nitrogen oxides and volatile organic compounds (VOCs), which are converted into their corresponding particulate phase upon oxidation/nucleation/condensation (Hallquist *et al*., 2009). Note that both primary and secondary aerosols undergo a dynamic change in both composition and properties resulting from oxidation, gas-to-particle partitioning, fragmentation and cloud processing (Kroll and Seinfeld, 2008; Gentner *et al*., 2017). Therefore, real-time and long-term measurements of aerosol particles are important to understand the temporal variations and to study changes in sources affecting air quality.

1.1 Historical Measurements of Particulate Air Pollution: Black Smoke

Black smoke (BS) measurements were the earliest systematic measurements of particulate air pollution in Ireland (Kelly and Clancy, 1984). BS data have been reported to be a useful metric for health studies, showing a strong correlation with morbidity and mortality in epidemiological studies (Kelly and Clancy, 1984; Clancy *et al*., 2002).

In the 1980s, Ireland experienced severe air pollution episodes due to coal burning for home heating. In 1982, a city-wide pollution event with BS concentrations reaching over 750 µg m^{-3} resulted in the doubling of fatality rates at a central Dublin hospital (Kelly and Clancy, 1984). After the introduction of a ban on the marketing, sale and distribution of smoky coal in 1990, a significant reduction in BS (up to 70%) was observed in Dublin (Goodman *et al*., 2009). Later, the coal ban was extended to other areas with populations over 15,000, including Cork and Galway (Goodman *et al*., 2009).

As BS measurements are based on the optical darkness of total PM, which is, however, dominated by submicron elementary carbon particles (Heal *et al*., 2005) (i.e. PM particles with a diameter of less than 1 µm – PM_1), BS is a good surrogate for primary combustion particles but is insensitive to

secondary inorganic aerosols such as sulfate and nitrate. Therefore, BS cannot represent the total mass concentration of PM, as the composition of PM has changed greatly, notably as coal burning in cities has declined. For example, Heal *et al*. (2005) reported that the daily BS to PM_{10} (the mass of all particles equal to and less than 10 µm in aerodynamic diameter) ratios at an urban background site in Edinburgh were significantly lower in summer than in winter because of the important contribution to PM mass in the summer of secondary aerosols, which are not included in BS measurements.

Despite these drawbacks, BS data are the only available long-term PM data (over 20 years) and enable the interpretation of PM and BC trends important for human health and climate change studies. For that reason, it is essential to understand similarities and differences between the historical BS and contemporary real-time BC measurements. Despite BC measurements being based on different instrumentation and data processing from BS measurement methods (Quincey, 2007), a simple quadratic relationship between BS and BC can be established (Quincey *et al*., 2007), which is useful in the interpretation of historical BS data.

1.2 Chemical Composition of Particulate Matter

Airborne aerosol particles have very complex and variable chemical compositions, ranging from inorganic compounds (e.g. sulfate, nitrate, sea salt and elemental carbon) to OM. Moreover, because of the various sources and transformations, the chemical composition of aerosols varies a lot depending on the location, time, season and weather conditions.

Inorganic compounds are found in both marine and continental aerosols. For example, primary sea salt particles are generated through bubble bursting and wave breaking (O'Dowd and de Leeuw, 2007), while sulfate ions (SO_4^{2-}) are formed from the gas-to-particle conversion of sulfur dioxide (SO_2). Sulfur dioxide can be emitted from both anthropogenic sources (e.g. coal burning) (Zhang *et al*., 2012) and natural ones (e.g. volcanoes or biological activity in oceans) (O'Dowd *et al*., 1997; Ovadnevaite *et al*., 2014). Nitrate ions (NO_3^-) are formed by the oxidation of atmospheric nitrogen dioxide (NO_2), which is almost exclusively emitted from anthropogenic sources, e.g. traffic emissions or other combustion sources (Geng *et al*., 2008).

Ammonium (NH_4^+) salts are formed when the gas ammonia (NH_3) reacts with various acids, such as sulfuric (H_2SO_4) or nitric acid (HNO_3), to form ammonium sulfate or nitrate. The availability of ammonia determines aerosol acidity or neutrality, ranging from fully neutralised salt particles to acidic ones.

BC is the sooty black material emitted by fossil fuel or biomass combustion, often with other compounds attached to its surface. BC, being a strong absorber of solar radiation, is the second largest contributor to current global warming after carbon dioxide (Ramanathan and Carmichael, 2008).

Finally, organic aerosol (OA) encompasses numerous individual organic compounds such as alkanes, fatty acids, sugars, alcohols, aldehydes and others, as well as some highly carcinogenic compounds such as polycyclic aromatic hydrocarbons (PAHs) (Bi *et al*., 2003). In contrast to inorganic aerosol, OA remains poorly understood as a result of its various sources and evolution (Jimenez *et al*., 2009).

As a result of strict regulations on sulfur-containing compounds, the atmospheric concentrations of SO_2 and sulfate have reduced significantly (by ~80% over a 35-year period), resulting in aerosol composition being dominated by OM (Grigas *et al*., 2017). As observed at the Mace Head research station on the west coast of Ireland, OA prevails over inorganic compounds under polluted conditions, contributing 60–90% of the PM_1 mass and exhibiting a trend whereby its contribution increases with increasing pollution levels (Grigas *et al*., 2017). Identifying OM sources is, therefore, crucial to developing efficient emission-reduction strategies.

1.3 Source Apportionment

Source apportionment identifies the specific types of aerosol particles that make up particulate air pollution and their sources. It improves our quantitative understanding of each source's contribution to particulate air pollution, enabling efficient mitigation. It is also very useful for refining emission inventories and predicting changes in air quality as a result of implementing various emission control strategies. Furthermore, source apportionment is important for studying the health effects of certain aerosol sources.

Receptor-based models are the most widely used source apportionment techniques (Lee *et al*., 2008). Typically, receptor models attribute observed concentrations of aerosol particles to specific sources using the chemical composition or mass spectra of those samples to trace the source type. The outcome of such analysis is the identification of pollution source types and their corresponding contributions to the observed concentrations.

Chemical mass balance (CMB) and positive matrix factorisation (PMF) are the two types of receptor-based bilinear algorithms that represent ambient time series as a linear combination of factor profile time series (Lee *et al*., 2008; Canonaco *et al*., 2013). CMB source apportionment requires a priori knowledge of major sources (e.g. chemical composition or mass spectra), while PMF source apportionment does not require any a priori assumptions about either source or time profiles. Both CMB (i.e. known sources) and PMF (i.e. unknown sources) methods have their own advantages and disadvantages. CMB source apportionment is based on using the source-specific chemical composition or mass spectra, as the input to the bilinear algorithm model, to assess the contribution of certain emission sources to air pollution. However, CMB source apportionment is unable to directly apportion secondary sources. Instead, the fraction that is not attributed to primary sources in the CMB model is regarded as the upper limit of the secondary sources.

Although PMF source apportionment does not require any a priori source information, this model often suffers from high rotational ambiguity, resulting in non-meaningful or mixed factors, especially when all species measured exhibit temporal co-variation, e.g. due to boundary-layer evolution or certain meteorological conditions such as rainfall.

As a PMF solver, multilinear engine 2 (ME-2) is capable of directing the PMF model towards an optimal solution by utilising a priori information in the form of the factor profiles and/or time series. ME-2 has been utilised in several source apportionment studies to find acceptable solutions in cases in which PMF modelling did not properly represent measurement data (Lanz *et al*., 2008; Canonaco *et al*., 2013; Reyes-Villegas *et al*., 2016).

The application of source apportionment techniques to high-time-resolution data (seconds to minutes) enables the identification and quantification of pollution sources on a near real-time basis. This is very important for gaining an understanding of the evolution and diurnal variations of highly variable and intense sources that might otherwise be missed by the poor time resolution (days to weeks) of filter-based sampling.

1.4 Application of Positive Matrix Factorisation to Aerosol Mass Spectrometer Data

The development of high-time-resolution aerosol mass spectrometry (AMS) has greatly improved our understanding of the chemical composition and sources of ambient aerosol particles (Jayne *et al*., 2000; Jimenez *et al*., 2009; Lanz *et al*., 2010). AMS determines the mass spectra of the major non-refractory (organic and inorganic) components of ambient aerosol in near real time (Canagaratna *et al*., 2007). Using the “fragmentation table” (i.e. typical mass spectral fragmentation patterns for compounds), measured mass spectra are assigned to several inorganic (i.e. sulfate, nitrate, ammonium and chloride) or organic compounds (Allan *et al*., 2004). The organic aerosol has been found to make up a large fraction (20–90%) of PM_1 mass and, thus, much attention has been paid to identifying its sources (Jimenez *et al*., 2009). However, the source apportionment of OA is still challenging because of very large chemical variability with respect to molecular weight, functional groups and polarity (Jimenez *et al*., 2009; Huang *et al*., 2014). Over the past decade, numerous studies have successfully exploited the resolving power of PMF to apportion AMS-measured organic mass to different sources based on the source-/process-specific factor profiles or time series (Zhang *et al*., 2011; Li *et al*., 2017). Typically, PMF interprets the time series of measured organic mass spectra as a linear combination of static factor profiles (i.e. mass spectra) and their time series (Paatero and Tapper, 1994; Canonaco *et al*., 2013).

AMS-PMF studies have been carried out at a variety of sites, including urban, rural and remote stations across the world (Jimenez *et al*., 2009; Lanz *et al*., 2010; Crippa *et al*., 2014; Li *et al*., 2017). Depending on the site, different sets of organic factors, including various primary OA (POA) and secondary OA (SOA) factors corresponding to different sources/processes, have been identified (Jimenez *et al*., 2009; Li *et al*.,

2017). For example, hydrocarbon-like OA (HOA) is a POA factor that is associated with vehicular emissions and is common in urban areas (Canagaratna *et al*., 2004; DeWitt *et al*., 2015). Cooking-related OA (COA) represents POA from cooking activities and its diurnal cycle usually exhibits mealtime peaks (He *et al*., 2010; Mohr *et al*., 2012). Biomass burning OA (BBOA) is associated with emissions from wood burning and crop residue burning (Zhang *et al*., 2015). Coal combustion OA (CCOA) is associated with emissions from coal combustion and has been identified in Beijing because of its widespread use in domestic heating (Sun *et al*., 2013) as well as in Ireland (Dall'Osto *et al*., 2013) and the UK. Oxygenated OA (OOA) is characterised by high oxygen content with a high atomic oxygen to carbon ratio (O:C) (0.25 to ~1) (Jimenez *et al*., 2009; Zhang *et al*., 2011). Most OOA is secondary and an increase in OOA mass is usually associated with strong photochemical activities and is accompanied by other secondary species, e.g. sulfate. Based on its volatility, OOA can be divided into semi-volatile OOA (SV-OOA) and low-volatile OOA (LV-OOA), representing newly formed and aged OOA, respectively (Zhang *et al*., 2011; Canonaco *et al*., 2015). The formation of SV-OOA depends on the emission of its precursor gases (e.g. VOCs) and a subsequent photo-oxidation process (Jimenez *et al*., 2009). The concentration of SV-OOA is usually higher in the afternoon as a result of stronger solar radiation at this time. Further oxidation of SV-OOA forms LV-OOA (Canonaco *et al*., 2015).

Figure 1.1, representing AMS-PMF studies conducted across Europe, shows that, for most sites, four organic factors can be retrieved, namely two POA factors (i.e. HOA and BBOA) and two SOA factors (SV-OOA and LV-OOA) (Crippa *et al*., 2014). COA was identified only at urban locations, while methane sulfonic acid (MSA) (marine-related sources) was identified only in marine environments. The traffic-related HOA was season independent and represented 11 ± 6% of total OA across Europe. In contrast, domestic heating-related BBOA was more intense during winter and represented 12 ± 5% of the total OA mass. However, SOA (the sum of SV-OOA and LV-OOA) was, usually,

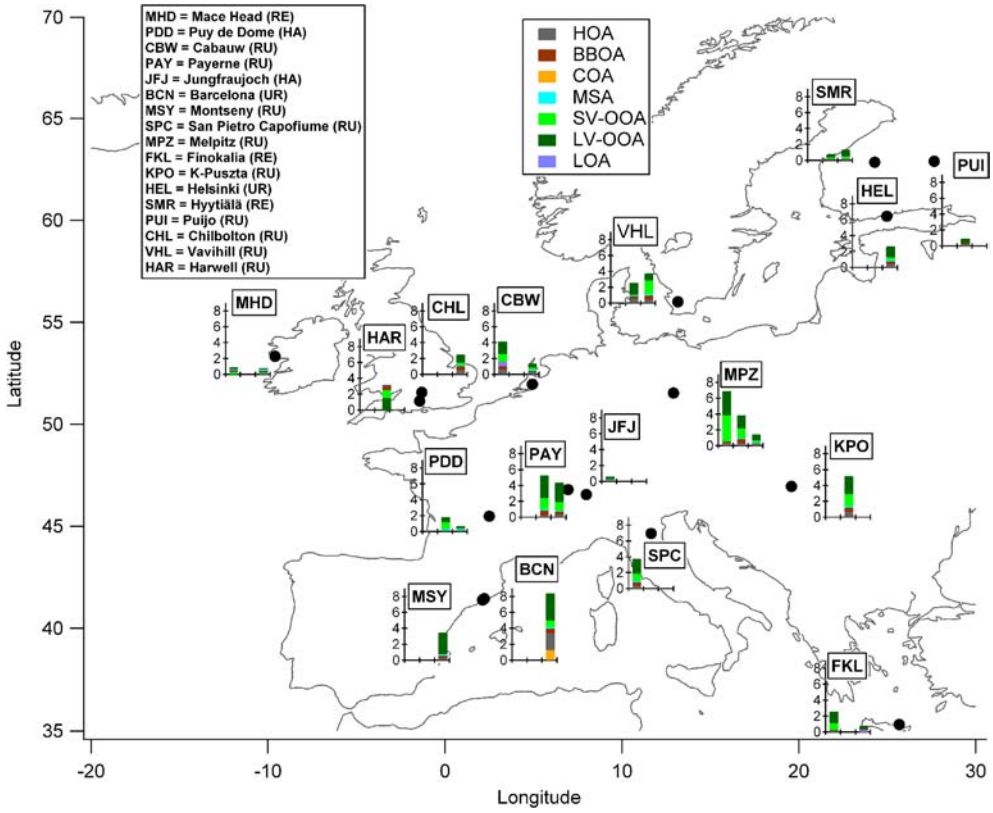

Figure 1.1. Seventeen measurement sites across Europe and average OA factor contributions resulting from PMF conducted on AMS organic spectra using ME-2. Reproduced from Crippa *et al*. (2014) under the terms and conditions of the Creative Commons Attribution license CC-BY-4.0 (https://creativecommons.org/licenses/by/4.0/).

the dominant fraction of OA (>70%), indicating the importance of the concurrent control of SOA precursors and governing of POA emissions.

1.5 Application of Positive Matrix Factorisation to Aerosol Chemical Speciation Monitor Data

Research-grade AMS provides valuable information about aerosol composition and sources; however, it is not well suited to routine air quality monitoring applications because of its high cost and the complexity of instrument maintenance (Ng *et al*., 2011). Most AMS studies are limited to a short sampling period, typically less than 2 months (Lanz *et al*., 2010; Sun *et al*., 2012). However, real-time and long-term aerosol measurements over several seasons or even years are important for gaining an understanding of the dynamic variation in aerosols. The Aerodyne aerosol chemical speciation monitor (ACSM), a simplified version of an aerosol mass spectrometer, is specially designed for long-term monitoring applications (Ng *et al*., 2011). The ACSM is smaller, weighs and costs less and requires less power than the aerosol mass spectrometer; therefore, it is easier to transport and requires less maintenance (Ng *et al*., 2011). The ACSM has been deployed for periods of up to 2 years (Petit *et al*., 2015; Sun *et al*., 2018), showing that this instrument can be used in an operational manner.

As part of the Aerosol, Clouds, and Trace Gases Research Infrastructure Network (ACTRIS) programme, which aims to pool high-quality data obtained using this state-of-the-art instrument, the ACSM is widely used throughout Europe (Crenn *et al*., 2015; Fröhlich *et al*., 2015; Minguillón *et al*., 2015). Throughout a 1-year campaign in Cabauw, the Netherlands, using an ACSM in combination with PMF, OOA was found to be the dominant factor in OA (constituting 61–84% of total OA) (Schlag *et al*., 2016). Because of the large secondary fraction (ammonium nitrate, sulfate and OOA), achieving a reduction in particulate air pollution is challenging on a local scale and therefore requires a regional effort (Schlag *et al*., 2016). The 1-year deployment of an ACSM at the Montseny regional background site in Spain in the western Mediterranean led to OA being found to be the major component of PM_1 mass (53%) (Ripoll *et al*., 2015). Source apportionment revealed that OOA dominated the OA, with its contribution being higher in summer (85% of total OA) than in winter (60%). Two POA factors (BBOA and HOA) were found to be present in OA in winter, while only one POA factor (traffic-related HOA) was identified in summer (Ripoll *et al*., 2015). Petit *et al*. (2015) also found, in a study of a 2-year campaign in the Paris region using an ACSM and other co-located instruments (e.g. an aethalometer), that OOA was a major component of OA during the spring and summer, while POA was more pronounced during the winter (Petit *et al*., 2015).

1.6 Source Apportionment Studies in Ireland

As mentioned above, Ireland experienced severe air pollution episodes in the 1980s due to solid fuel, especially coal, burning (Kelly and Clancy, 1984). After the introduction of a ban on the marketing, sale and distribution of coal in 1990, the air quality improved significantly (Goodman *et al*., 2009). However, a more recent study in Cork (Kourtchev *et al*., 2011) found that domestic solid fuel is still the major source of organic carbon during the autumn (66%) and winter (75%), despite the ban on bituminous coal. Later, an AMS-PMF study in winter in Cork (Dall'Osto *et al*., 2013) found four types of POA (HOA, BBOA, COA and peat/coal burning OA) and one type of OOA (LV-OOA). In total, POA accounted for 82% of OA, indicating an important role for local emissions, especially from wood, peat and coal burning (Figure 1.2). These studies suggest that the ban on bituminous coal alone is not enough to improve air quality, as peat and wood emit similar or higher amounts of PM.

The two studies mentioned above were conducted in Cork city, located in the southern part of Ireland (Kourtchev *et al*., 2011; Dall'Osto *et al*., 2013). Sources contributing to reducing air quality in other locations, such as Dublin or the west coast of Ireland, remain poorly understood.

1.7 Health Effects of Airborne Particulate Matter

Numerous studies have shown that exposure to ambient PM has damaging effects on health (Samet *et al*., 2000; Brunekreef and Holgate, 2002; Pope *et al*., 2004; Schaumann *et al*., 2004; Pope and

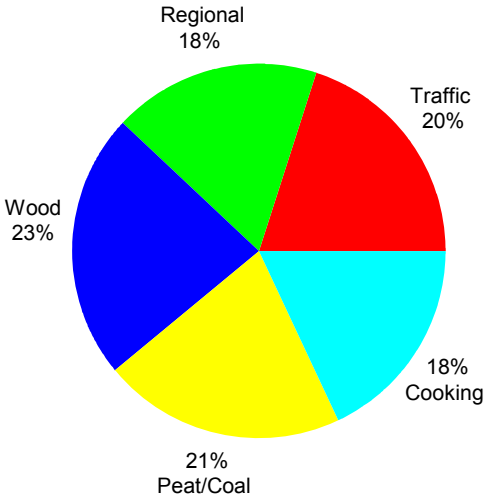

Figure 1.2. Average relative source contributions to OA in the winter in Cork, Ireland. Reproduced from Dall'Osto *et al.* (2013) under the terms and conditions of the Creative Commons Attribution license CC-BY-4.0 (https://creativecommons.org/licenses/by/4.0/).

Dockery, 2006). To reduce the damage to health, current air pollution regulations aim to reduce total particulate mass (Directive 2008/50/EU). However, atmospheric aerosol consists of a wide range of chemical components of potentially varying toxicity, implying that particulate mass is not an ideal air quality metric for assessing health impacts. For example, components such as ammonium, sulfate, nitrate and chloride, and some chemical fractions of mineral dust may be more benign than transition metals (Kodavanti *et al*., 2005; Gasser *et al*., 2009; Akhtar *et al*., 2010), BC (or elemental carbon and associated species) (Brunekreef, 1997; Kleinman *et al*., 2007) or PAHs (Burchiel *et al*., 2005; Lundstedt *et al*., 2007). Although constituting only a small fraction of aerosol mass, these components could play a disproportionally large role in causing adverse health effects. In addition, aerosol from certain sources such as traffic and biomass burning has been reported to be more closely associated with mortality and adverse health effects than other sources (Sbihi *et al*., 2013; Kamal *et al*., 2015). Therefore, elucidating the links between pollution sources and their corresponding adverse health effects is important to ensure that air quality regulations target the relevant sources and maximise the protection of health.

Despite the importance of elucidating these links, no comprehensive set of mechanisms explaining the observed linkage between aerosol concentrations and adverse health effects has been established to date. It has been hypothesised that one way in which aerosol could cause physiological effects is through its ability to induce oxidative stress (Delfino *et al*., 2005, 2013; Nel, 2005). Oxidative stress is a state of biochemical imbalance in which the presence and formation of reactive oxygen species (ROS) in the human body overwhelms antioxidant defences, eventually leading to various adverse health outcomes (Donaldson *et al*., 2001; Li *et al*., 2003; Delfino *et al*., 2011).

ROS are molecules or ions that can be present in PM (exogenous) or produced inside the cell as by-products of oxygen metabolism (endogenous) (Zhou *et al*., 2018). ROS include the superoxide radical ($O_2^{\bullet}$), hydrogen peroxide (H_2O_2), the hydroxyl radical ($^{\bullet}OH$), the alkoxyl radical ($RO^{\bullet}$), the carbon-centred radical ($C^{\bullet}$) and singlet oxygen (O_2) (Lakey *et al*., 2016). The oxidative potential (OP) of PM is defined as the ability of atmospheric aerosol to generate ROS. The OP of PM integrates various biologically relevant properties of the constituent particles, including their size, surface area and chemical composition. OP may be a better indicator of the biological responses to aerosol exposure and consequently may be more informative than PM mass or details of specific chemical components when attempting to link aerosols to adverse health effects.

A number of different assays have been developed to quantify the OP of aerosol samples (Cho *et al*., 2005; Venkatachari *et al*., 2005; Jung *et al*., 2006; Ayres *et al*., 2008; Zomer *et al*., 2011), avoiding the need for more expensive and time-consuming *in vitro* cell studies. The dithiothreitol (DTT) assay, introduced by Kumagai *et al*. (2002), is one of the most commonly used to measure the OP of fine particles (i.e. the OP of fine particles as measured using the DTT assay – OP_DTT). DTT acts as a surrogate for cellular reductants such as NADH/NADPH. The assay is based on mimicking interactions between physiological reductants and aerosol components through purely chemical analysis. When the reaction is monitored under conditions of excess DTT, DTT consumption over time is proportional to the concentration of redox-active species in the PM, and this is quantified as the PM's OP (OP_DTT).

The DTT-active aerosol components identified are organic species, including water-soluble organic

carbon (Cho *et al*., 2005; Verma *et al*., 2009a) or, more specifically, humic-like substances (Lin and Yu, 2011; Verma *et al*., 2012; Verma *et al*., 2015a) and quinones (Kumagai *et al*., 2002; Chung *et al*., 2006). Recent studies have also shown that SOA may cause significant DTT activity (McWhinney *et al*., 2013a; Lin *et al*., 2016) and that SOA OP is linked to SOA formation conditions (e.g. in high- vs low-NO_x conditions) (Jiang *et al*., 2017; Jiang and Jang, 2018). Other studies have emphasised the role of transition metals in OP_DTT, such as Cu and Mn (Charrier and Anastasio, 2012; Vejerano *et al*., 2015). However, in studies comparing the DTT assay with other OP tests, the DTT assay has always been reported to be the least sensitive to metals (Janssen *et al*., 2014; Hedayat *et al*., 2015).

The OP_DTT per volume of air sampled has been found to correlate with biological markers, such as cellular haem oxygenase expression (Li *et al*., 2003) and fractional exhaled nitric oxide, in human subjects (Delfino *et al*., 2013; Janssen *et al*., 2015). Epidemiological studies have linked OP_DTT to adverse health outcomes, such as asthma, rhinitis (Yang *et al*., 2016), asthma or wheezing, and congestive heart failure (Bates *et al*., 2015; Fang *et al*., 2016).

The OP_DTT of water-soluble PM components is a common focus of OP studies. All the above-cited DTT-active species were identified in aerosol water extracts. Water-insoluble species can also be an important fraction in terms of the overall redox activity of PM, with recent publications providing evidence for the role of water-insoluble aerosol components in generating OP (Akhtar *et al*., 2010; Daher *et al*., 2011; Li *et al*., 2013, McWhinney *et al*., 2013a). According to Gao *et al*. (2017), including the contribution of water-insoluble species in an OP assessment gives a more realistic picture of actual PM exposure. Nevertheless, few methods allow total OP_DTT to be measured and these are still not well characterised and involve more complicated procedures.

1.8 Air Quality Network

An air quality monitoring network provides real-time, publicly accessible data from monitoring stations in a specific region or country. However, regulatory air quality networks mainly focus on PM mass monitoring and are not required to routinely measure the chemical composition of PM, let alone perform source apportionment. Without source apportionment capabilities and information on the sources contributing most to worsening air quality, effective emission reduction strategies are only a shot in the dark. Sophisticated emission reduction strategies are clearly required and need to be accurately informed by next-generation observational air quality networks.

During historical air pollution events, sulfur (sulfur dioxide and sulfate) and BS often dominated pollution and were relatively straightforward to quantify; however, as sulfate emissions have decreased by an order of magnitude since the acid rain days (Grigas *et al*., 2017), carbonaceous aerosol has typically replaced sulfur as the main contributor to PM_1 pollution. In most regions, including Europe and the USA, the contribution of carbonaceous aerosol has increased and now accounts for up to 95% of PM_1 pollution (Jimenez *et al*., 2009; Grigas *et al*., 2017). Therefore, the problem in characterising PM_1 now lies in the diversity of sources, both natural and anthropogenic, and the chemical complexity of the OM, and is further compounded by the analytical challenges related to source apportioning organic species, many of which have not yet been identified.

In an attempt to address these challenges, we have established the first pilot national AMS network aimed at enabling the quantification and source apportionment of OM (Lin *et al*., 2017). The pilot network is essentially a subnetwork of the Irish National Transboundary Air Pollution Network, incorporating three ACSM nodes strategically positioned in urban (Dublin residential background and kerbside), regional (Carnsore Point; background) and marine/coastal (Mace Head; background) locations to capture and quantify contributions from local sources and transboundary air pollution (see the AQ network section on the Macehead.org website).

1.9 Aim and Objectives

The overall aim of this project was to deploy a state-of-the-art PM characterisation technique, namely AMS, in conjunction with source apportionment and meso-scale modelling analysis, to elucidate and quantify the most important air pollution sources affecting air quality in Ireland and determine their potential health impacts.

1.9.1 Objectives

- To identify and quantify aerosol sources affecting Dublin's air quality by deploying AMS.
- To assess the contribution of transboundary and local air pollution by means of the Weather Research and Forecasting Model coupled with Chemistry (WRF-Chem), a regional air quality model, along with AMS speciation data.
- To evaluate the historical "black smoke" data and relate them to modern BC measurement techniques.
- To assess the health effects of atmospheric aerosol particles.

2 Methods

2.1 Site Selection

Measurement locations were selected to cover a variety of aerosol types, from a coastal/marine background location to the most polluted kerbside location. Mace Head Atmospheric Research Station (53°33′ N, 9°54′ W), located on the west coast of Ireland, is exposed to air masses of very distinct origins, from very clean marine air masses to polluted air masses arriving from central Europe, making it a control station without significant contribution from local anthropogenic sources. The stations in two urban locations cover distinct local sources: measurements made at University College Dublin (UCD) (conducted on the roof of the science building, ~30 m above the ground, 53.3053° N, 6.2207° W) represent residential background sources and those made at Trinity College Dublin (TCD) (Pearse Street, street level, 53.3449°N, 6.2542°W) characterise traffic contributions. Finally, the station at Carnsore Point (52.1775°N, 6.3676°W) is exposed to long-range pollution from the UK and Europe (Figure 2.1).

2.2 Chemical Composition Measurements

The Aerodyne Research Inc. ACSM was used to characterise the chemical composition of non-refractory PM_1 (NR-PM_1) in ambient measurements, but also to obtain unique mass spectral signatures of aerosols produced from the burning of solid fuels. ACSM is providing near real-time concentrations and chemical speciation of non-refractory PM with further source apportionment capability (Ng *et al.*, 2011). For ambient measurements, sampling was performed from every 5 to every 30 minutes, depending on the location; when measuring high aerosol loads during burning experiments, sampling was performed approximately every 1 minute. ACSM spectra analysis was performed using the standard ACSM analysis software (version ACSM_local_1.5.12.0) written within Wavemetrics Igor and provided by Aerodyne Research Inc. BC and other refractory components cannot be measured by the ACSM and, thus, an aethalometer (AE-33, Magee Scientific) was used, in addition to

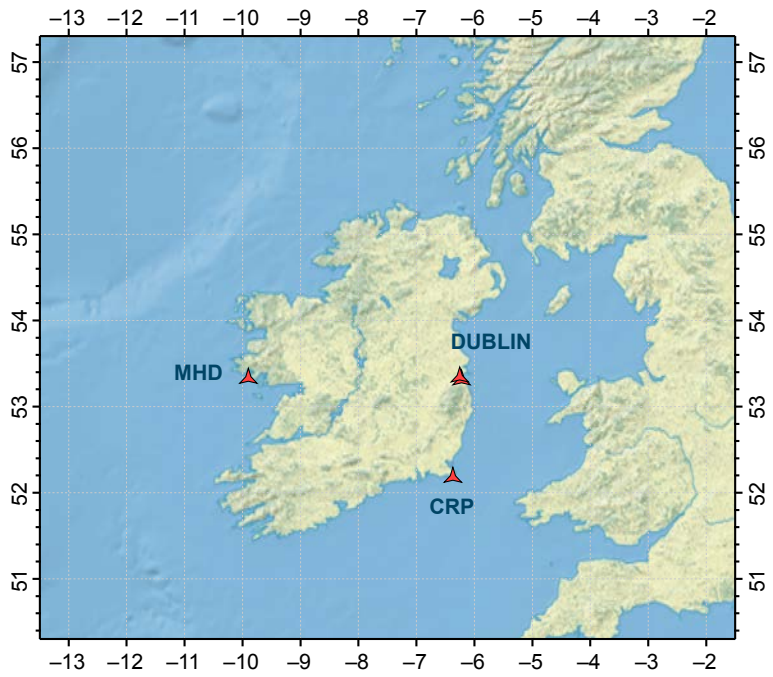

Figure 2.1. Map of the measurement locations. MHD, Mace Head; CRP, Carnsore Point.

the ACSM, for BC concentration measurements and source apportionment (see section 2.7.1 for a description of the AE-33).

2.3 Fingerprinting Solid Fuels

To enable the ME-2 to separate various solid fuels, solid fuel fingerprinting experiments were performed at the beginning of this project. Wood, sod peat, peat briquettes, bituminous coal and coal ovoids, locally sourced in County Tipperary, were used to obtain solid fuel burning fingerprints. The difference between dry (moisture <20%) and wet (>40%) wood/peat fingerprints was also investigated.

2.3.1 Experiment set-up

The burning experiments were performed using a solid fuel stove, set up in different ways: (1) a standard set-up, with the front window of the stove closed and the air supply regulated (filtered) to maintain the fire; and (2) an adjusted set-up intended to mimic open-fire conditions, with the front window of the stove open all the time. While these different set-ups might have affected emission factors (not measured here), they did not affect the fingerprints of the solid fuels used. The mass spectrum obtained for burning peat using a stove mimicking open-fire conditions showed very good agreement with the mass spectrum obtained for burning peat using standard stove set-up (the correlation coefficient – R – between the two mass spectra was 0.98, and the slope was 0.95 ± 0.02). Samples of the fuels were ignited using paper and left for about 15 minutes to reduce any effects of paper ignition. While sampling each type of fuel, new fuel was added to maintain the combustion and mimic the burning behaviour in a real house. The stove was cleared of residue following the combustion of each fuel sample. The NR-PM_1 aerosol generated from the fuel combustion was collected using a copper sampling line connected to the chimney. The total length of copper line between the chimney and the mobile station was around 10 metres, which meant that the aerosol had cooled down to ambient temperature by the time of measurement. An ACSM (Aerodyne Research Inc.) was used to characterise the chemical composition and obtain mass spectral signatures of the fuels.

2.3.2 Aerosol composition

Organic matter constituted the largest fraction (~98% for dry wood, ~91% for peat briquettes and ~94% for smoky coal) of total NR-PM_1 emissions for all fuel types except for the “smokeless” coal (~26%). For smokeless coal, chloride ions were the major component of the aerosol particles, constituting about 53% of total NR-PM_1 emissions, followed by organics (26%), sulfate (11%) and ammonium (8%). Burning conditions had only minor effects on the relative contributions of the species identified.

2.3.3 Mass spectra profiles

The averaged and normalised ACSM unit mass resolution (UMR) mass spectra of OA particles obtained from burning dry wood, peat and coal are shown in Figure 2.2. All three mass spectra were dominated by C_nH_{2n+1} (29, 43, 57, 71…) and C_nH_{2n-1} (27, 41, 55, 69…), indicating that saturated alkanes, alkenes and possibly cycloalkanes make large contributions to POA emissions from burning wood, peat and coal. However, the relative abundance of ions with specific mass-to-charge ratios (m/z) varied significantly depending on the fuel type. For example, for wood burning, the most prominent ion identified in the aerosol mass spectrum profile has a m/z of 29, followed by an ion with a m/z of 43, while, for peat burning emissions, the most abundant ion has a m/z of 43, followed by an ion with a m/z of 29. In contrast, ions of m/z 43 and m/z 41 were the most abundant in the coal emission mass spectrum. In addition, heavier ions ($m/z > 100$), most likely coming from PAH emissions, were much more prominent in the coal emission spectra than in the peat or wood emission spectra.

The prominent signals at m/z 29 and 43 in the wood emission spectra (Figure 2.2a) are consistent with previous reports using high-resolution time-of-flight AMS (HR-ToF-AMS) (He *et al*., 2010). High levels of CHO^+ and $C_2H_3O^+$ ions were found to be responsible for the strong signals at m/z 29 and m/z 43, respectively. Mass fragments at m/z 60 are often regarded as markers for wood burning aerosols (Alfarra *et al*., 2007) and mainly arise from the thermal decomposition of cellulose, the pyrolysis of which produces levoglucosan. The mass spectrum of POA from peat burning shows that

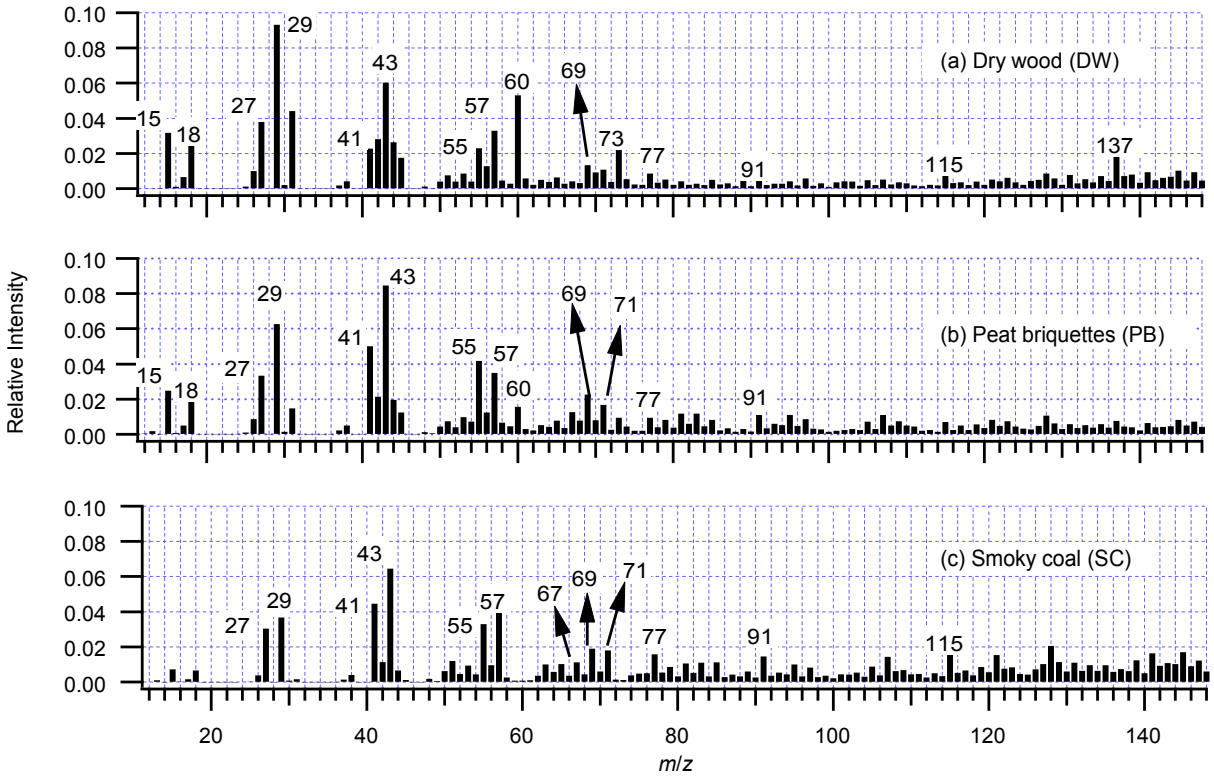

Figure 2.2. Normalised mass spectra of OM from the combustion of (a) dry wood, (b) peat briquettes and (c) smoky coal. Reproduced (adapted) with permission from Lin *et al.* (2017). Copyright 2017 American Chemical Society.

the highest signal is at *m/z* 43 (Figure 2.2b), which is consistent with HR-ToF-AMS measurements of open-grate peat burning (Dall'Osto *et al.*, 2013). Ions with *m/z* 43 are dominated by $C_3H_7^+$ ions in peat emissions, while $C_2H_3O^+$ ions dominate the *m/z* 43 signal in wood emissions. $C_xH_y^+$-type ions make up 71% of the peat mass spectra, which implies that there is a high fraction of hydrocarbons in peat emissions (Dall'Osto *et al.*, 2013). In addition, signals at *m/z* 77 and 91, typical of aromatic ion series, are present in the peat mass spectra and are more prominent than in the wood mass spectra. The presence of a *m/z* 60 signal in peat mass spectra profiles is due to the incomplete decay of vegetation, which contains cellulose (Szajdak *et al.*, 2007). Cellulose is one of the most common chemical substances in peat (Szajdak *et al.*, 2007). Although these ion series in the peat profile are not as prominent as in the wood profile, ions at *m/z* 60 are enough to distinguish the peat mass spectrum profile from those of coal and oil, the formation of which involves the complete decay of vegetation. For example, the most prominent peak in spectra of HOA from traffic emissions is typically at *m/z* 57, characteristic of saturated hydrocarbons, with no signal at *m/z* 60 (Lanz *et al.*, 2010; Ng *et al.*, 2010). A high degree of similarity in mass spectrum profiles for dry peat, wet raw peat and peat briquettes can be observed, which suggests that the state of the peat (i.e. raw, wet, shredded or compressed into briquettes) does not affect the OA mass spectra. For peat, 34.4% of mass spectrometry fractions have a signal of *m/z* > 80, which is slightly higher than for wood, indicating that high molecular weight compounds form in peat.

While burning smoky coal produces visibly more BC than smokeless coal, the OA mass spectral signatures of smoky and smokeless coal were very similar. This similarity indicates that the composition of the smokeless coal ovoids responsible for the emission of POA is similar to that of smoky coal. The strongest peak in the smoky coal mass spectrum was the signal at *m/z* 43, followed by *m/z* 41 (Figure 2.2c). This is similar to peat and consistent with previous HR-ToF-AMS measurements of emissions from open-grate coal burning (Dall'Osto *et al.*, 2013). $C_xH_y^+$-type ions dominate the mass spectrum for coal, accounting for

71% of fractions, which is the same as for the peat mass spectrum profile (Dall'Osto *et al*., 2013). Coal is formed through a process called "coalification" (Ibarra *et al*., 1996), where peat is physically and chemically altered as a result of bacterial decay, compaction, heat and time. No signal at *m/z* 60 was observed in the smoky coal mass spectrum (Figure 2.2c) as a result of the complete decomposition of cellulose. The absence of a signal at *m/z* 60 distinguishes the smoky coal mass spectrum from the mass spectrum obtained from contemporary biomass burning. In addition, the signal at *m/z* 57 is stronger than that at *m/z* 55 in the coal profile, while the opposite is the case for peat, indicating that coal has more saturated hydrocarbons than peat. Furthermore, fragment signals at *m/z* 77, 91 and 115 are stronger in the coal mass spectrum than in the peat mass spectrum, and this is most likely due to the high fraction of aromatic compounds in coal. The signal at *m/z* > 80 was ~51% of the total coal mass spectrum, which is significantly higher than for wood or peat.

2.3.4 Differences between aerosol chemical speciation monitor profiles and implications for positive matrix factorisation analysis

The mass spectra shown in Figure 2.2 are compared by plotting the individual *m/z* value intensities for dry wood and coal relative to the *m/z* value intensities for peat: $(m/z_{wood/coal,i} - m/z_{peat,i})/m/z_{peat,i}$ (Figure 2.3). The peat mass spectrum was chosen as the reference mass spectrum because peat is an intermediate state between wood and coal. The main differences between the wood and peat spectra are in the intensities at *m/z* 29, 31, 41, 60, 73, 83, 96 and 137: the intensities at *m/z* 29, 31, 60, 73 and137 are higher for wood than for peat (positive relative difference for wood), while the intensities at *m/z* 41, 83 and 96 are higher for peat (negative relative difference). In the case of the coal and peat comparison, the intensities at *m/z* 29, 31, 45, 60 and 73, being higher for peat, and at *m/z* > 115, being higher for coal, contribute mainly to the difference.

These differences in *m/z* value intensities mentioned above are expected to play an important role when applying PMF to determining the contributions of wood, peat and coal to OA.

2.4 Organic Aerosol Source Apportionment Method

A multilinear engine (ME-2) (Paatero, 1997; Paatero *et al*., 2014) within the Igor-based software package SoFi (version 6.1) was used for the source apportionment of OA. A detailed description of ME-2 and the software package can be found in Canonaco

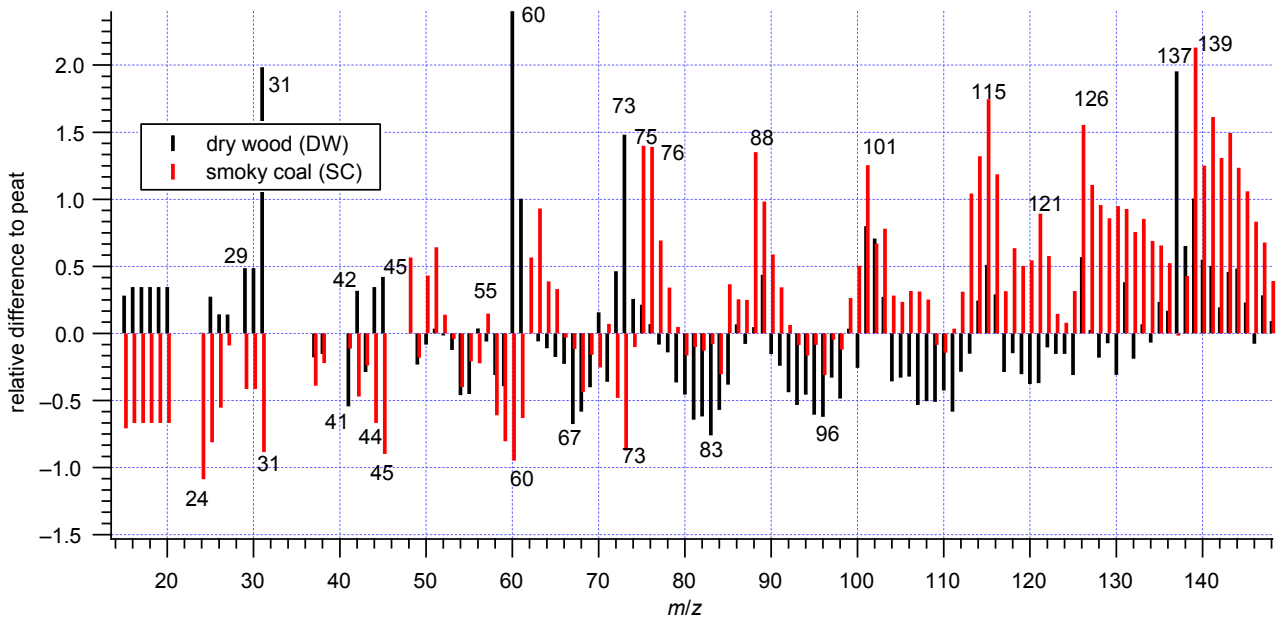

Figure 2.3. The difference between dry wood and smoky coal mass spectrum profiles relative to the peat mass spectrum profile for each *m/z* value. Reproduced (adapted) with permission from Lin *et al*. (2017). Copyright 2017 American Chemical Society.

et al. (2013). An a-value approach within ME-2 has been successfully used to explore rotational ambiguity in online and offline datasets, where users can direct the algorithm towards environmentally reasonable rotations by constraining reference-factor profiles or time series based on a priori information (Crippa *et al*., 2014; Elser *et al*., 2016). The a-value indicates the extent to which a reference profile can vary (e.g. an a-value of 0.1 allows a variability of 10%). Primary solid fuel profiles, obtained from the burning experiments described above, and a primary HOA profile, obtained from Crippa *et al*. (2014), were used to constrain primary emissions in PMF solutions, while secondary and unknown sources were left unconstrained (free PMF). HOA usually represents emissions from traffic; however, oil burning produces similar particulate emissions to those of traffic in terms of mass spectra, as indicated in the diesel-burning work by Schneider *et al*. (2006).

A 10% variation in profiles (i.e. an a-value of 0.1) was allowed, corresponding to the expected variation in profiles of freshly emitted OA as compared with the burning experiment fingerprints; however, the effects of applying other a-values were also investigated. For example, the effects of using a-values of 0, 0.05, 0.1 and 0.2 were investigated and no or only insignificant effects on the contributions of factors from oil, coal and wood burning to total OA were observed, while secondary OA and peat profiles were most reasonable when an a-value of 0.1 was used. Using an a-value of 0.1 was found to be optimal because it allowed sufficient freedom for variation in secondary sources, but prevented mixing between factors, which was the case for larger a-values (Lin *et al*., 2017).

2.5 Quasi-Lagrangian Method

The Lagrangian analysis tool LAGRANTO (Sprenger and Wernli, 2015) was used to evaluate contributions from local sources versus regional or long-range transport. Four back-trajectories (00:00, 06:00, 12:00 and 18:00) were calculated for each measurement day and for each station, with a 1-hour time resolution, based on meteorological reanalysis data of the European Centre for Medium-Range Weather Forecasts (ECMWF). Figure 2.4 shows an example of daily back-trajectory plots characterised by connecting flows between AEROSOURCE measurement stations. The contributions of the various sources on different spatial scales (urban, regional and continental) were considered (Figure 2.5, left panel).

Connecting flow conditions were analysed by comparing concentrations between upwind and downwind stations. Two approaches were deployed: a case-study approach, with a focus on the most relevant conditions, and a holistic approach, focusing on statistically significant differences in the atmospheric concentrations of the main aerosol components, providing a more general characterisation of pollution sources.

In addition, the following connecting flow selection criteria were applied: only back-trajectories passing horizontally within a range of ~20 km from the station (0.2° latitude–0.3° longitude) (horizontal restriction) and vertically within 1 km from the station (vertical restriction) were considered.

2.6 Air Quality Model

2.6.1 Technical description

For this study, WRF-Chem Version 3.9 was used to simulate PM concentrations in Ireland. WRF-Chem is the Weather Forecasting Research (WRF) model, which is fully coupled with the online chemical mechanism with aerosol module.

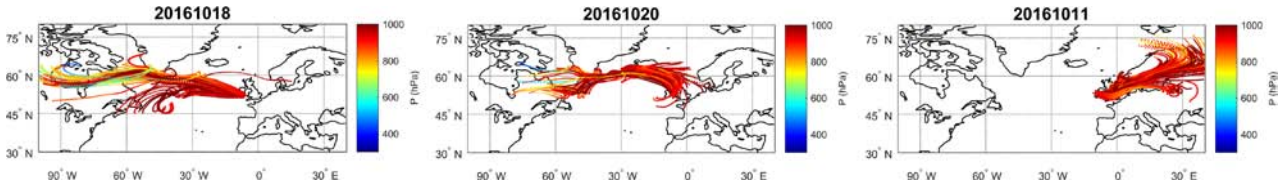

Figure 2.4. Daily back-trajectory charts calculated using LAGRANTO, showing connecting flow conditions between Mace Head and Carnsore Point in westerly wind conditions (left); between Dublin and Carnsore Point in northerly wind conditions (centre); and between Dublin and Mace Head in easterly wind conditions (right).

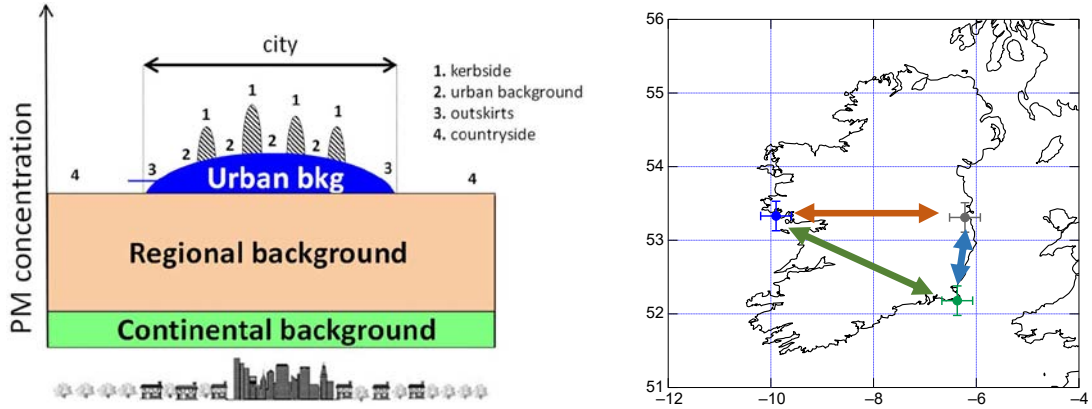

Figure 2.5. Left: graphical representation of PM sources; right: representation of connecting flows between three locations (Mace Head, left; Dublin, upper right; Carnsore Point, bottom right). Reproduced (adapted) from Fuzzi *et al*. (2015) under the terms and conditions of the Creative Commons Attribution license CC-BY-4.0 (https://creativecommons.org/licenses/by/4.0/).

The centre of domain (the centre of the area covered by the analysis) was located at 52.32°N, 1.51°W, and the whole area covered the majority of northern Europe with a 0.25° resolution. The vertical structure was divided into 30 levels, and terrain, land use and soil data were interpolated into grids from the United States Geological Survey (USGS) global elevation model. Simulations were performed using the second-generation Regional Acid Deposition Model (RADM2) (Stockwell *et al*., 1990) and the organic gas-phase chemical mechanism model CRIMECH v2 (Archer-Nicholls *et al*., 2014). The aerosol scheme used was the Modal Aerosol Dynamics Model for Europe (MADE/SORGAM) (Ackermann *et al*., 1998; Schell *et al*., 2001).

2.6.2 Emission inventory

Emission inventories (7 km × 7 km) of the Netherlands Organisation for Applied Scientific Research (TNO) are currently used in the operational model version; however, a comparison of model simulations with measurement data indicates that state-of-the-art emission inventories (of the European Monitoring and Evaluation Programme, EMEP, and of TNO, and even MapEIre, for the national mapping of greenhouse gas and non-greenhouse gas emission sources) fail to reproduce pollution events in simulations, highlighting the need to develop an emission dataset with a sophisticated representation of domestic solid fuel consumption.

Quantification of the emission sources in Dublin required an estimation of the amount of secondary fuel used per household in the Greater Dublin Area. This was done by referring to tabulated emission factors, which quantify the amount of PM released per unit of heat energy, and calorific values, which quantify the amount of heat energy created per mass unit of fuel consumed. These values allowed the amounts of $PM_{2.5}$ emissions per mass unit of fuel consumed to be calculated (see Table 2.1). An assumption that 40% of households use an additional solid fuel heating source during the winter was made. The amount of fuel consumed per unit of time was estimated from non-academic online forums and articles. The ratios of fuels burned per household were taken from census data, assuming that the same ratio applies to those using solid fuel as a primary source and those using solid fuel as a secondary source. The chemical speciation of PM emitted from solid fuel combustion was based on the chemical composition of PM_1 measured during extreme pollution events in Dublin (Lin *et al*., 2018). Hourly emissions data were prepared using a pre-processor developed at the University of Manchester, with time variance based on scaling factors estimated from meteorological observations. Emissions from burning solid fuel as a secondary/supplementary fuel for the grid cell representing Dublin city were then added to the TNO emission inventory. The hourly emission profile was set to reflect the diurnal fingerprint of solid fuel use, as depicted in Figure 2.6.

Table 2.1. Emission factors, calorific values and $PM_{2.5}$ emissions per kg of fuel undergoing combustion

Fuel type	Calorific value ($MJ\,kg^{-1}$)	Emission factor ($kg\,PM_{2.5}\,TJ^{-1}$)	$PM_{2.5}$ emissions ($mg\,PM_{2.5}\,kg^{-1}$ fuel)
Bituminous coal	27.84	30	835.2
Sod peat	13.1	60	786
Briquettes	18.55	60	1113
Petroleum coke	32.1	30	963
Fuel oil	41.24	40	1649.6
Gas oil	14.31	5	71.55
Kerosene	44.2	5	221
LPG	47.16	0.2	9.432
Natural gas	52.3	0.2	10.46
Biomass (wood)	16	270	4320

Source: data from TNO database, 2001. Reprinted with permission from Lin *et al.* (2017). Copyright 2017 American Chemical Society.

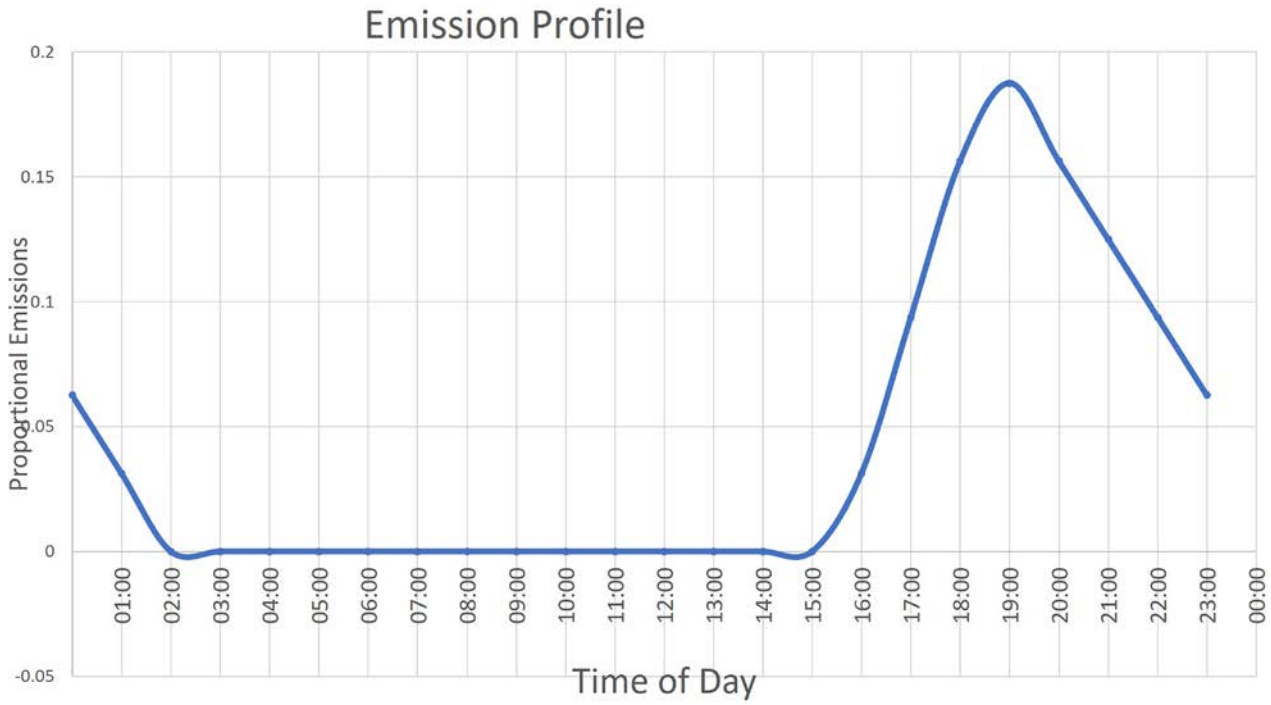

Figure 2.6. Diurnal profile of secondary solid fuel emissions used in WRF-Chem simulations.

To automate the generation of solid fuel emission data, the estimated enhancement in PM emissions as a result of solid fuel burning was inversely correlated with temperature in Dublin city. It was assumed that residential fuel burning starts at an air temperature of ≤12°C and the percentage of households burning fuel will increase linearly with decreasing temperatures, resulting in 40% of households burning solid fuel as a secondary heating source at 0°C and an even higher percentage at below-freezing temperatures.

The reference temperature is taken from ECMWF dissemination data at 18:00 for each forecasting day in the grid cell corresponding to Dublin.

This method represents a crude first attempt at proof of concept, and the refinement of the system is desirable to robustly characterise fuel-burning habits. However, the operational model results presented in section 3.6 are very encouraging and demonstrate proof of concept for the modelling system, which enables the pre-empting of harmful pollution events and mitigating actions to be taken for the protection of health.

2.7 Black Carbon and Black Smoke Measurements

2.7.1 Black carbon

BC measurements were made using an aethalometer (model AE-33, Magee Scientific). The aethalometer collects particles on filter tape and measures the attenuation of light at seven different wavelengths, ranging from ultraviolet (370 nm) to infrared (950 nm). The equivalent BC (eBC) mass concentration is calculated from the change in optical attenuation at 880 nm in a selected time interval using a mass absorption cross-section of 7.77 $m^2 g^{-1}$ (Drinovec *et al*., 2015).

The aethalometer exploits the different light absorption properties of BC particles originating from different sources to perform basic source apportionment. It has been shown that light absorption by BC particles from traffic sources, i.e. petrol and diesel emissions, is less dependent on wavelength than it is for BC particles emitted from biomass burning, i.e. the combustion of wood, etc., with the latter displaying particularly high levels of absorption in the near-ultraviolet and blue parts of the light spectrum (Sandradewi *et al*., 2008).

The absorption coefficients for wavelengths of 470 nm and 950 nm, along with the absorption Ångström exponent (α), are used to split the measured eBC into two source components, one for traffic (eBC_{TR}) and one for wood burning (eBC_{WB}) (Sandradewi *et al*., 2008). Given that several different solid fuels are used in Ireland, it is appropriate to change the wood burning component to solid fuel, to encompass wood, peat, turf and coal. In this work, the contributions from traffic (eBC_{TR}) and solid fuel burning (eBC_{SF}) were determined using the α values most recently recommended in the literature ($\alpha_{TR} = 0.9$ and $\alpha_{SF} = 1.68$) (Zotter *et al*., 2017). Although the studies described in this paper were conducted in a different environment from that in Zotter *et al.* (2017), it has been found that the parameters provide a good approximation for sources in Ireland. The use of these "Zotter values" as a basis for analysis was shown to be effective during the Environmental Protection Agency (EPA) SAPPHIRE research project (Wenger *et al*., 2020), where source apportionment using these parameters was in line with other source apportionment models and not greatly different from the source apportionment performed using an "optimised" set of values (also see Buckley, 2020).

2.7.2 Black smoke

Measurements of BS are based on the optical reflectance of a PM sample collected on a filter by pumping a known volume of air through a known area of filter. The reflectance, volume and filter area values are converted to a BS index, given in units of $\mu g\, m^{-3}$.

BS measurements were made in accordance with the methods detailed in British Standards Institution document BS-1747–2 (BSI, 1969). In brief, ambient air is drawn through a clean Whatman No. 1 filter paper, at a flow rate of between 1.5 $m^3 h^{-1}$ and 2.5 $m^3 h^{-1}$. Air was typically sampled for a period of 24 hours. Upon completion of sampling, the filter is removed from the housing and inserted into the reflectometer. White light is shone onto the filter and the amount of light reflected back is measured. The greater the amount of PM collected on the filter, the darker the filter and hence the lower the reflectance measured. The reflectance value measured is then compared with a calibration curve established by the BS-1747 document. This value, expressed in $\mu g\, cm^{-2}$, can be converted to $\mu g\, m^{-3}$ using equation 2.1:

$$C_z = Sa/V \quad (2.1)$$

where C_z is the BS concentration, V is the volume of air sampled, a is the area of the stain on the filter paper and S is the equivalent surface concentration of smoke on the filter, determined by comparing the reflectance reading with the calibration curve (Goodman, 1999).

2.8 Measurements of the Oxidative Potential of Atmospheric Aerosol Particles

Aerosol samples ($PM_{2.5}$) were collected on 150-mm diameter quartz fibre filters by a high-volume sampler, sampling every 6 hours for 1 week (2–8 December 2015). Half of each filter was used for the analysis of water-soluble aerosol OP using the DTT assay, following the procedure introduced by Cho *et al*. (2005) and Verma *et al*. (2009a). The filter portions were extracted in deionised water via sonication (for 30 minutes) and the extracts were filtered using PTFE

(polytetrafluoroethylene) 0.45-µm pore syringe filters to remove insoluble materials and any filter debris. The extracts were stored at 4°C if they could not be analysed immediately.

For the DTT assay, 2.5 ml of extract were added to 0.5 ml of potassium phosphate buffer (0.5 M, pH 7.4) in an amber vial (the primary vial). The solution obtained was heated at 37°C using a water bath. When the temperature reached the desired value, 30 ml of the DTT solution, with a concentration of 10 mM, were added to the vial (time zero). After 5, 10, 15, 20 and 25 minutes, 0.5-ml aliquots were removed from the vial and added to a second amber vial (the secondary vial) containing 0.5 ml of 10% trichloroacetic acid to stop the reaction. After all solutions had been collected, 50 ml of 10 mM 5,5'-dithiobis-(2-nitrobenzoic acid) (DTNB) solution in phosphate buffer at pH 7.4 were added to all secondary vials, mixed thoroughly and allowed to react for 5 minutes in the dark. Then, 2 ml of a solution of 0.4 M Tris-HCl buffer at pH 8.9 and 20 mM EDTA were added. The reaction between the residual DTT and DTNB forms 2-nitro-5-thiobenzoic acid (TNB), which was quantified at its maximum absorption wavelength of 412 nm using a TIDAS E (J&M) UV/VIS spectrophotometer.

The kinetics of DTT oxidation were followed by measuring the decrease in the concentration of DTT added to the sample (at 100 µmol) over the reaction course. The DTT depletion rate (nmol DTT min^{-1}), which is proportional to ROS production, was computed from the value of the slope of the straight line obtained by plotting the five experimental points of DTT concentration against reaction time (5, 10, 15, 20 and 25 minutes). The values of the slopes obtained for the field blank filters, treated following the same approach, were subtracted from the values of the slope obtained for the experimental samples, to compensate for signals coming from the filter matrix. The reproducibility of the method was confirmed on repeated tests of standard DTT-active organic compounds, which showed that the degree of uncertainty was in the order of 6%.

3 Quantification of Particulate Matter Sources in Ireland

3.1 Extreme Air Pollution Events in the Dublin Residential Area

PM_1 mass concentration, chemical speciation and size distribution have been continuously measured at the residential background site in Dublin (UCD) since August 2016. Here we present detailed results from a 1-year measurement period covering August 2016–August 2017, with a specific focus on the source apportionment of PM arising during extreme air pollution events.

Extreme pollution events were observed frequently between 15 November 2016 and 31 January 2017 (Figure 3.1), with the WHO-recommended daily value for $PM_{2.5}$ (25 µg m^{-3}) being exceeded ~20% of the time, or on 1 in 5 days (Figure 3.1c). Two events, on 19 November 2016 (P1) and 22 January 2017 (P2), were selected as the focus of this study because of the particularly high concentrations of PM detected. PM_1 peak concentrations were 302 µg m^{-3} during the first event and 273 µg m^{-3} during the second event.

$PM_{2.5}$ mass concentration was simultaneously monitored at the EPA's Rathmines regulatory air quality station, approximately 3 km from the UCD measurement site. A good correlation [coefficient of determination (R^2) = 0.87] between PM concentrations at both locations indicates that these events were not due to a single local source (e.g. a car passing by or a plume from a nearby chimney) but were simultaneously influenced by a pollution plume, covering an area of at least 3 km in radius. Indeed, for a wind speed of 2 m s^{-1}, a 30-minute sampling resolution (instrument averaging time) corresponds to a spatial scale of 3.6 km. The slope of the correlation between PM_1 and $PM_{2.5}$ (0.74) indicates that PM_1 mass, on average, accounted for 74% of $PM_{2.5}$

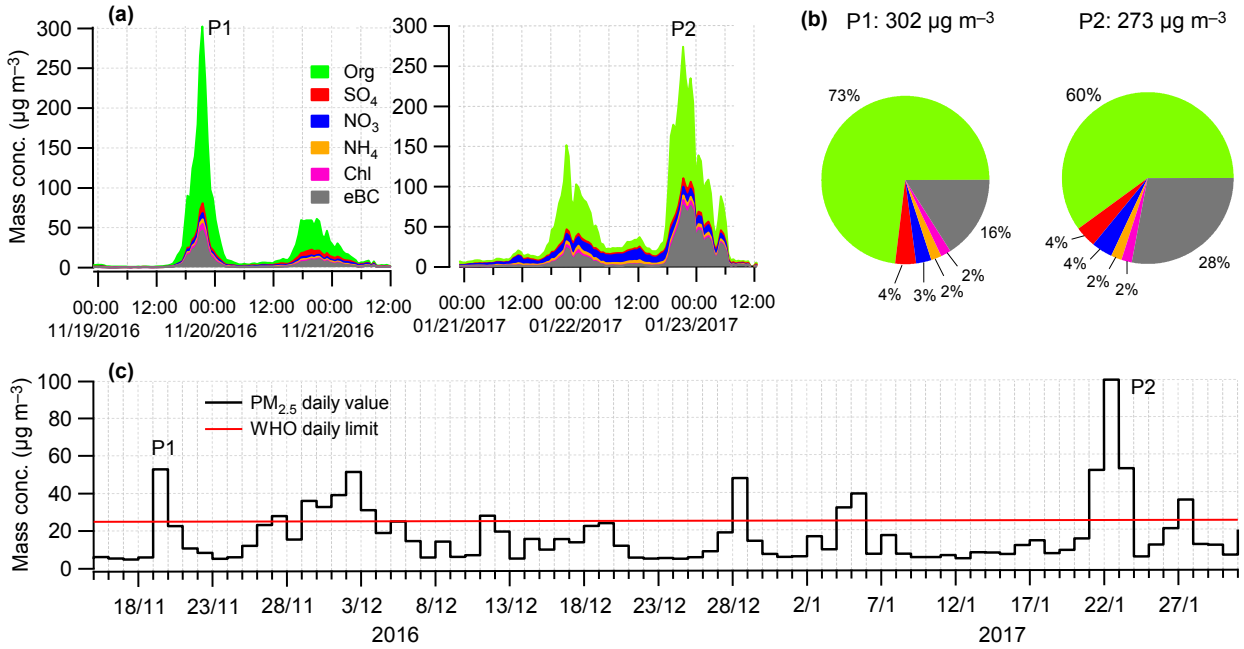

Figure 3.1. Chemical composition of PM_1 during extreme pollution events. (a) Mass concentrations of PM_1 components during two extreme pollution events, on 19 November 2016 (P1) and 22 January 2017 (P2), measured at UCD. (b) Relative contribution of the PM_1 components to the peak PM_1 concentrations of 302 µg m^{-3} (P1) and 273 µg m^{-3} (P2), measured at UCD. (c) Time series of $PM_{2.5}$ mass concentration, measured with a tapered element oscillating microbalance (TEOM) at Rathmines station, ~3 km away from UCD, compared with the WHO recommended daily value (25 µg m^{-3}). Reprinted from Lin *et al.* (2018) with permission from Springer Nature. Copyright 2018. https://www.nature.com/natsustain/

during the entire measurement period. However, the mass ratios of PM_1 to $PM_{2.5}$ were close to 1 during both events, indicating the dominance of smaller particles during extreme pollution events. For the two events, a monomodal size distribution with modal diameter at 90 nm was observed for PM_1, present at concentrations 20–25 times higher than concentrations observed during non-event periods.

As shown in Figure 3.1b, carbonaceous aerosol (OA + BC) was the major component of PM_1, accounting for 89% of the total PM_1 measured during the pollution peak on 19 November and 88% in the pollution peak on 22 January, while inorganic components, sulfate (4%), nitrate (3–4%), ammonium (2%) and chloride (2%), accounted for only a minor part of the PM_1. During the pollution events, OA increased by 20–170 times compared with levels experienced during the previous days, while BC increased by 40–100 times.

Natural gas, electricity, oil, coal, peat and wood are the main fuel sources used for heating in Dublin (CSO, 2011), with natural gas and electricity being the most popular. However, neither natural gas nor electricity is expected to emit PM. In contrast, liquid (oil) and solid fuels (peat, coal and wood) are potential sources of PM_1 as a result of emissions from incomplete combustion. To evaluate their contributions, ME-2 source apportionment analysis, using the a-value approach, was utilised (see section 2.4). The reference profiles of peat, coal and wood were obtained from locally sourced fuels that were burned in a stove typical for Irish households, while that for oil was taken from the literature (see section 2.3). Based on a correlation with BC, ME-2 solutions with an a-value of 0–0.2 were selected as environmentally reasonable ones. All acceptable solutions were then averaged to obtain the mean concentration and contribution of each factor, while the variation between the solutions represented the uncertainty of the overall approach and ranged from 9% to 28%.

A five-factor (oil, peat, coal, wood and OOA) solution was deemed to be appropriate (Lin *et al.*, 2018), with the first four arising from primary emissions from residential heating and the OOA factor arising mainly from the regional transport of aged/oxidised aerosol. In this study, a moderate correlation of OOA with sulfate ($R^2 = 0.59$) indicates a contribution from long-range transport or secondary formation processes during the day; however, its simultaneous increase with primary factors during the evening–early night (from ~18:00 to 01:00–02:00) suggests that the condensation of semi-volatile species is also an important source of OOA during pollution events. The concentrations and contributions of each factor during the extreme pollution events are presented in Table 3.1.

The peat factor shows the highest concentrations, 101.7 $\mu g\,m^{-3}$ during the first event (P1) and 89.6 $\mu g\,m^{-3}$ during the second event (P2), and its contributions to OA mass were 46% and 55%, respectively. As shown in Figure 3.2, peat burning made the largest contribution to OA in the evening–early night (18:00–23:00 local time) and, in the case of the stagnant meteorological conditions during the second event (P2 in Figure 3.2), this dominance was persistent until the next morning (06:00). Such a significant contribution

Table 3.1. Average mass concentrations and relative contributions of OA factors for all environmentally reasonable model runs during extreme pollution events: P1 on 19 November 2016 and P2 on 22 January 2017

	P1 on 19 November 2016				P2 on 22 January 2017			
Factor	Mean ± SD ($\mu g\,m^{-3}$)	SD as proportion of mean (%)	Fraction of OA (%)	Fraction of PM_1 (%)	Mean ± SD ($\mu g\,m^{-3}$)	SD as proportion of mean (%)	Fraction of OA (%)	Fraction of PM_1 (%)
Oil	63.2 ± 5.9	9.4	28.6	20.9	38.4 ± 6.3	15.8	23.6	14.1
Peat	101.7 ± 12.5	12.3	46.0	33.6	89.6 ± 9.1	10.3	55.0	33.0
Coal	13.9 ± 1.33	9.6	6.3	4.6	3.4 ± 1.3	25.5	2.1	1.3
Wood	32.7 ± 7.7	23.6	14.8	10.8	27.2 ± 4.4	16.2	16.7	10.0
OOA	9.5 ± 1.1	11.4	4.3	3.1	4.2 ± 1.1	27.5	2.6	1.6

The standard deviation (SD) values are based on three selected ME-2 model runs.

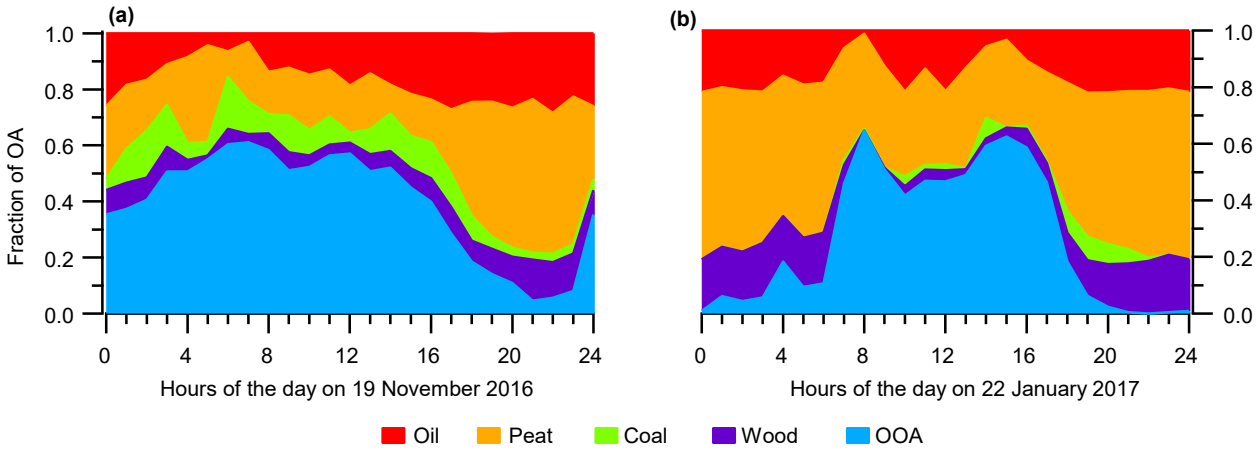

Figure 3.2. Contribution of organic factors, oil, peat, coal, wood and OOA, to total OA mass during extreme pollution events: (a) P1 on 19 November 2016 and (b) P2 on 22 January 2017. Reprinted from Lin *et al.* (2018) with permission from Springer Nature. Copyright 2018. https://www.nature.com/natsustain/

from peat burning is rather surprising because, to the best of our knowledge, no other countries have ever reported a similarly large contribution from peat burning. The other solid fuel factors, the coal factor (3.4–13.9 μg m^{-3}) and the wood factor (27.2–32.7 μg m^{-3}), contributed 2–6% and 15–17% to total OA (Table 3.1), respectively. Solid fuels (peat, coal and wood) contributed 67–74% of total OA in the evening–early night. Peat and wood collectively contributed 61–72% to total OA, which was greater than the sum of oil and coal (26–35%). During daytime, however, the concentrations and contributions of solid fuel factors decreased (to 0.5–3.4 μg m^{-3} and 36–59%, respectively; Figure 3.2), corresponding to a reduction in domestic heating activities. In contrast, OOA was the dominant OA factor (0.8–4.0 μg m^{-3}, 41–64%) during the day, which is most likely related to secondary production and/or aerosol ageing.

For this study, BC source apportionment, using the Ångström exponent (α) model, separated BC into fossil fuel (eBC_{FF}) and biomass burning (eBC_{BB}) sources, rather than traffic (eBC_{TR}) and solid fuel (eBC_{SF}) sources, because of the limited knowledge available at the time of the study. All following studies have deployed the latter separation. The combination of the OA peat and wood factors together with eBC_{BB} (peat possesses similar α values to wood and is attributed to the biomass factor in eBC source apportionment) contributed 52–70% of PM_1 mass during the pollution events. The fossil fuel factor (the sum of the oil and coal factors and eBC_{FF}) contributed 17–34% of PM_1 mass, about 1.5–4.1 times less than the biomass- and peat-related contribution. Inorganic aerosol species (sulfate, nitrate, ammonium and chloride) and OOA accounted for the remaining 13–14% of PM_1, but we could not apportion them into biomass or fossil fuels. More details can be found in a paper by the authors (Lin *et al.*, 2018).

3.2 Seasonality of Particulate Matter Sources Affecting Dublin's Residential Background

As for the extreme pollution events discussed above, on average, emissions from peat burning dominate the aerosol composition in winter in Dublin's residential background location (Figure 3.3a). For example, on average in winter, peat burning emissions contributed 35% of total OA mass, with an absolute concentration value of 1.5 μg m^{-3}, and were approximately seven times higher than in autumn (0.2 μg m^{-3}) and in spring (0.2 μg m^{-3}). Likewise, coal and wood emissions contributed more in winter (11% and 8% of total OA, respectively) than in either autumn or spring (less than 5% of total OA). OA arising from solid fuel burning was below the detection limit in summer. The contribution of HOA (8–15% of total OA) and its absolute concentrations (0.1–0.2 μg m^{-3}) were comparable in autumn, spring and summer, pointing to its predominantly traffic-related origin.

However, the HOA contribution and concentration were significantly higher in winter (approximately eight times that in other seasons), which is consistent with additional HOA coming from domestic heating

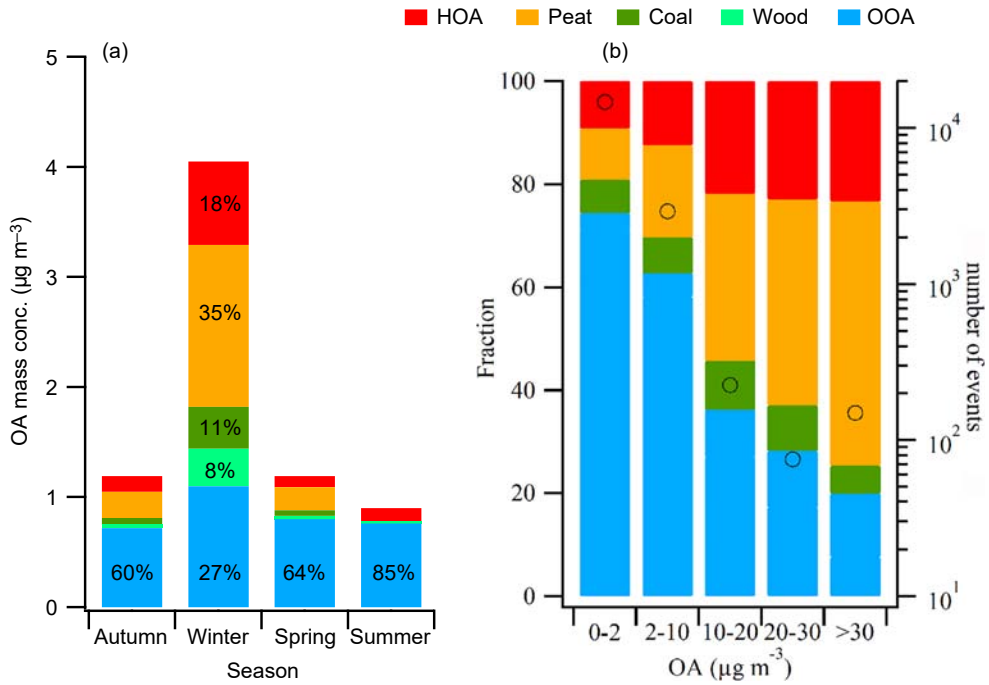

Figure 3.3. (a) Overview of the average contributions (%) of OA factors (i.e. HOA, peat, coal, wood and OOA) to total OA mass during autumn, winter, spring and summer; and (b) factors as fractions (%) of total OA mass as a function of OA mass category (left axis) and number of pollution events, displayed as open circles (right axis). Note that each data point corresponds to a 30-minute average.

activities such as oil burning, as discussed above. In addition, favourable conditions for primary semi-volatile HOA condensation, due to colder temperatures, higher pressure and higher relative humidity, in winter could also result in higher aerosol-phase HOA concentrations.

The contributions of peat, wood and oil burning (the last of which is displayed as HOA here) increased with increasing total OA mass concentrations (Figure 3.3b), confirming that residential heating was the main cause of extreme air pollution events, with solid fuel burning contributing ~70% to total PM.

Combining the above information with BC source apportionment data provides an overall picture of the contributions of various source to PM_1, as presented in Figure 3.4. On average, residential heating emissions dominate aerosol concentrations during the winter, with peat and wood combined contributing 47% to total PM_1, followed by coal/oil (contributing 19%), while regional, ammonium nitrate and traffic sources contribute 16%, 12% and 6%, respectively. During the summer, contributions from heating emissions are minimal and most PM_1 (70%) is accounted for by the regional/long-range sources. Concentrations of PM_1 from traffic emissions remain similar throughout the seasons (~0.5 µg m^{-3}), but their relative contribution varies from 6% in the winter to 23% in the summer.

3.3 Differences in Sources Affecting Air Quality at Residential Background and Kerbside Locations in Dublin

To better assess the effects of traffic emissions on local air quality, mass concentrations, chemical composition and sources of PM_1 were evaluated simultaneously at the urban kerbside location (TCD) and the residential site (UCD) in Dublin from September to November 2018. Figure 3.5 shows the time series of PM_1 components (i.e. OM, sulfate, nitrate, ammonium, chloride and BC) at the kerbside location at TCD and the residential site at UCD, as well as showing the mass concentrations of $PM_{2.5}$ at the EPA's Rathmines station.

The two sites show distinct pollution patterns in the period 11–15 September (marked as E1 in Figures 3.5 and 3.6), before residential heating use begins to increase, with the TCD kerbside location affected by traffic and experiencing typical morning

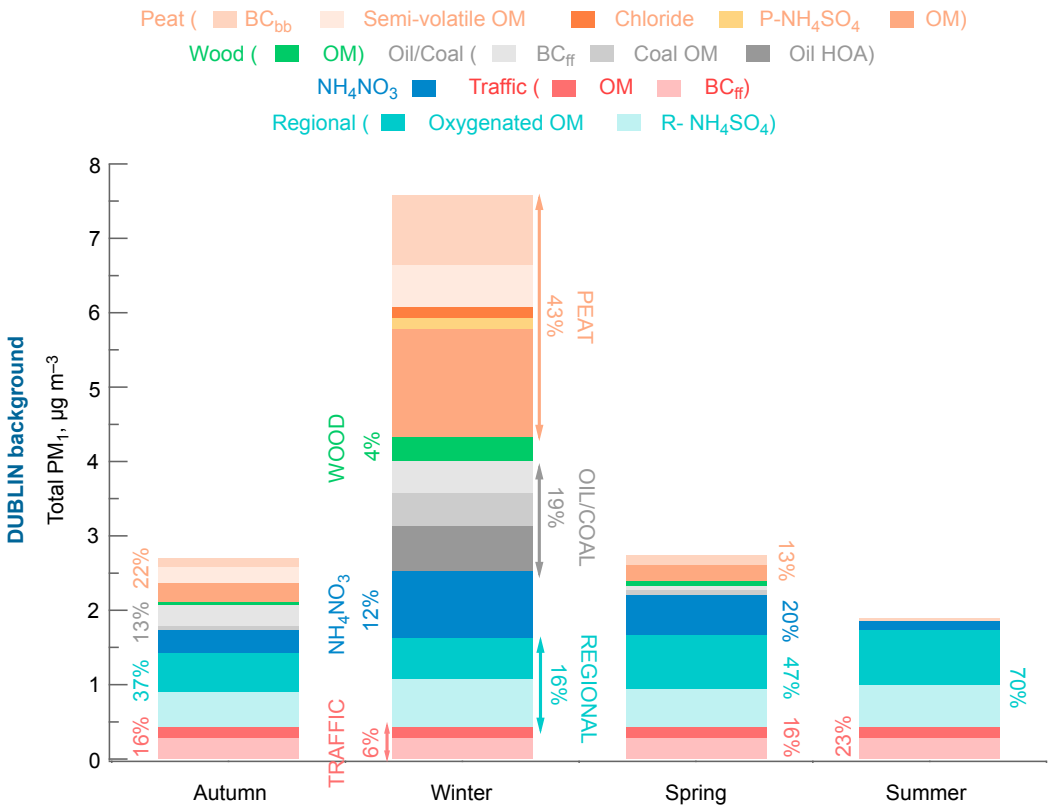

Figure 3.4. Seasonal variation in source contributions to PM_1. The colours and shades represent distinct sources. Orange: peat, comprising "BC_{bb}", BC from biomass burning as apportioned by the AE-33 source apportionment method and mainly representing emissions from peat in this case; "semi-volatile OM", oxygenated OM that ACSM source apportionment attributed to secondary/primary peat emissions; "chloride", also from peat in this case; "P-NH_4SO_4", ammonium sulfate attributed to peat emissions; and "OM", a primary OM factor also attributed to peat burning by the ACSM-PMF. Green: wood, comprising "OM", a wood factor derived from ACSM source apportionment. Grey: oil and coal combined, comprising "BC_{ff}", BC assigned to fossil fuels by the AE-33 source apportionment method; "coal OM", OM coming from coal; "oil HOA", a primary organic factor assigned to oil burning. Blue: ammonium nitrate (NH_4NO_3), which was not attributed to any particular sources because of a lack of reliable methods available; it can come from local sources (traffic) via secondary production, primary peat emissions or regional long-range transport. Red: traffic, comprising "OM", a primary OM factor attributed to car emissions; "BC_{ff}", fossil fuel BC attributed to traffic. Cyan: regional sources, comprising "oxygenated OM", regional oxygenated OM; and "R-NH_4SO_4", regional ammonium sulfate.

and evening rush hour peaks at 09:00 and 18:00, respectively (Figure 3.6c), and the residential UCD site showing lower pollution levels and flat diurnal trends (Figure 3.6d). On the other hand, from 28 October to 1 November (E2), when residential heating use increases, PM concentrations increased significantly at both sites, as well as at the Rathmines location (Figure 3.5a–c), with simultaneous pollution peaks occurring in the evening–early night (at ~22:00; Figure 3.6e and f).

At the kerbside location, the overall average PM_1 concentration was 10.4 µg m^{-3}, with a dominant contribution from BC (Figure 3.7a), accounting for 54% of total PM_1, followed by OA (36%). The remainder was composed of sulfate (4%), nitrate (3%), ammonium (2%) and chloride (1%). However, the PM_1 concentration during E1 was half of that seen during E2, with concentrations of 9.9 µg m^{-3} and 19.4 µg m^{-3}, respectively. In addition, the contribution of OM was lower during E1 than during E2 (31% and 41%, respectively), while the BC fraction was higher (63% and 43%) (Figure 3.7c and e).

At the residential site, however, the overall average PM_1 concentration was 5.2 µg m^{-3} (Figure 3.7b), half

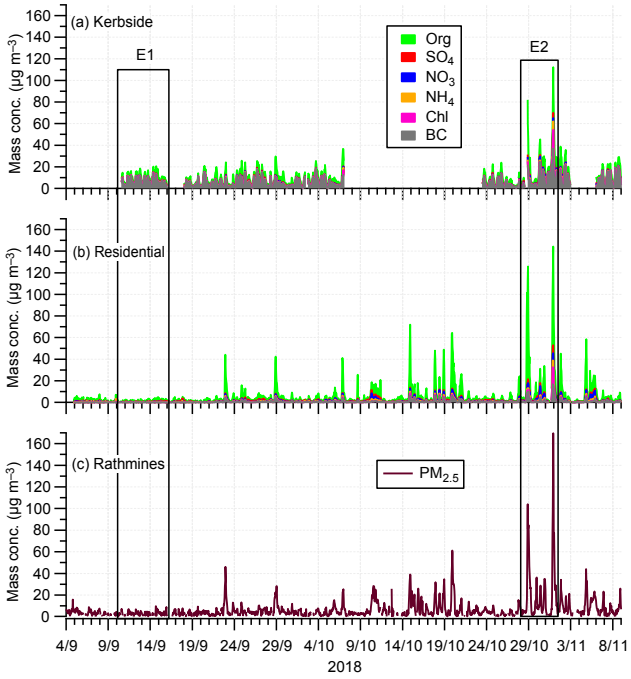

Figure 3.5. (a) Kerbside location (TCD) and (b) urban residential site (UCD) time series of PM_1 components – organics (org), sulfate (SO_4^{2-}), nitrate (NO_3^-), ammonium (NH_4^+), chloride (Chl) and BC; and (c) $PM_{2.5}$ at the EPA's Rathmines monitoring station. E1 and E2 represent periods of the year when the level of residential heating use is high and low, respectively, and are marked for further discussion. Data for the kerbside location covering 8–19 October were missing as a result of the instrument overheating. Reproduced from Lin *et al.* (2020) under the terms and conditions of the Creative Commons Attribution license CC-BY-4.0 (https://creativecommons.org/licenses/by/4.0/).

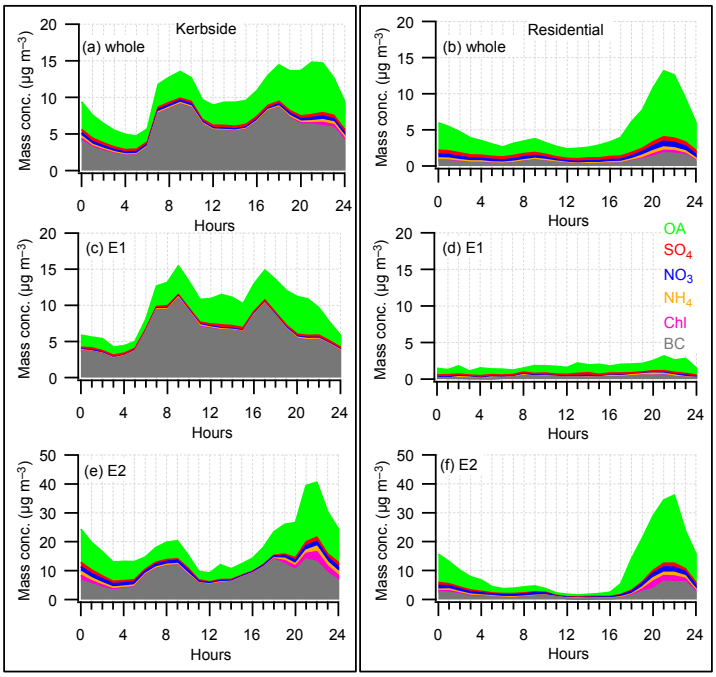

Figure 3.6. Diurnal pattern of PM_1 components – organics (OAA), sulfate (SO_4^{2-}), nitrate (NO_3^-), ammonium (NH_4^+), chloride (Chl) and BC – during the entire period (a, b), E1 (c, d) and E2 (e, f) at the kerbside location (left panel) and residential site (right panel). Reproduced from Lin *et al.* (2020) under the terms and conditions of the Creative Commons Attribution license CC-BY-4.0 (https://creativecommons.org/licenses/by/4.0/).

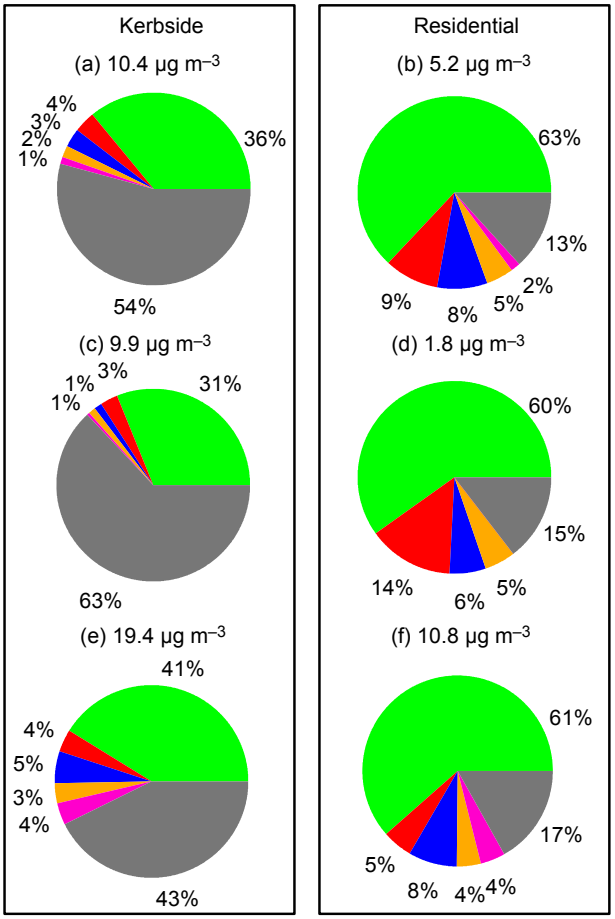

Figure 3.7. Relative fractions of PM_1 components – OA, sulfate (SO_4^{2-}), nitrate (NO_3^-), ammonium (NH_4^+), chloride (Chl) and BC – during the entire period (September to November 2018) (a, b), E1 (c, d) and E2 (e, f) at the kerbside location (left panel) and residential site (right panel). The values above each pie chart are the average PM_1 concentrations. Reproduced from Lin *et al.* (2020) under the terms and conditions of the Creative Commons Attribution license CC-BY-4.0 (https://creativecommons.org/licenses/by/4.0/).

of that at the kerbside location, which was mainly due to low concentrations (1.8 µg m^{-3}) before the heating season (Figure 3.7d). However, the PM concentration increased significantly (~6 times) after the start of the heating season (to 10.8 µg m^{-3}) (Figure 3.7f). In terms of chemical composition, OA was the most dominant compound in PM_1 in the residential Dublin area, accounting, on average, for 60–63% of total PM_1, followed by BC (13–17%). The rest was sulfate (9–14%), nitrate (6–8%), ammonium (4–5%) and chloride (<1–4%).

OA source apportionment separated PM_1 into six factors (HOA, peat, coal, wood, COA and OOA) at the kerbside location and five factors (HOA, peat, coal, wood and OOA) at the residential site (Figure 3.8). HOA is the POA factor usually associated with traffic emissions. During the morning rush hour (09:00 local time), HOA accounted for 35–42% (or 1.2–2.3 µg m^{-3}) of total OA at the kerbside site, while its contribution to OA was much lower (15–29% or 0.1–1.0 µg m^{-3}) at the residential site. COA identified at the kerbside site was due to emissions from nearby restaurants, with COA exhibiting a diurnal pattern of lunch and evening–early night peaks (Figure 3.8). The contribution from peat burning was found to increase in the early evening, with the concentration peaking at around 22:00 at both sites.

The overall contributions of the OA factors during the entire measurement time and during the E1 and E2 periods are shown in Figure 3.9. Although directly adjacent to a street with heavy traffic, HOA, or the traffic contribution, amounted to only 19–21% at the kerbside location (Figure 3.9a, c and e). However, while the single highest contribution to OA came from secondary and aged OOA (30–37%), the primary sources (HOA, COA and solid fuel burning emissions) combined dominated (63–70%) at the kerbside location (Figure 3.9a, c and e). COA, traffic and coal contributions were similar for both the E1 and E2 periods (18–22%, 20–21% and 11–8%, respectively), but contributions from peat and wood were higher for the E2 period (19% and 5%, respectively) than for the E1 period (9% and 2%, respectively).

It is worth noting that, as mentioned in section 3.1, the origin of OOA is ambiguous. The most likely and common source is the regional transport of aged/oxidised aerosol; however, its simultaneous increase with primary factors, during the evening–early night, points to the condensation of semi-volatile species also being important.

The OOA factor was as important if not more important at the residential site (41–61% of total OA), pointing to an important influence of secondary aerosol and long-range transport during the day and the E1 period, while, during the E2 period, OA was dominated by sources arising from the condensation of semi-volatile species, as evidenced by higher OOA concentrations during the late evening (Figure 3.8e). Nevertheless, primary factors accounted for up to 59% of OA during

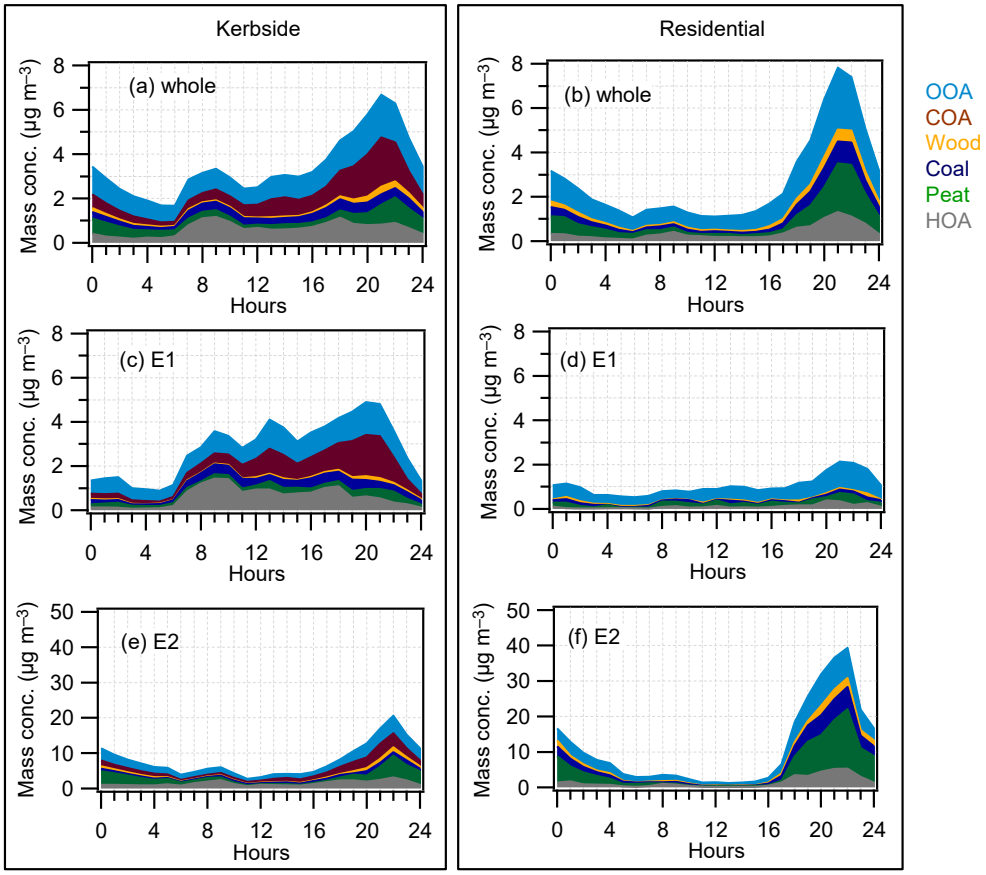

Figure 3.8. Diurnal pattern of HOA, peat, coal, wood, COA and OOA factors during the entire period (September to November 2018) (a, b), E1 (c, d) and E2 (e, f) at the kerbside location (left panel) and residential site (right panel). Reproduced from Lin *et al.* (2020) under the terms and conditions of the Creative Commons Attribution license CC-BY-4.0 (https://creativecommons.org/licenses/by/4.0/).

E2, with peat burning being the most important POA factor, accounting for 16–25%, followed by HOA (9–14%), coal (9–14%) and wood (5–7%) (Figure 3.9). Moreover, the contributions of primary factors at the residential site were even higher for the colder winter months, as shown in section 3.1; however, the period in question here did not include calendar winter and, thus, did not include extreme pollution episodes.

Source apportionment of black carbon: black carbon contributions were attributed to traffic (BC_{TR}) and solid fuel burning (BC_{SF}), as described in section 2.7.1. The primary PM emitted by traffic is mainly composed of BC_{TR} and HOA; therefore, the diurnal pattern of BC_{TR} is like that of HOA (Figure 3.10, left panel), while the BC_{SF} diurnal trend is comparable to that of solid fuel (the sum of peat, coal and wood factors) (Figure 3.10, right panel). During the morning rush hour, the HOA-to-BC_{TR} ratio was 0.21, which is consistent with the ratios typical of a diesel-dominated fleet (DeWitt *et al.*, 2015). In contrast, the solid fuel burning emission concentrations went up in the evening–early night and peaked at ~22:00 (Figure 3.10, right panel), corresponding to domestic heating activities. Finally, in contrast to traffic, emissions from solid fuel burning have a higher OA fraction than BC fraction, resulting in an $OA_{SOLID\ FUEL}$-to-BC_{SF} ratio of ~2.3 during the evening–early night peak, which is comparable to the residential site ratio discussed in section 3.1.

Overall sources of PM_1: BC and OA are the major components of PM_1; therefore, grouping their source apportionment results gives an overall distribution of PM_1 sources (Figure 3.11). As discussed above, BC_{TR} and HOA can come from both traffic and oil burning, so, to resolve this, daytime BC_{TR} and HOA were combined to determine the contribution of traffic sources, while evening–early night BC_{TR} and HOA, coinciding with solid fuel burning activities, were

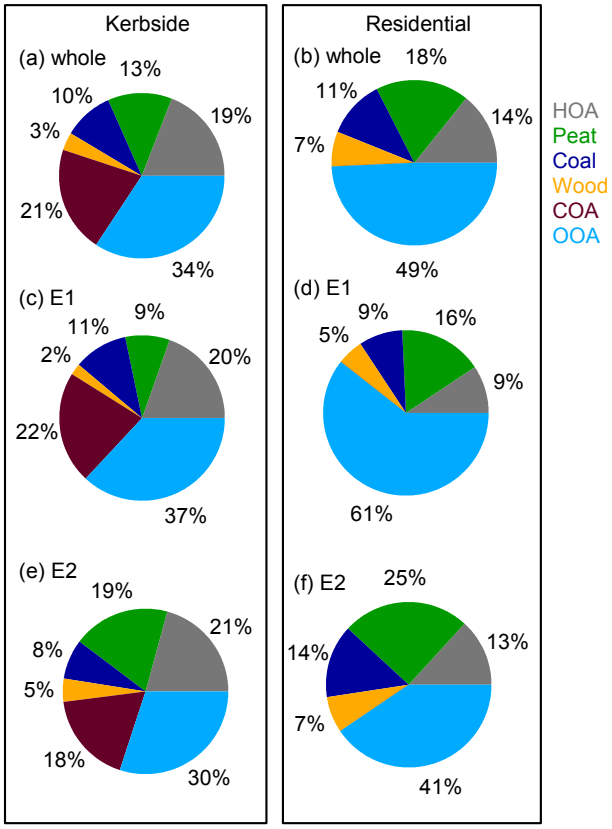

Figure 3.9. Relative contribution of HOA, peat, coal, wood, COA and OOA during the entire period (September to November 2018) (a, b), E1 (c, d) and E2 (e, f) at the kerbside location (left panel) and residential site (right panel). Reproduced from Lin *et al.* (2020) under the terms and conditions of the Creative Commons Attribution license CC-BY-4.0 (https://creativecommons.org/licenses/by/4.0/).

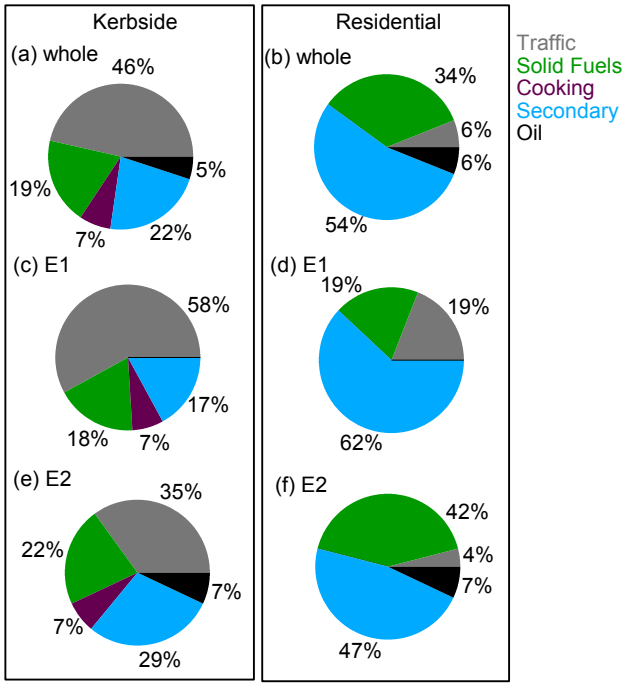

Figure 3.11. Source apportionment of PM_1 into traffic ($HOA_{TR} + BC_{TR}$), solid fuels (the sum of peat, coal, wood and BC_{SF}), cooking, secondary and oil ($HOA_{OIL} + BC_{OIL}$) sources during the entire period (September to November 2018) (a, b), E1 (c, d) and E2 (e, f) at the kerbside location (left panel) and residential site (right panel). Secondary sources include OOA, sulfate, nitrate and ammonium, which cannot be exclusively included as traffic or heating sources. Reproduced from Lin *et al.* (2020) under the terms and conditions of the Creative Commons Attribution license CC-BY-4.0 (https://creativecommons.org/licenses/by/4.0/).

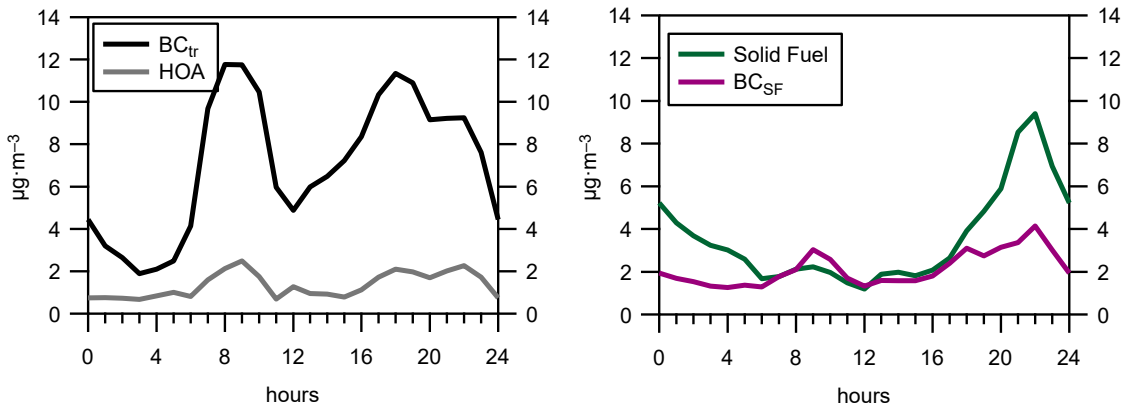

Figure 3.10. The diurnal cycle of BC from traffic (BC_{tr}) and HOA (left); and the solid fuel OA factor and BC from solid fuel burning (BC_{SF}) (right) at the kerbside location during the period E2. Reproduced from Lin *et al.* (2020) under the terms and conditions of the Creative Commons Attribution license CC-BY-4.0 (https://creativecommons.org/licenses/by/4.0/).

used to determine the contribution of oil burning. At the kerbside location, traffic sources, on average, accounted for 35–58% of the total PM_1 and oil burning for 5–7%. On the other hand, while contribution of oil burning at the residential site was similar to that at the kerbside location (6–7%), the traffic contribution was significantly lower at the residential site (4–19%). Adding BC_{SF} to combined solid fuel factors (peat, wood and coal) resulted in 19–42% contribution from solid fuel burning at the residential site and 18–22% at the kerbside location. Cooking accounted for ~7% of PM_1 at the kerbside location, but was not identified in the residential background site. Secondary sources, including OOA, sulfate, nitrate and ammonium, which cannot be exclusively included as traffic or heating sources, accounted for 17–29% of PM_1 in TCD and 47–62% at UCD over the September–November 2018 period.

For more details of the sources contributing to PM air pollution at the kerbside and residential sites, see the study by the authors (Lin *et al.*, 2020).

3.4 Overview of Winter Particulate Matter Sources in Ireland

In addition to Dublin, regional background (Carnsore Point) and coastal (Mace Head) sites were selected for chemical characterisation and source apportionment. As expected, overall concentrations in Carnsore Point and Mace Head were lower than those in Dublin (Figure 3.12); however, similarly to Dublin, carbonaceous compounds dominated the total PM_1 composition (accounting for >50%). On average, PM in both regional and coastal sites was dominated by secondary aerosol including OOA, nitrate, sulfate and ammonium, demonstrating the important role of regional transport. Nevertheless, solid fuel burning contributed significantly during cold stagnant periods, with peat contributing 32% and 40% of PM during these periods at the Mace Head and Carnsore Point sites, respectively (Table 2 in Lin *et al.*, 2019b).

Overall in winter, local emissions were found to contribute 26% and 41% of total PM at Carnsore

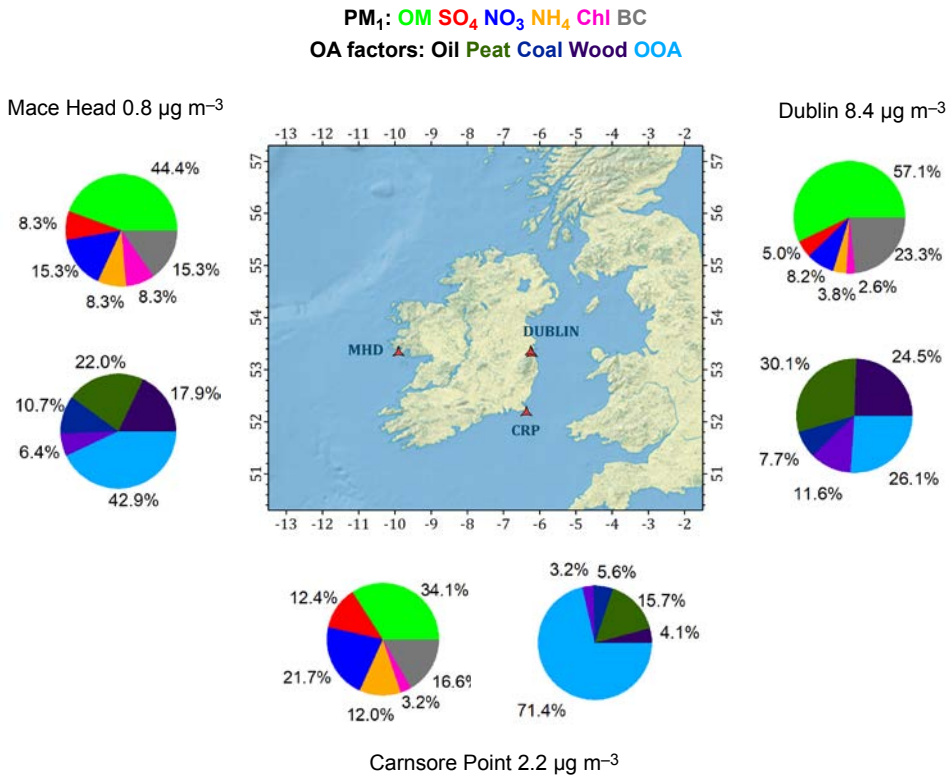

Figure 3.12. Average mass concentrations and composition of PM_1 and OA factors in Dublin (right), Carnsore Point (bottom) and Mace Head (left) in winter. Reproduced from Lin *et al.* (2019b) under the terms and conditions of the Creative Commons Attribution license CC-BY-4.0 (https://creativecommons.org/licenses/by/4.0/).

Point and Mace Head, respectively, compared with the 74% and 59% contributions of secondary inorganic aerosol, including OOA (marker for regional secondary production and long-range transport), at these sites (Figure 3.12). Based on a study in Galway in the summer (Lin *et al*., 2019a), it is expected that contributions from local sources are even smaller in seasons other than winter. Several pollution spikes have occurred at Carnsore Point and Mace Head in winter (Figure 3.13b and d, respectively). However, these were observed under specific low wind speed and wind direction conditions, pointing to sources from nearby villages (Figure 3.14b and d, respectively). In contrast, sulfate and OOA concentrations at Carnsore Point originated from a south-easterly direction and concentrations at Mace Head from an easterly direction with a wind speed of >5 m s^{-1}, indicating regional and long-range transport of sulfate and OAA.

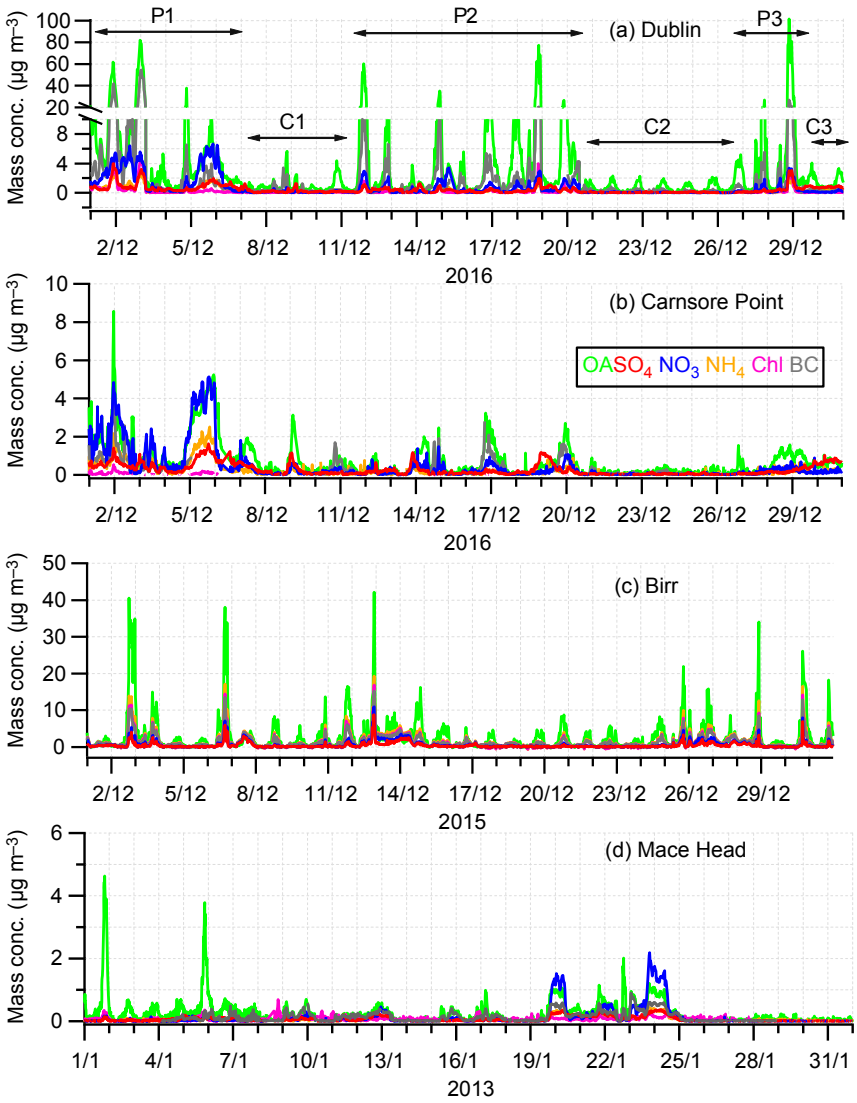

Figure 3.13. Time series of OA, sulfate (SO_4^{2-}), nitrate (NO_3^-), ammonium (NH_4^+), chloride (Chl) and BC at (a) the urban background site in Dublin; (b) the rural site at Carnsore Point; (c) a midland town site (in Birr); and (d) the coastal site at Mace Head. The measurements at the Dublin and Carnsore Point sites were conducted simultaneously in December 2016. The campaign in Birr was carried out in December 2015 and in Mace Head in January 2013. BC, measured by AE-33 with 1-minute resolution or by Multi Angle Absorption Photometer (MAAP) with 5-minute resolution, was averaged to 30 minutes to match the time stamp of the ACSM. Pollution periods (P1–P3) and clean periods (C1–C3) in Dublin are marked. Reproduced from Lin *et al.* (2019b) under the terms and conditions of the Creative Commons Attribution license CC-BY-4.0 (https://creativecommons.org/licenses/by/4.0/).

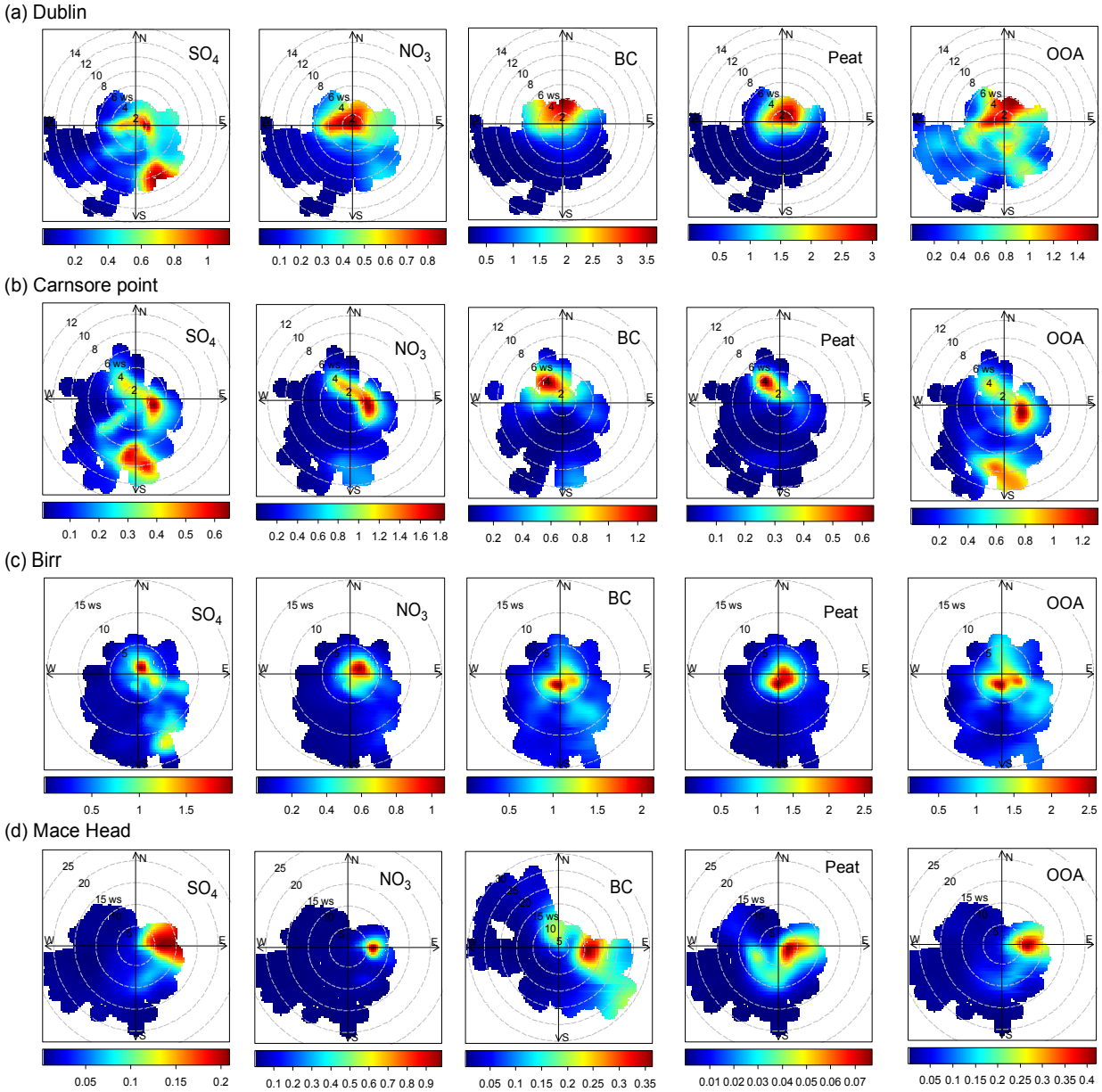

Figure 3.14. Polar plots of sulfate (SO_4^{2-}), nitrate (NO_3^-), BC, peat and OOA factors in (a) Dublin, (b) Carnsore Point, (c) Birr and (d) Mace Head. The plots are colour-coded based on the concentration of each species in µg m^{-3}. Wind rose plots were generated with OpenAir software in R (Carslaw and Ropkins, 2012). Reproduced from Lin *et al.* (2019b) under the terms and conditions of the Creative Commons Attribution license CC-BY-4.0 (https://creativecommons.org/licenses/by/4.0/).

See the study by the authors (Lin *et al.*, 2019b) for more details.

3.5 Quantification of Transboundary Contribution by Quasi-Lagrangian Method

To quantify the contribution of aerosol sources on different spatial scales (urban, regional, long-range transport, etc.), connecting flow condition cases were analysed and concentrations of the main aerosol components (Org, SO_4^{2-}, NO_3^-, NH_4^+ and BC) between the upwind and downwind stations were compared.

Analysing the flow connecting Mace Head and Carnsore Point (MH–CP) provides an estimate of the aerosol sources located over rural Ireland (along the ideal route connecting Mace Head and Carnsore Point). Measurements performed under westerly conditions at Mace Head are representative of the

North Atlantic background; thus, the difference in concentrations between Mace Head and Carnsore Point can be attributed to additional sources and/or to removal processes along the route. Higher concentrations were systematically observed at Carnsore Point than at Mace Head, which, as expected, points to a net input of aerosol particles from sources located over rural Ireland and its superposition on to the North Atlantic background (Figure 3.15). For example, in the autumn/winter, BC, Org and NO_3^- concentrations along the MH–CP route increased by an order of magnitude, while a lower effect was observed for SO_4^{2-} and NH_4^+ (an approximately twofold increase). In the spring/summer, lower contributions from Irish sources were observed for all the aerosol species, except NO_3^-, which remained quite similar to the contribution in the autumn/winter, pointing to a contribution from traffic rather than biomass or residential solid fuel burning (which is strongly seasonal). In contrast, the reduction in the rural contribution of Org and BC in the spring/summer points to a contribution from residential solid fuel

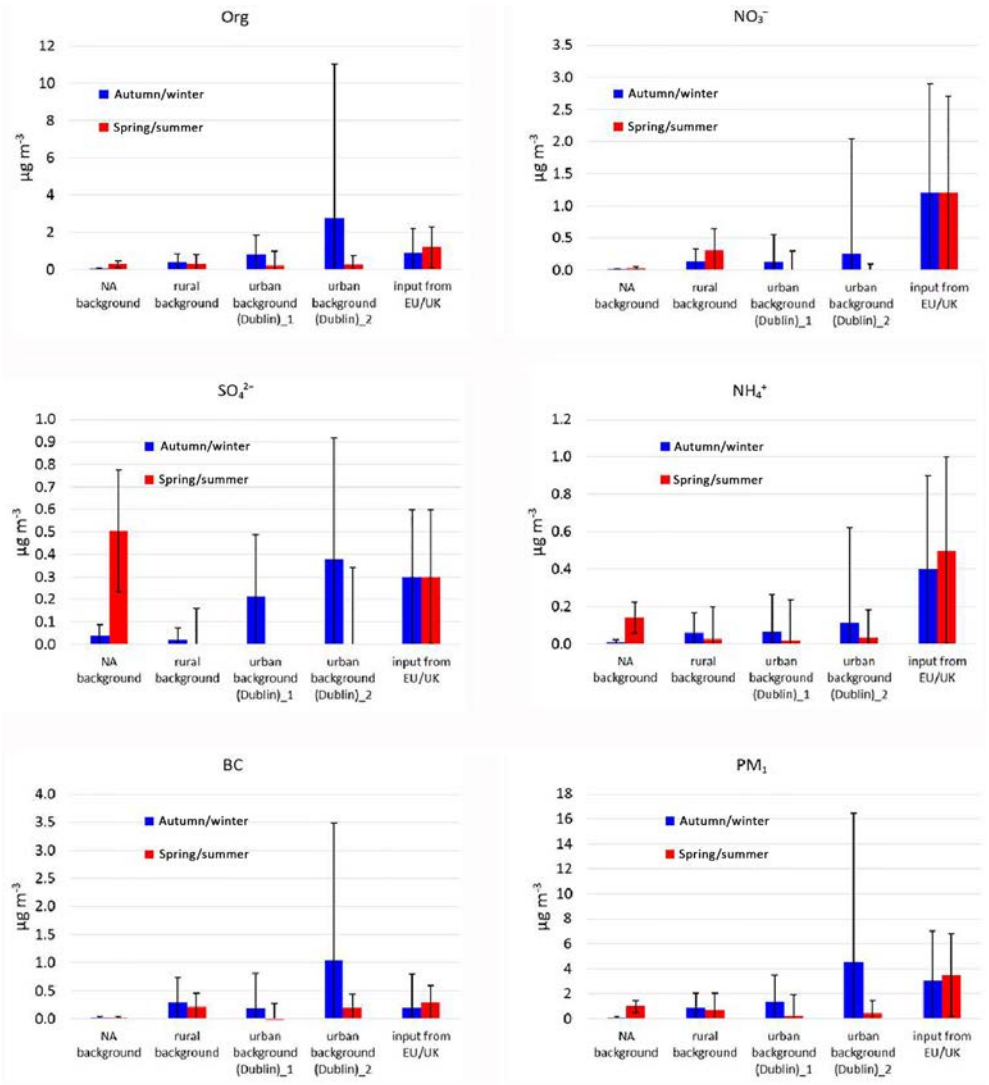

Figure 3.15. Tentative estimates of the main inputs contributing to air quality in Ireland. The North Atlantic background was derived from the MH–CP and MH–Dub connecting flow cases. The rural background concentrations were derived from the MH–CP connecting flow cases (differences between concentrations measured at Carnsore Point and Mace Head). The (Dublin)_1 urban background was estimated from the MH–Dub connecting flow cases by subtracting the rural contribution derived from the MH–CP cases. The (Dublin)_2 urban background was derived from the CP–Dub connecting flow cases. The contributions made by transboundary aerosol sources (from the EU and the UK) were estimated from a cluster analysis study performed on the Carnsore Point data.

burning during the autumn/winter. Interestingly, SO_4^{2-} levels decline on going from Mace Head to Carnsore Point in spring/summer, suggesting that Ireland may be a sink for biogenic SO_4^{2-} aerosol produced from natural oceanic sources.

Analysing the flow connecting Mace Head and Dublin (MH–Dub) provides an estimate of the combined contribution of aerosol sources located both over rural Ireland and within the Dublin urban area. A significant increase in concentrations was observed for all the aerosol components on going from Mace Head to Dublin in the autumn/winter period. On average, OM concentrations increased by ~80 times, NO_3^- by ~40 times and BC by ~20 times. The increase in concentration on going from Mace Head to Dublin was lower during the spring/summer, with OM showing the highest difference between autumn/winter and spring/summer conditions. This again suggests that residential solid fuel burning makes a significant contribution in the Dublin urban area. Similar behaviour can be observed for BC, while NO_3^- once more shows a similar contribution in both seasons, confirming that traffic is likely to be a more important source than residential solid fuel burning. SO_4^{2-} shows similar behaviour in the spring/summer as in the MH–CP case discussed above.

Analysing the flow connecting Carnsore Point to Dublin (CP–Dub) provides an estimate of the urban background contribution to air quality within the Dublin area, virtually isolated from the rural background contribution (measured at Carnsore Point). The source contribution pattern is similar to those previously discussed. While the Dublin urban area is a strong source of OM during the cold months, this contribution is significantly lower in the spring/summer, pointing again to strong seasonal variation due to domestic heating. The same applies to BC, which is co-emitted with OM during solid fuel combustion. In autumn/winter, NO_3^- concentrations in southerly flows (flows connecting Carnsore Point with Dublin) were several times higher (~4) for both Dublin and Carnsore Point than in the westerly flows discussed above, with only a modest increase due to the urban background, showing the significant contribution made by long-range transport in winter.

However, the limited number of connecting flow cases and, particularly, the disposition of the stations restricted the ability of the quasi-Lagrangian approach to quantify transboundary aerosol contributions from the EU and the UK in Ireland. For this reason, a cluster analysis of the back-trajectories reaching Carnsore Point during the 1-year measurement period was performed. Back-trajectories were grouped through a centroid-based cluster analysis technique (*k*-means clustering) to elucidate the main circulation patterns reaching Carnsore Point.

Tentative estimates of North Atlantic background, Irish rural background and Dublin urban background concentrations and transboundary inputs from the EU and the UK were derived based on the above quasi-Lagrangian study and the cluster analysis results for each of the main aerosol components. The estimate of the North Atlantic background was achieved by considering the average concentrations measured at Mace Head in the connecting flow cases MH–CP and MH–Dub. The rural background concentrations were derived from the results of the MH–CP connecting flow cases (differences between concentrations measured at Carnsore Point and Mace Head). Two estimates are provided for the Dublin area urban background. The first was derived by subtracting the rural contribution derived from the MH–CP cases from the "urban + rural" contributions obtained from the MH–Dub connecting flow cases. The second estimate was produced from the CP–Dub connecting flow cases by subtracting Carnsore Point concentrations from Dublin concentrations. Figure 3.15 shows that the two estimates are not always consistent within each other, reflecting difficulties in measuring urban background concentrations in an environment rich in aerosol sources. Finally, the contributions of transboundary aerosol sources from outside Ireland were derived from the cluster analysis study performed on the Carnsore Point data. It is worth highlighting that the results presented in Figure 3.15 are estimates based on assumptions that are generally sound but could lose their validity under specific conditions. Longer observation periods are needed for meaningful statistical characterisation. Therefore, the source attributions of the main aerosol components presented must be considered with caution.

In summary, quasi-Lagrangian and cluster analyses show the importance of OA sources located over the Irish territory and within the Dublin urban area during the autumn/winter. This demonstrates the important contribution of domestic heating. In the spring/summer, the contribution of organic sources is more evenly distributed between the Dublin area and rural

Ireland, suggesting that traffic and photochemistry are the main OA sources in the spring/summer. The contribution of transboundary sources to OA seems to be more important in the warm period than in the autumn/winter. A similar pattern can be observed for BC. Transboundary inputs appear to be very important for the ammonium nitrate burden over Ireland, while, for sulfate, the role of biogenic sources from the ocean is evident during the spring/summer.

3.6 Modelling Air Quality in Ireland

3.6.1 Sensitivity studies

An offline sensitivity test was performed to investigate the ability of the WRF-Chem model to reproduce heavy pollution events recorded by the ACSM network in Dublin in winter 2017/2018. The performance of WRF in terms of forecasting meteorology has been well documented (Powers *et al*., 2017). To assess the ability of the model to simulate nocturnal pollution events in Dublin, we looked at the various planetary boundary layer (PBL) schemes available within the model and compared the results with light detection and ranging (Lidar) measurements (Figure 3.16). It is noted that the most significant pollution event occurred during stagnant conditions (very low nocturnal PBL) between 22 and 23 January 2017, so the scheme selected for the model should be capable of reproducing this very low PBL. The Yonsei University (YSU) PBL scheme performed most favourably when compared with Lidar measurements, so this was the scheme employed in the simulations.

In addition to meteorology, chemical aerosol representation and reactions are very important for successfully modelling air pollution concentrations. The chemical mechanism model used was the Common Representative Intermediates Mechanism (CRIMECH) scheme for VOC degradation (Jenkin *et al*., 2008). This is an explicitly detailed chemical mechanism scheme, considering 1183 reactions and 434 chemical species, and is deemed to be appropriate for this purpose. Figure 3.17 shows that, even using this state-of-the-art chemical scheme (CRIMECH) and an appropriate PBL scheme, but standard emissions, the

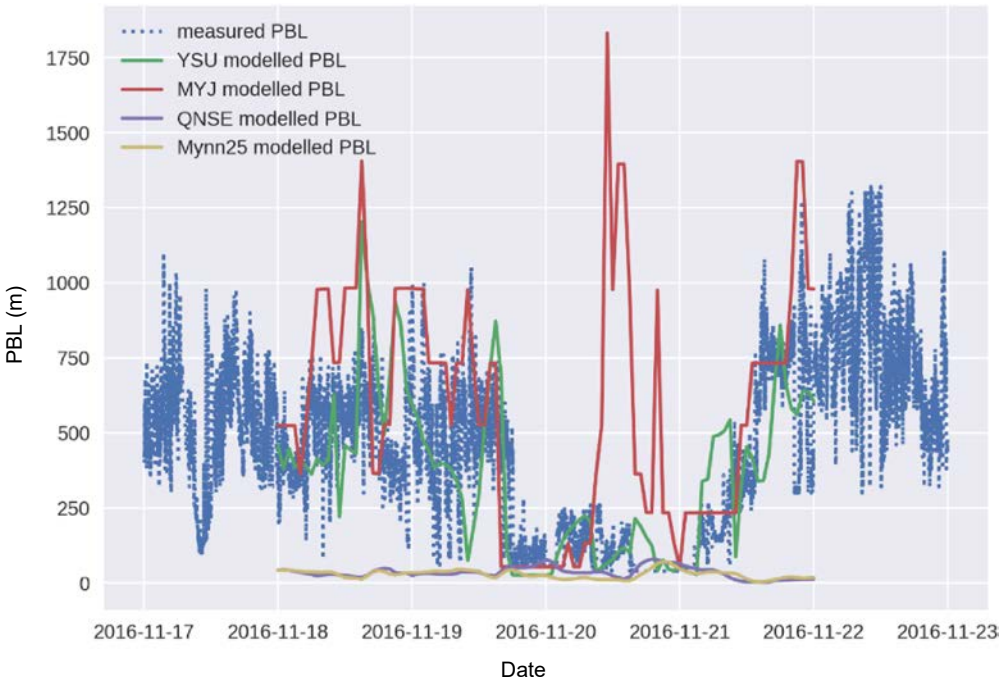

Figure 3.16. WRF-Chem-modelled and Lidar-measured PBL schemes in Dublin, November 2016. MYJ, Mellor Yamada Janjic; Mynn25, Mellor-Yamada Nakanishi and Niino Level 2.5; QNSE, Quasi-Normal Scale Elimination; YSU, Yonsei University. The models were developed by Mellor and Yamada (1982), Nakanishi and Niino (2004), Sukoriansky *et al*. (2005), Hong *et al*. (2006) and Hong (2010). Figure reproduced from Hu *et al*. (2019) under the terms and conditions of the Creative Commons Attribution 3.0 Unported License (http://creativecommons.org/licenses/by/3.0/).

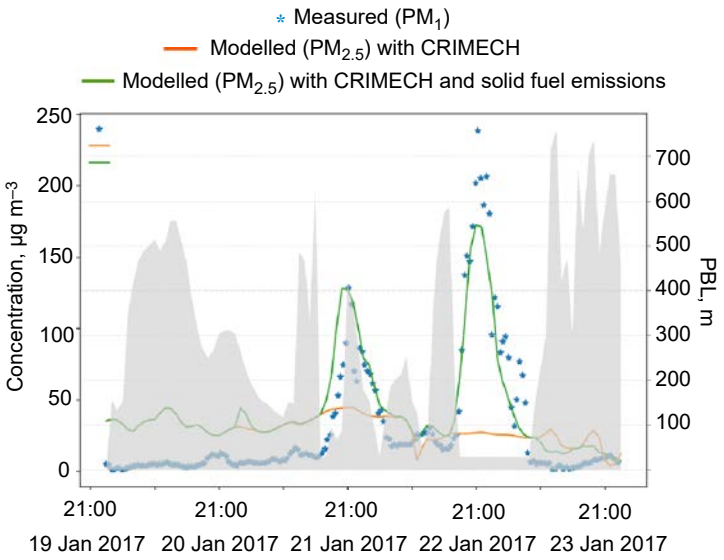

Figure 3.17. PM measured using an ACSM and modelled by WRF-Chem using the CRIMECH scheme, as well as a PBL scheme (grey background), January 2017, Dublin.

pollution event could not be reproduced by the model. For example, modelled $PM_{2.5}$ concentrations were still significantly below the measured values and did not show any evening–early night increases, as indicated by the observations.

Emission inventories were, thus, enhanced using additional emission sources to represent solid fuel burning as a secondary heating source in the residential sector, as outlined in section 2.6. The emissions showed diurnal variation, with a profile that was assumed to be characteristic of residential fuel burning (section 2.6). Using the enhanced emission inventory, the pollution events were successfully simulated using the WRF-Chem model, which now captured the nocturnal pollution episodes on 21 and 22 January (Figure 3.17). Modelled concentrations were still slightly lower than the measured ones due to the wider area represented by the model grid cell (17 km × 28 km), at a resolution of 0.25° × 0.25°, which also included low-emission areas (parks, etc.), as opposed to the point measurements used for observations.

3.6.2 Integration into StreamAIR

The emission pre-processing technique, as outlined in section 3.6.1, was integrated into the operational state-of-the-art meteorology and air quality forecasting system StreamAIR. To maintain computational efficiency, the model was set to run with the RADM2 chemical mechanism (Stockwell *et al*., 1990) and the Goddard Chemistry Aerosol Radiation and Transport (GOCART) (Chin *et al*., 2000) bulk aerosol module. Work is ongoing on a sensitivity test to elucidate the optimal set-up for operational air quality forecasting in Europe and Ireland (manuscript in preparation). A sample of the StreamAIR web app is shown in Figure 3.18 (available online: http://streamair.nuigalway.ie/).

The results from the StreamAIR system with enhanced emissions, to account for residential solid fuel burning, are shown in Figure 3.19. The model forecast predicts the time and duration of the pollution events. Similar to the sensitivity test, discrepancies between the magnitude of modelled and measured PM peaks can be attributed to the difference between point measurement and the grid-cell average of the model, as discussed above. Although the results are very encouraging, the system would benefit from comprehensive detailed emission inventories at hourly temporal resolution, accurately portraying characteristics of domestic solid fuel burning in terms of the distribution of fuel types, the duration of burning and the seasonality of solid fuel burning. Without such a dataset, the nationwide forecasting of air pollution events is impossible.

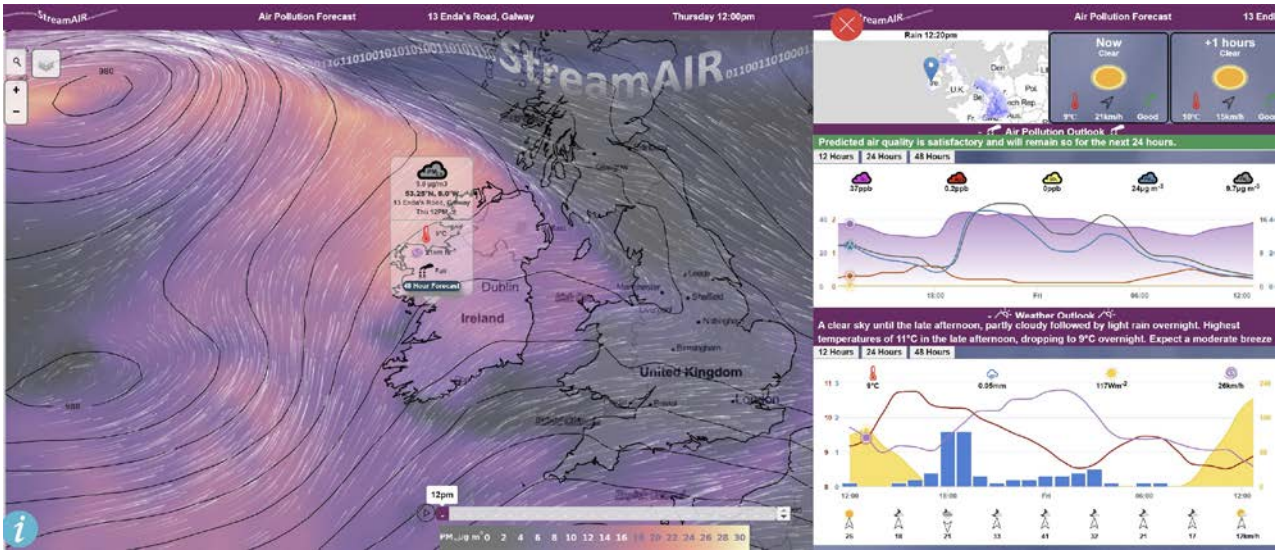

Figure 3.18. Screenshot from the web app StreamAIR. The map (left) shows simulated $PM_{2.5}$ and the plots (right) show 48-hour forecasts for Dublin with meteorological and air quality components.

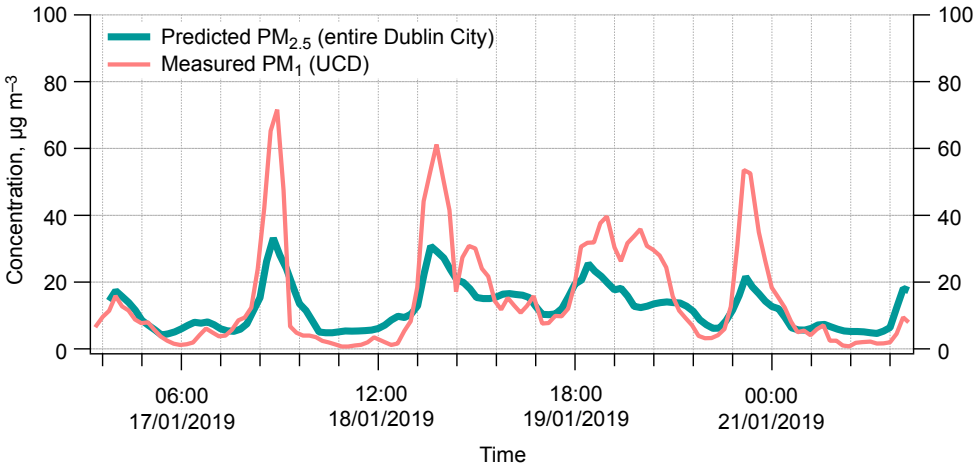

Figure 3.19. StreamAIR-modelled $PM_{2.5}$ and measured PM_1 (ACSM total + BC measured by the AE-33) at UCD campus, Belfield.

4 Black Smoke versus Black Carbon

Measurements of eBC in Dublin show a trend where BC levels are highest in the winter and lowest in the summer (Table 4.1), in agreement with measurements of OM made using the ACSM, as discussed above. Spikes in eBC reached up to 70 µg m^{-3} and were dominated by the solid fuel burning fraction (eBC_{SF}) during the winter months, while the traffic fraction (eBC_{TR}) was dominant in the summer months.

Winter eBC measurements made in Dublin were compared with measurements made in London and Paris (Sciare *et al*., 2011; Fuller *et al*., 2014). The average eBC value for London during the winter months from 2009 to 2011 was ~1.89 µg m^{-3}, and the average for Paris during the winter months for 2010–2011 was ~1.45 µg m^{-3}. The methods for calculating these values were based on those described in Sandradewi *et al*. (2008) and the percentage contributions from "wood burning" were found to be ~17% and ~23% for Paris and London, respectively. The average winter eBC values for Dublin were 0.92 µg m^{-3} (2016/17) and 0.71 µg m^{-3} (2017/18), with "solid fuel" contributions of 56% and 52%, respectively.

The differences seen in emission profiles during the different seasons can also be seen in the relative contributions of traffic and solid fuel burning. The higher contribution of "solid fuel" burning in winter is due to the increased use of solid fuels for residential heating in that season, mainly in the evening–early night, as discussed in Chapter 3.

Table 4.1. Monthly averages of total eBC, eBC_{SF} and eBC_{TR}

Month and year	Total eBC (µg m^{-3})	eBC_{TR} (µg m^{-3})	eBC_{SF} (µg m^{-3})	Solid fuel (% of total BC)
August 2016	0.46	0.37	0.09	20
September 2016	0.40	0.32	0.08	20
October 2016	1.1	0.67	0.43	39
November 2016	1.37	0.62	0.75	55
December 2016	1.16	0.48	0.68	59
January 2017	0.88	0.33	0.55	63
February 2017	0.72	0.38	0.34	47
March 2017	0.51	0.23	0.28	55
April 2017	0.45	0.24	0.21	46
May 2017	0.45	0.32	0.13	28
June 2017	0.27	0.21	0.06	20
July 2017	0.34	0.29	0.05	15
August 2017	0.30	0.23	0.07	23
September 2017	0.52	0.33	0.19	37
October 2017	0.48	0.38	0.10	21
November 2017	0.56	0.40	0.16	29
December 2017	0.72	0.42	0.30	42
January 2018	0.67	0.29	0.38	57
February 2018	0.73	0.31	0.42	58
March 2018	0.74	0.38	0.36	49
April 2018	0.57	0.33	0.24	42
May 2018	0.67	0.45	0.22	33
June 2018	0.58	0.48	0.17	29
July 2018	0.46	0.32	0.14	29
August 2018	0.30	0.21	0.09	30

4.1 Long-term Trends in Black Carbon Based on Data Derived from Historical Black Smoke Measurements

Historical BS data for the Dublin area were collected from several sources. Data for the period 1963–1989 were received from Martin Fitzpatrick of Dublin City Council. These data came in the form of reports that had been compiled on an annual basis by the council. Data for the period 1991–2009 were downloaded directly from the EPA's archive of black smoke monitoring data (available at https://www.epa.ie/researchandeducation/research/safer/). These two datasets were compiled into a single set, and any gaps in the time series, including the period 1989–1991, were filled in with data received from Dr Pat Goodman of the Dublin Institute of Technology. The selection of a suitable site was largely dependent on the availability of data for the entire period. In an effort to avoid any preferential sampling bias (Zidek *et al*., 2014), a single site was selected. This site was located on Baggot Street at the beginning of the period of analysis, but was relocated to Herbert Street, ~350 m away, in 1979, where it remained for the rest of the period. Note that data from Dr Goodman's archive were from city-wide averages taken from a network of six stations.

Details of all legislation changes in Ireland are available at www.irishstatutebook.ie. A comprehensive search of this site was carried out, focusing on the keywords "Air", "Pollution", "Environment" and "Smoke". In 1973, Ireland joined the European Economic Community (EEC) and adopted the legislation of the Community; the relevant acts drafted and enforced by the Community were gathered from www.eur-lex.europa.eu after searching for the same keywords. The data from Baggot Street and Herbert Street were averaged over monthly periods, and data from 1963 to 2009 are presented in Figure 4.1. A clear seasonal pattern can be observed. This is consistent with the increased use of solid fuels for residential heating in the winter months. Although, in general, BS concentrations show a decreasing trend, there are some clear exceptions. These exceptions can be explained by meteorological data and legislative changes that occurred during the study period.

The first instance of air quality-related legislation in Ireland came in the form of the Local Government (Sanitary Services) Act (No. 26 of 1962), which provided powers to local authorities for the regulation of smoke, dust grit and gas pollution sources. This was built upon in 1970 with the Control of Atmospheric Pollution Regulations (S.I. No. 156/1970), which defined permissible levels of "dark" or "black" smoke, in accordance with the Ringlemann chart. Following on from the oil crises in 1973/74 and 1979, the Irish Government introduced a grant scheme for the installation of solid fuel-fired boiler systems, which accounts for the increase in pollution in the following

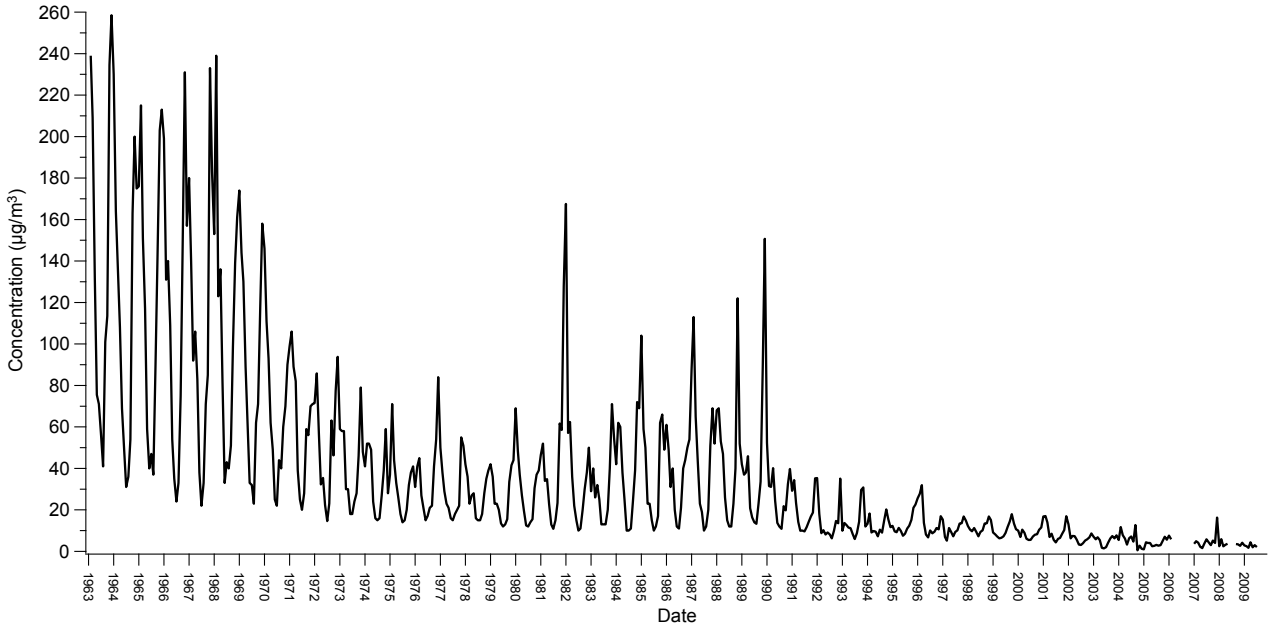

Figure 4.1. Dublin black smoke trends from 1963 to 2009.

years. The particularly large increase in pollution in 1982 can be explained by the extremely low temperatures recorded in the January of that year. Temperatures as low as –19.6°C were recorded during a phenomenon known as "The Big Snow" (data available at www.met.ie/climate/available-data/historical-data). In 1987, the Air Pollution Act (No. 6 of 1987) was introduced. This Act set out the definition of air pollution for Ireland, and under it several regulations relating to air quality standards, air quality management plans and permitted fuels were introduced.

The nationwide air quality standards introduced under this Act adopted the EU standards for suspended particles (Commission Decision 82/779/EEC). The next piece of legislation to have an impact on air quality in Ireland was the Retail Sale of Fuels Regulations (S.I. No. 333/1989); this required retailers of solid fuels to stock "low-smoke" alternatives to bituminous coal and wood, namely Bord na Móna peat briquettes and Rheinbraun Union nuggets/briquettes. These regulations were expanded in September 1990 with the Marketing, Sale and Distribution of Fuels Regulations (S.I. No. 123/1990), which prohibited the sale and distribution of bituminous coals in the Dublin city area. All regulations are reflected in the BS/BC concentrations presented in Figure 4.3.

4.2 Black Smoke–Black Carbon Relationship in Dublin

To establish a relationship between contemporary black carbon (BC) and historical black smoke (BS) records, concurrent BC and BS measurements were performed at the Dublin UCD site. The types of BS sources and their relative contributions have changed since the early BS records were compiled; therefore, BS data derived using modern instruments are not comparable with historical BS data. Nevertheless, BC derivation from historical BS measurements is appropriate. The relationship between BC and BS derived from data covering a 1-year period is presented in Figure 4.2 and the conversion can be expressed via equation 4.1:

$$\mathrm{BC}\ (\mu g\,m^{-3}) = (0.1 \pm 0.002) \times \mathrm{BSI}_{\mathrm{British}} - (2.0 \pm 0.4) \times 10^{-4} (\mathrm{BSI}_{\mathrm{British}})^2 \qquad (4.1)$$

where $\mathrm{BSI}_{\mathrm{British}}$ (black smoke index) is as defined in British Standard BS1747:2 (BSI, 1969).

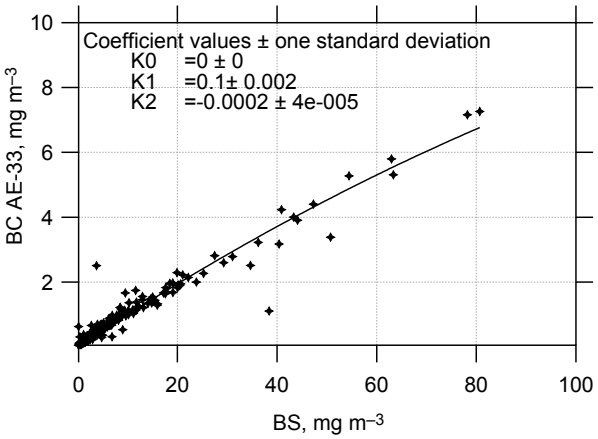

Figure 4.2. The relationship between BC measurements obtained using the AE-33 (a modern instrument) and BS measurements (obtained using a historical instrument) in Dublin UCD for a 1-year period: August 2016–August 2017. Polynomial fitting with three coefficients was used (Heal and Quincey, 2012).

The relationship shown in Figure 4.2 was derived from measurements obtained in one location in Dublin and might not be applicable to other areas, even in the same city, as was indicated by London examples (Quincey *et al*., 2011).

A more general method, based on the basic similarities between the physical principles of BS and BC measurements, is more appropriate for deriving a common relationship. Although the use of reflectance to measure BS and transmittance to measure BC means that there is no exact correspondence between parameters, Heal and Quincey (2012) stated that the BS method is analogous to the BC aethalometer method when the appropriate correction is applied. This postulation allows a conversion between BS and BC to be made with much more explicit assumptions based on first principles (Heal and Quincey, 2012).

Therefore, for the further derivation of BC data from BS measurements, an equation developed by Mathew R. Heal and Paul Quincey (Quincey, 2007; Quincey *et al*., 2011; Heal and Quincey, 2012) was used here:

$$\mathrm{BC}\ (\mu g\,m^{-3}) = (0.27 \pm 0.03) \times \mathrm{BSI}_{\mathrm{British}} - (4.0 \pm 0.2) \times 10^{-4} (\mathrm{BSI}_{\mathrm{British}})^2 \qquad (4.2)$$

Annual averages of the Dublin BS data were converted to BC values and were compared with the annual average of the values collected at UCD. As 2017 was

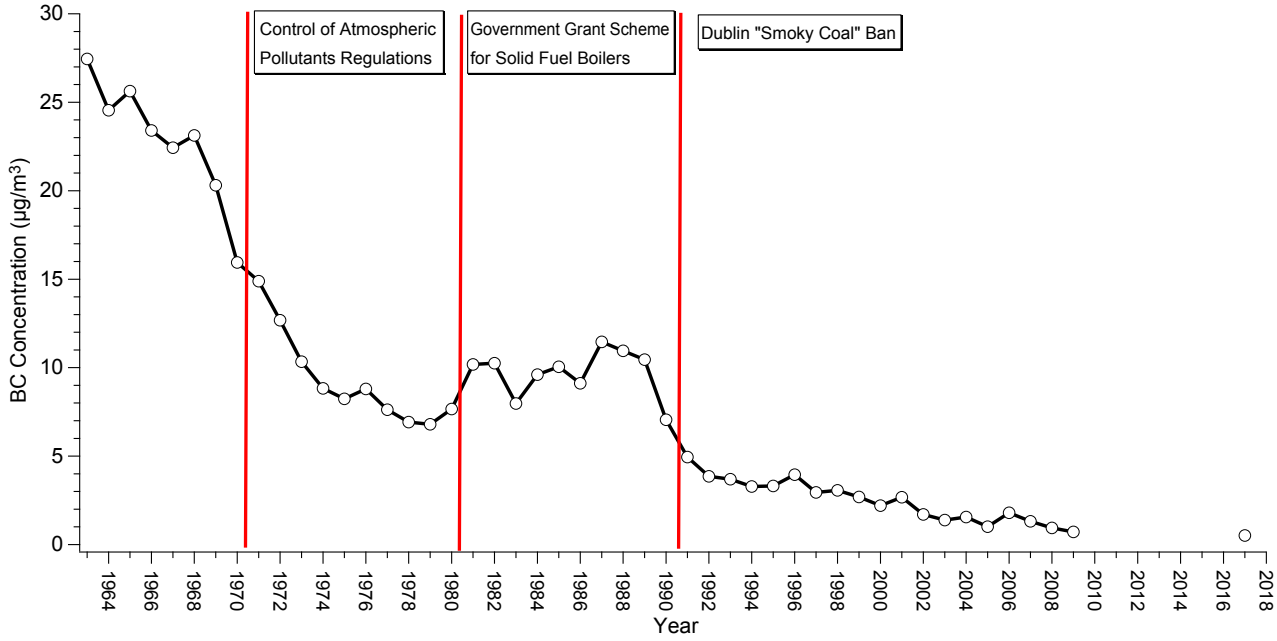

Figure 4.3. Mean Dublin BC values from 1963 to 2018.

the only full year covered during the campaign, it was the only year included in the comparison (Figure 4.3).

Average annual BC values show a declining trend similar to that observed for the monthly BS values (Figure 4.1). The final average annual BC value calculated from the BS data taken from the EPA's Research Data Archive (https://www.epa.ie/researchandeducation/research/safer/), for 2009, is 0.71 µg m^{-3}. The average annual eBC for UCD in 2017, from the AE-33 measurements, was 0.51 µg m^{-3}. This represents a 28% decrease in BC pollution in Dublin (between 2009 and 2017), although it should be noted that the UCD site is further away from the city centre than the Baggot Street/Herbert Street site.

5 Aerosol Health Effects

To investigate the relationship between the chemical composition of PM and potential adverse health effects for the population exposed, $PM_{2.5}$ samples collected at Birr and Dublin, Ireland, were analysed for aerosol OP. The DTT assay (see section 2.8) was used for the OP evaluation. The sampling period in Birr covered 2–8 December 2015, with a 6-hour sampling resolution, while the Dublin kerbside location sampling period covered 6 February–6 March 2019, with a 12-hour sampling resolution.

5.1 Chemical Speciation of Particulate Matter, Birr

Figure 5.1 shows the atmospheric concentrations (hourly means) of the main PM_1 chemical components, measured at Birr, during the selected period. OM, SO_4^{2-}, NO_3^- and NH_4^+ concentrations were measured using an ACSM, while the eBC concentrations were measured using an aethalometer (see sections 2.2 and 2.7). OA was apportioned into five components using PMF, following the approach described in section 2.4. Four components were attributed to primary emissions from combustion processes. One of these, HOA, is associated with fossil fuel combustion and traditionally corresponds to traffic; however, a contribution from oil combustion for domestic heating is also likely at the site, with oil potentially being used for heating (see sections 2.4 and 3.2). Three more components were attributed to the combustion of solid fuels for domestic heating: peat, coal and wood. In addition to these fuel factors, an OOA factor was also resolved, which is representative of the secondary OA formed in the atmosphere or aged during long-range transport.

The average concentrations of the main aerosol components during the campaign were 5.4 ± 9.8, 0.4 ± 0.8, 0.3 ± 0.4, 0.3 ± 0.5 and 0.8 ± 1.2 µg m^{-3} for OM, SO_4^{2-}, NO_3^-, NH_4^+ and eBC, respectively. OA dominated the aerosol mass (Figure 5.1), with a contribution of 63 ± 20%, followed by eBC (17 ± 13%). SO_4^{2-}, NO_3^- and NH_4^+ contributed 10% ± 13%, 5% ± 5% and 5% ± 6%, respectively. On average, OOA dominated the OA mass (44% ± 76%), followed by peat (17% ± 14%), HOA (12% ± 10%), wood (11% ± 27%) and coal (10% ± 11%). Five per cent of OA was not attributed to any factor.

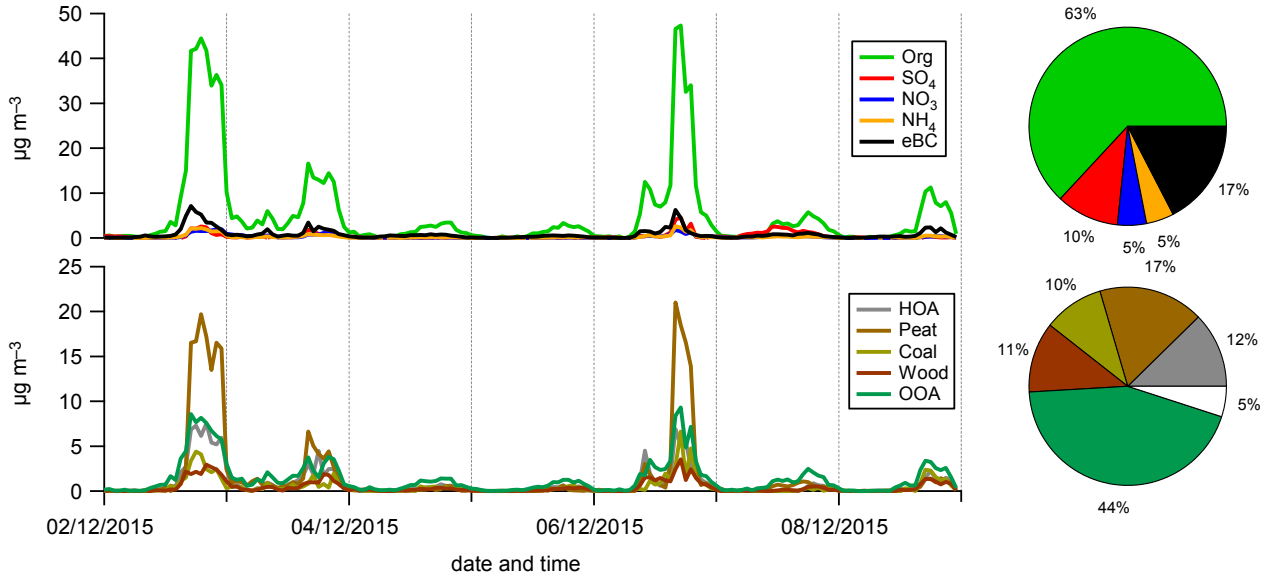

Figure 5.1. Top: atmospheric concentrations (left) and average contributions (right) of the main aerosol components at Birr, between 2 and 8 December 2015. Bottom: atmospheric concentrations (left) and average contributions (right) of the OA components isolated by PMF.

Several evening–early night high-concentration aerosol events were observed during the week selected, with hourly PM_1 average peak concentrations reaching as high as 56 µg m^{-3} and the OA peak concentration reaching 47 µg m^{-3} (75% contribution). During these events, the contribution of OOA to total OA reduced to 28% ± 9%, while most of the POA contributions increased, with the peat contribution increasing to 27% ± 14%. This demonstrates that the extreme pollution events observed were mainly driven by POA sources, with domestic heating contributing the most. The occurrence of these events is favoured by meteorological conditions, such as a stagnant and shallow mixing boundary layer, which prevents the dilution of locally emitted particles and mostly occurs during the night. For more details on the Birr site, see the study by Lin *et al*. (2019b).

5.2 Aerosol Oxidative Potential Measurements, Birr

Temporal differences in water-soluble DTT activity are discussed to provide an overview of the ROS-generation potential of PM in Birr. The rate of DTT consumption is presented in Figure 5.2, normalised by both the volume of sampled air (OP_DTTv, or extrinsic DTT activity, expressed in units of nmol min^{-1} m^{-3}) and the particulate mass (OP_DTTm, or intrinsic DTT activity, expressed in units of nmol min^{-1} mg^{-1}) (Charrier *et al*., 2015).

OP_DTTv shows high daily and weekly variability, ranging from 0.004 to 3.2 nmol min^{-1} m^{-3} [with a relative standard deviation (RSD) of 144%]. The time trend of OP_DTTv shows a striking similarity to the non-refractory aerosol mass concentrations measured using the ACSM plus the eBC concentration measured using the aethalometer, with maximum values at evening–early night and minimum values in day-time (R = 0.88). This OP_DTTv feature has previously been observed in different environments (Delfino *et al*., 2013; Janssen *et al*., 2014; Fang *et al*., 2015). It is worth highlighting that different slopes have been observed for the correlation between PM concentration and OP_DTTv for different sites and periods (Fang *et al*., 2015), indicating that the aerosol chemical composition has an effect on determining the specific ROS-generation potential of atmospheric aerosols. This aspect will be addressed in more detail in the following section.

The intrinsic DTT activity (OP_DTTm) trend shows less variability (RSD = 64%) and no clear correlation with evening–early night aerosol accumulation events. This is consistent with previous findings published in the literature and reporting limited OP_DTTm variability in space and time compared with OP_DTTv (Verma *et al*., 2014; Shafer *et al*., 2016; Patel and Rastogi, 2018a). To further investigate this aspect, we have grouped the samples corresponding to three evening–early night aerosol accumulation events, dominated by solid fuel combustion sources as discussed above, and compared them with the remaining samples. Statistically significant differences (p < 0.02) for the main aerosol component concentrations, PMF factors and OP_DTTv can be observed between the pollution

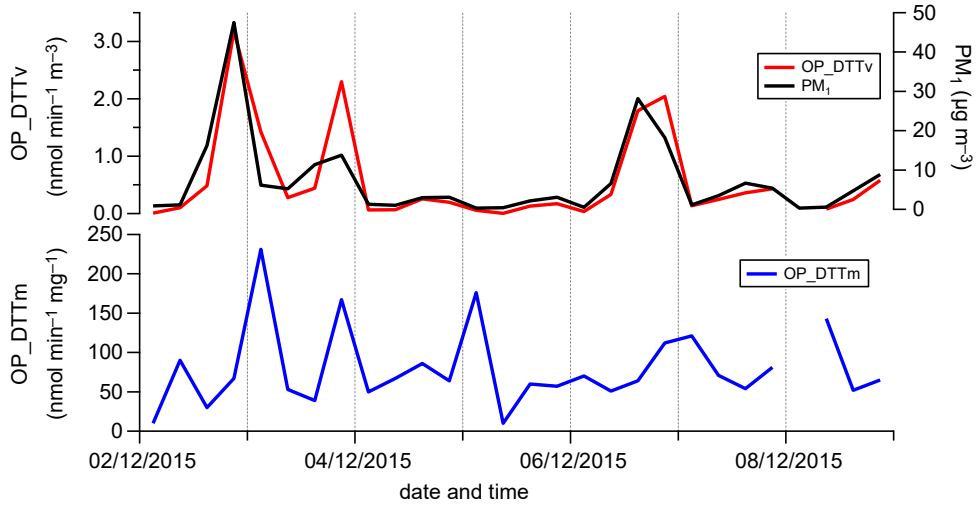

Figure 5.2. Time trends of OP_DTTv (top) and OP_DTTm (bottom) at Birr. The top panel shows the PM_1 aerosol mass, averaged over the filter sampling time, for comparison.

events and the background samples. However, no significant differences were observed between the mass contributions of the main aerosol species and PMF factors, with the only exception being the peat factor ($p < 0.05$). Consistently, OP_DTTm does not show a statistically significant ($p > 0.1$) difference between the two subsets of data. Therefore, in the Birr dataset, the lower variability in OP_DTTm can be explained by the low variability in the soluble aerosol chemical composition between peak and background samples, while the high variability in OP_DTTv is related to the large differences in absolute concentrations observed between the two subsets of samples.

To compare these results with those of other published studies that focus mainly on daily aerosol samples, we calculated the daily means of DTT activity observed at Birr. The variability in OP_DTTv values observed at Birr (from 0.09 to 1.1 nmol min^{-1} m^{-3}) is somewhat higher than the variability documented over Los Angeles, CA (0.10–0.16) (Hu *et al*., 2008), Beijing (0.11–0.49) (Liu *et al*., 2014) and various cities in Europe (0.10–0.46) (Shafer *et al*., 2016). Nevertheless, it is similar to the variability reported over Orinda, CA (0.37–2.50) (Ntziachristos *et al*., 2007), Greece (0.84–3.10) (Argyropoulos *et al*., 2016), the Netherlands (1.4) (Janssen *et al*., 2014), the south-west USA (~0.1 to ~0.9) (Fang *et al*., 2015) and the wider Los Angeles area (~0.2 to ~1.2; ~0.1 to ~0.9) (Cho *et al*., 2005; Verma *et al*., 2009b). At the same time, the OP_DTTm values (49–122 nmol min^{-1} mg^{-1}) obtained in Birr were found to be at the upper end of the ranges reported in the literature (~10 to ~100, according to the studies cited above). The good level of agreement between OP_DTTv values and those in the literature indicates that aerosol collected at Birr is particularly redox active. Nevertheless, it is also worth noting that OP_DTTm was derived by normalising online-measured PM_1 mass, under the assumption that this is representative of the $PM_{2.5}$ aerosol mass collected on the filter. Although this assumption is reasonable, considering the characteristics of the sampling site, a discrepancy between the two aerosol mass metrics may have led to higher OP_DTTm values. However, this fact does not affect the considerations below, which discuss attributing the aerosol OP to different sources, as this is based on correlations between absolute concentrations and OP_DTTv values.

5.3 Sources of Aerosol Oxidative Potential, Birr

To identify the contribution of specific aerosol components to OP_DTT, both simple and multivariate linear regression analyses were employed. Pearson's correlation coefficients between OP_DTT values (OP_DTTv and OP_DTTm) and aerosol species concentrations (volume and mass normalised) are presented in Table 5.1.

Table 5.1. Pearson's correlation coefficient (*R*) of volume-normalised and mass-normalised species concentrations with OP_DTTv and OP_DTTm, respectively

Volume-normalised aerosol species/PMF factor	*R* (DTTv)	PM_1-mass-normalised aerosol species/PMF factor	*R* (DTTm)
Org	0.88*	Org/PM_1	0.12
SO_4^{2-}	0.59*	SO_4^{2-}/PM_1	–0.25
NO_3^-	0.94*	NO_3^-/PM_1	0.50*
NH_4^+	0.87*	NH_4^+/PM_1	0.11
eBC	0.75*	eBC/PM_1	–0.03
PM_1	0.88*	–	–
HOA	0.87*	HOA/PM_1	0.17
Peat	0.86*	$Peat/PM_1$	0.13
Coal	0.83*	$Coal/PM_1$	0.05
Wood	0.90*	$Wood/PM_1$	0.05
OOA	0.87*	OOA/PM_1	0.06
n.a.-OA	0.85*	$n.a.\text{-}OA/PM_1$	–0.17

***Significant at $p < 0.05$.**

n.a.-OA, OA not apportioned (i.e. the mass of OA not attributed to any source by the source apportionment algorithm).

Table 5.1 shows significant and high correlation coefficients for all the main aerosol species and PMF factors when looking at extrinsic DTT activity (OP_DTTv). This is due to the high levels of correlation observed in the time series of all the aerosol species measured during the study period. High levels of correlation between all the aerosol components suggest common processes such as meteorological conditions (PBL dynamics) or common source variations.

Despite generally good correlations being observed between OP_DTTv and PM_1 concentration, differences can be observed among the correlation coefficients for individual PM species. The highest correlation coefficient is observed for OP_DTTv and nitrate ($R = 0.94$). A significant correlation between OP_DTT and NO_3^- (in terms of both volume-normalised or mass-normalised values) has already been observed in the literature (Bates *et al*., 2015; Argyropoulos *et al*., 2016; Perrone *et al*., 2016; Patel and Rastogi, 2018a). This correlation has always been considered indirect, as ammonium nitrate and sulfate have been demonstrated to be DTT-inactive in laboratory studies (Fang *et al*., 2016; Patel and Rastogi, 2018a,b). However, considering that many studies have shown a high level of correlation between NO_3^- and some OOA factors (usually identified as SV-OOA) (Lanz *et al*., 2007; Ulbrich *et al*., 2009; Chakraborty *et al*., 2016; Sullivan *et al*., 2016), the high OP_DTTv–NO_3^- correlation may be attributed to a highly DTT-active SOA fraction co-variant with NO_3^- that cannot be isolated using UMR source apportionment. A higher OOA-resolving potential would be desirable in future work (possibly by deploying a high-resolution aerosol mass spectrometer) to test this hypothesis.

A good level of correlation between OA factors and OP_DTTv was also observed, with wood showing the highest correlation ($R = 0.9$), followed by OOA ($R = 0.87$), HOA ($R = 0.87$), peat ($R = 0.86$) and coal ($R = 0.83$). This links ROS-generating potential to the organic fraction of solid fuel combustion, particularly emissions from wood burning. A significant contribution of wood burning to aerosol OP has been reported in the literature (Verma *et al*., 2014, 2015a; Bates *et al*., 2015; Argyropoulos *et al*., 2016; Fang *et al*., 2016; Zhou *et al*., 2018). Other biomass burning (e.g. rice crop residue burning) emissions were also reported to contribute to OP_DTT (Fushimi *et al*., 2017), but with lower intrinsic ROS-generation potential than wood burning.

The lowest correlation coefficients are associated with eBC ($R = 0.75$) and sulfate ($R = 0.59$). Although sulfate is not expected to contribute to the ROS-generating potential of atmospheric aerosol, eBC has previously been associated with DTT activity (Cho *et al*., 2005; Patel and Rastogi, 2018b). Nevertheless, in principle, eBC should not contribute to water-soluble DTT activity, as measured in this study, considering its water-insoluble nature (Patel and Rastogi, 2018a).

No significant correlation is observed between the mass contribution of aerosol species and OP_DTTm, apart from in the case of NO_3^-, as discussed above.

To investigate the role of OA in OP in more detail, PMF factors were used as independent variables in a multilinear regression model for OP_DDTv, following the approach presented by Verma *et al*. (2015b). The OP_DTTv variability was explained reasonably well by the linear regression model, with the R^2 value between modelled and measured OP_DTTv being 0.82.

The coefficients of the regression equation (the multiplication factors associated with each independent variable; shown in Table 5.2) represent the intrinsic ability of each of the specific aerosol species to generate ROS, as measured by the DTT assay (i.e. OP_DTT per total mass of the specific component). It is important to note that only the DTT activity of the water-soluble fraction of PM is measured in this study, while the online measurements included total mass concentrations of the OAs; thus, the values reported in Table 5.2 should be considered to represent intrinsic "water-soluble" DTT activity and not

Table 5.2. Results of the multilinear regression model analysis performed using OP_DTTv (dependent variable) and PMF OA factors (independent variable)

OA factor	Multilinear regression coefficient (nmol min^{-1} μg^{-1})
HOA	3.15e-007 ± 1.01
Peat	0.049 ± 0.396
Coal	–5.08e-010 ± 1.6
Wood	0.92 ± 1.96
OOA	4.12e-006 ± 0.85
n.a.-OA	0.061 ± 1.23
Intercept	0.035 ± 0.29

n.a.-OA, OA not apportioned (i.e. the mass of OA not attributed to any source by the source apportionment algorithm).

"total" activity. Another important caveat to consider is that, in the present study, no information on aerosol metal components were available; therefore, we have attributed total aerosol ROS-generating potential to the organic fraction, which could lead to an overestimation. However, considering the site characteristics (e.g. away from heavy traffic, industry, railways), this assumption is reasonable. Moreover, the DTT assay is less sensitive to metals (Hedayat *et al*., 2015) than other assays and therefore the role of metals should be further investigated using different methodologies.

Similarly to the results in Table 5.1, the wood factor yielded the highest regression coefficient (intrinsic water-soluble DTT activity), being 0.92 ± 1.96 nmol min^{-1} µg^{-1}. It is noteworthy that this value is higher than the intrinsic water-soluble DTT activity of wood burning obtained by Verma *et al*. (2015b) (0.151 ± 0.020 nmol min^{-1} µg^{-1}) and much higher than the typical total intrinsic activity measured by McWhinney *et al*. (2013b) for diesel exhaust particles (0.020–0.060 nmol min^{-1} µg^{-1}), which have been associated with several detrimental health effects (Kagawa, 2001; Pandya *et al*., 2002; Duscio *et al*., 2003; Garshick *et al*., 2006). The fact that intrinsic DTT activity of wood burning aerosol was found to be higher at Birr than that found by Verma *et al*. (2015b) may be due to different burning conditions at the sites or a result of differences in the atmospheric ageing of the OA generated by wood burning (Zhou *et al*., 2018), but could also be an effect of metal components not being addressed in our DTT activity "source attribution". In any case, these results imply that biomass burning emissions might pose a potentially serious health hazard.

The regression coefficients were also significant for the peat factor and the "not-apportioned-OA" factor. This suggests that peat burning also produces DTT-active aerosols, but with an intrinsic DTT activity (0.049 ± 0.396 nmol min^{-1} µg^{-1}) that is one order of magnitude lower than the wood burning activity. No significant contribution to DTT activity was observed for the HOA, coal or OOA factors in the short time period covered by this study. A similar result for HOA was reported by Verma *et al*. (2015b). It is worth highlighting that HOA and coal burning PM are mainly water insoluble and therefore are not expected to contribute to the water-soluble DTT activity measured in the present study (Verma *et al*., 2015b). A similar multilinear regression analysis was performed by including eBC as an independent variable, but no significant contribution to OP_DTTv was observed for eBC either, which, again, might be due to the insoluble nature of this compound.

OOA was reported to contribute to aerosol OP in several works (Verma *et al*., 2015b; Lin *et al*., 2016); therefore, the result for OOA obtained in this study is somewhat surprising, considering the high average contribution of OOA to OA at Birr during the measurement period. The insignificant contribution of OOA to OP_DTTv can probably be explained by the fact that OOA is treated as a whole in this study, without distinctions between the different SOA-formation processes. In our opinion, the significant OP_DTTv–NO_3^- correlation hints at some sort of SOA-formation process, leading to highly DTT-active SOA (as mentioned above), the contribution of which is masked by other, more DTT-neutral, SOAs.

The average intrinsic water-soluble DTT activities of the different PMF factors were multiplied by their respective ambient concentrations for each sample to reconstruct the total OP_DTTv associated with those OA components (Figure 5.3).

Overall, the major contribution to water-soluble DTT activity came from the wood factor (average 80 ± 13%). Despite a lower intrinsic water-soluble activity than wood, the high concentrations of the peat factor mean that it also contributes substantially to OP_DTTv at Birr (10 ± 6%), particularly during evening–early night episodes (16 ± 5%) when aerosol concentrations are high. A similar average contribution is associated with the fraction of OA not apportioned by the PMF algorithm. The contributions from other OA components were negligible, as evident from the very low intrinsic DTT-activity coefficients.

5.4 Aerosol Oxidative Potential Measurements, Dublin

Chemical speciation of PM and source apportionment results for the Dublin TCD (kerbside) location are presented in section 3.3; here, we discuss the measurements of only OP.

Figure 5.4 shows the OP_DTTv and OP_DDTm values measured at the TCD location in Dublin. OP_DTTv ranges from 0.06 to 1.58 nmol min^{-1} m^{-3} and OP_DDTm from 4 to 132 nmol min^{-1} mg^{-1}.

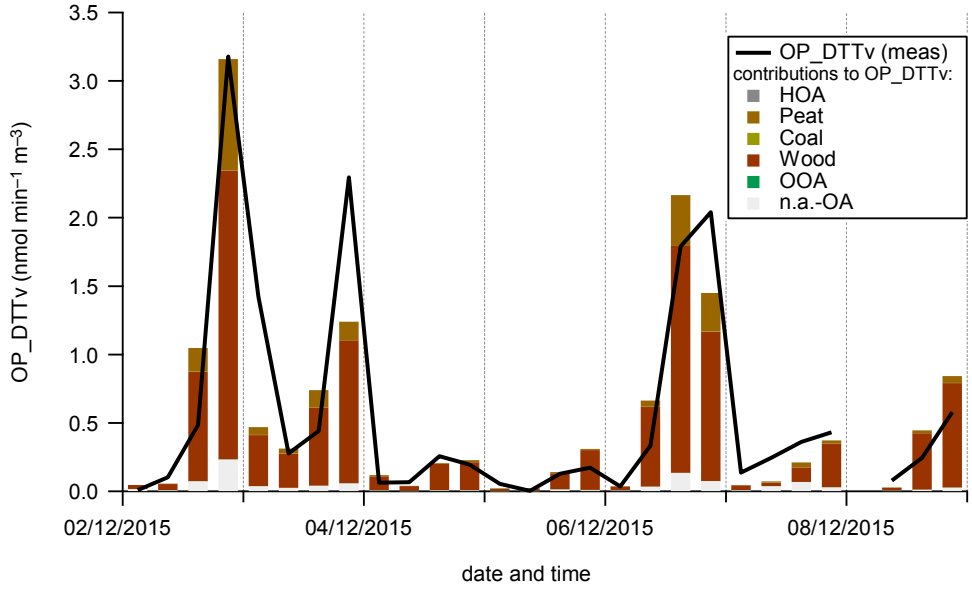

Figure 5.3. Reconstructed and measured water-soluble OP_DTTv. The reconstructed OP_DTTv is fractionated into the contributions of the main OA components.

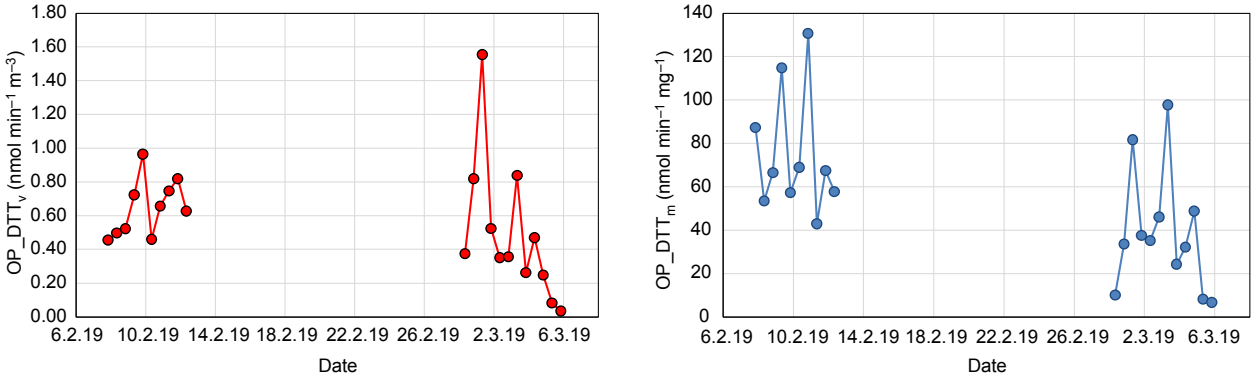

Figure 5.4. OP_DTT values obtained at the kerbside location at TCD.

As can be seen from the figure, diurnal variations at the Dublin TCD site are not as pronounced as in Birr and show an opposite trend. Slightly higher OP was observed during the day in TCD as opposed to evening–early night in Birr. This points to different sources contributing to OP at these two locations. The higher OP during the day potentially indicates a dominant contribution from traffic at the Dublin TCD location, while the Birr location was affected more by solid fuel burning. However, proper OP source attribution analysis is required to provide quantitative information for the Dublin site, as was done for Birr and is the focus of further investigations.

In terms of daily averages, OP_DTTv ranges between 0.09 and 1.11 (median 0.30) nmol min^{-1} m^{-3} and between 0.06 and 1.04 (0.60) nmol min^{-1} m^{-3} in Birr and Dublin TCD, respectively, while OP_DTTm ranges between 49 and 122 (76) nmol min^{-1} mg^{-1} and 7.5–91 (61) nmol min^{-1} mg^{-1} in Birr and Dublin, respectively. Although the comparison of short-term non-overlapping periods for these different sites is not robust, general consistency between the OP ranges is observed in terms of extrinsic aerosol ROS-generating capacities, with slightly higher OP_DTTm values obtained at Birr suggesting that biomass burning aerosol may have a higher OP, at least as determined by the DTT assay. This agrees with the limited set of comparative data available in the literature, as already discussed in the report, but further measurements covering longer periods and seasons are needed to quantitatively address this issue.

Moreover, preliminary investigations of OP contributions from the insoluble OM fraction were carried out and, although results are still very preliminary, an interesting pattern has emerged, namely that of the insoluble OP fraction having a larger contribution at Birr's residential site than at the Dublin kerbside site. This result is unexpected, as traffic emissions supposedly contribute more to the insoluble OM fraction than solid fuel burning does, and, thus, insoluble OP from traffic was anticipated to make a larger contribution at the Dublin site than at the Birr site. These conflicting results reinforce the importance of studying the OP relationship for specific sources and chemical compositions and merit further investigation.

Finally, it is worth noting that the OP evaluation assay deployed in this study provides only a partial overview of aerosol OP and its negative effects on human health; other assays have been shown to be more sensitive to different chemical species (e.g. metals) than the DTT assay. Moreover, the present study evaluated the ROS-generating potential of water-soluble aerosol components (which is standard for OP studies), and this may highlight some sources of potential toxicity more than others. For instance, BBOA is more water soluble than OA from fossil fuel burning (represented by HOA, coal and, partly, eBC in this study), and this may, in part, explain the high contribution to OP attributed to BBOA in this study. It is also worth pointing out that, while non-cellular assays, such as the DTT assay, are useful tools for determining the ROS activity of PM, they have their limitations in terms of physiological relevance, as they do not take into account any additional biological responses occurring within a PM-exposed cell.

6 Conclusions and Recommendations

6.1 Conclusions

AEROSOURCE, a pilot AMS network, was successfully implemented to enhance the National Transboundary Air Pollution Network with near real-time aerosol chemical speciation (including OM) and source apportionment capabilities. The AEROSOURCE network comprised three sophisticated aerosol mass spectrometer nodes positioned in strategic locations: Carnsore Point (regional background), Dublin (urban environment) and Mace Head (marine background). The success and power of the next-generation network became evident after 3 months of operation, when it provided real-time data on aerosol composition and sources during extreme pollution events in south Dublin.

Carbonaceous aerosol (OM and BC) dominated the aerosol composition in Dublin, contributing up to 89% and 94% of total PM_1 at the residential background and kerbside locations, respectively. However, the OM and BC contributions differed between the sites: OM dominated PM_1 at the residential background location and B&BC was the dominant compound at the kerbside location.

Source apportionment of OM and BC revealed that four major sources contribute to aerosol concentrations in Dublin city: (1) residential heating; (2) traffic; (3) long-range transport of aged aerosol; and (4) cooking. However, the contributions from these different sources were dependent on the season and location.

On average, residential heating emissions made a dominant contribution to aerosol concentrations during winter in residential Dublin, with peat and wood combined contributing 47% of total PM_1, followed by coal/oil heating (19%), and regional aerosol, ammonium nitrate and traffic sources contributing 16%, 12% and 6%, respectively. On the other hand, during the summer, contributions from heating emissions were minimal, and regional/long-range sources contributed most (70%) to total PM_1. The absolute concentrations contributed by traffic remained similar throughout the seasons at the residential location (~0.5 $\mu g\,m^{-3}$), but the relative traffic contribution varied from 6% in the winter to 23% in the summer. The PM concentrations at Dublin's kerbside location, on the other hand, were dominated by the traffic contribution (35–58%), followed by secondary PM (17–29%), solid fuel burning (18–22%), cooking (7%) and oil burning (0–7%). During the winter, contributions from solid fuel burning emissions related to residential heating (22%) approached those from traffic (35%) at the kerbside location.

In addition to the overall dominant contribution from solid fuel burning during the autumn/winter, extreme air pollution events (with PM_1 surpassing 100 $\mu g\,m^{-3}$) frequently occurred over the entire country in winter, including Dublin. Using sophisticated fingerprinting techniques, AEROSOURCE revealed that the consumption of peat and wood, although contributing little to the total energy budget, contributed up to 70% of the PM (i.e. PM_1) mass.

These extreme events accounted for all air quality exceedances during which PM (i.e. $PM_{2.5}$) limits, recommended by WHO, were breached in Dublin. Our estimates show that specifically targeting 100% reduction of emissions of wood and peat would reduce the PM_1 concentrations by 52–70%. Assuming that the $PM_{2.5}$ concentration would be reduced proportionally, the elimination of wood and peat burning would reduce the exceedance of the WHO $PM_{2.5}$ daily limit value to 1 in 75 days, from the currently observed 1 in 5 days (over winter) in Dublin. Even though a 100% reduction in peat and wood emissions is unlikely in reality, even reducing peat and wood consumption by 50% would mean that limit values would be exceeded on only approximately 1 in 10 days; in contrast, increasing peat and wood emissions by 50% would lead to limit values being exceeded on 1 in 3 days.

As expected, overall concentrations at the regional background Carnsore Point and coastal Mace Head sites were lower than those in Dublin; however, carbonaceous compounds dominated total PM_1 composition (>50%) at those sites too. On average, long-range transport and regional sources, producing OOA, ammonium nitrate and sulfate, were the dominant PM_1 sources; however, solid fuel burning emissions were important during cold stagnant

periods, with peat contributing 32% and 40% of PM_1 at the Mace Head and Carnsore Point sites, respectively. Overall, winter contributions from solid fuels were ~39% at the Mace Head site and 25% at the Carnsore Point site.

In addition, quasi-Lagrangian and cluster analyses were performed to evaluate local source contributions as opposed to the contribution of the regional and long-range transport of pollutants. These analyses indicated the importance of local sources during the autumn/winter, pointing to significant contributions from domestic heating, while, in the spring/summer, traffic and photochemical secondary particle formation were the main sources. Overall, the contribution from transboundary sources was more important during the spring/summer than in the autumn/winter, when local sources dominated OA. Long-range transport of pollutants contributed significantly to ammonium nitrate concentrations over Ireland, particularly during the spring/summer. While, for sulfate, the role of biogenic sources from the ocean was evident during the spring/summer period in addition to the transport of anthropogenic pollutants.

Modelling analysis, performed to elucidate and quantify air pollution sources affecting air quality in Ireland, highlighted deficits in the current Irish emission inventory. An update of the inventory, to include high-temporal-resolution solid fuel emission data, was thus required to reproduce the evening–early night peak events in Dublin in both the residential and kerbside locations. After the addition of solid fuel emissions, the model was able to match the time and duration of pollution events, whereas without it, PM levels were underestimated by an order of magnitude. Although the modelling results are very encouraging, the system would benefit from comprehensive Ireland-wide detailed emission inventories with hourly temporal resolution that accurately portray characteristics of domestic solid fuel burning in terms of the distribution of fuel types, the duration of solid fuel burning and the seasonality of burning. Without such a dataset, nationwide modelling of air pollution with an acceptably low uncertainty level is not possible.

Furthermore, the investigation of the potential for detrimental health effects arising from different emission sources in this study provided an indication that solid fuel burning contributes significantly to PM toxicity. In this short preliminary study, the source attribution based on DTT activity, performed using multilinear regression, attributed most of the observed OP of water-soluble aerosol to wood burning, with a smaller but significant contribution attributed to peat combustion, pointing to an important role for solid biomass and peat burning in determining health effects, alongside coal or oil combustion. It is also worth noting that the regression analysis highlighted the effect of local PM sources on the observed aerosol OP as opposed to the effect of regional sources.

The absolute values of volume-normalised DTT activity measured in Birr in this study were comparable to or higher than those measured in big cities in Europe, the USA and Asia. This is highly important considering that sampling was performed in a small town (Birr) and shows that solid fuel burning for domestic heating, coupled with unfavourable meteorological conditions, can cause severe pollution episodes, with potential negative effects on the exposed population. Moreover, mass-normalised DTT activity was among the highest levels ever reported in the literature. Although a certain overestimation of this parameter cannot be completely ruled out, given that online-measured mass was used to infer aerosol loadings on the filters, this most likely indicates a high intrinsic ROS-generation capability of emissions from solid fuel combustion. Further studies are necessary to address this issue more quantitatively.

Finally, historical BS measurements, spanning several decades (1960–2009), extended by contemporary BC measurements encompassing current concentrations, demonstrate the success of air pollution legislation and its implementation. Observations show an overall trend of declining BC, with significant step-like drops in concentrations after the implementation of pieces of milestone legislation (the Control Atmospheric Pollution Regulations, the smoky coal ban, etc.).

6.2 Recommendations

AEROSOURCE has made some unique findings that should lead to better-informed and more targeted clean air policy development with the aim of removing key pollutants, particularly those with disproportionate effects on air quality. Moreover, the findings highlight the risks of adopting an ill-informed, monotonic approach to policy development rather than a common-issue and co-beneficial approach. The particular policy issue exposed by this study relates

to the Europe-wide promotion of solid biomass as an alternative to fossil fuels. The use of biomass is of course somewhat beneficial when considering the resulting reductions in greenhouse gas emissions; however, as AEROSOURCE demonstrates, solid fuel burning leads to extreme pollution events, resulting in PM levels well in excess of WHO guideline values. Therefore, instead of promoting the use of solid fuel, new emission controls on residential solid fuel burning should be introduced as a matter of urgency.

Moreover, we recommend that emission reduction legislation should encapsulate the toxicity aspects of different PM sources rather than being solely based on total particulate mass concentrations. This recommendation demands conceptual advances in the design and implementation of focused air pollution–health source apportionment studies, to elucidate the health effects in a deterministic manner, considering aerosol physicochemical properties, sources, and PM toxicity and effects on mortality.

AEROSOURCE results indicate that solid fuel emissions make large contributions to OP, which is regarded as an indirect proxy for the toxicity effects of PM; however, more comprehensive studies, involving a wide array of assays and direct cell toxicity measurements covering longer than 2-week periods (ideally 1 year or more), are needed to progress scientific understanding in this area and provide more definitive answers. Ireland, owing to its relatively distinctive collection of pollution sources and the advanced AEROSOURCE network, possesses high potential to significantly contribute to this knowledge.

The current advanced AEROSOURCE network, comprising three strategically positioned nodes, augments the national air quality monitoring network, which is now capable of supporting sophisticated and better-informed policy development and implementation to address the scientific challenges outlined above. Without analytically advanced chemical speciation and source apportionment capabilities, the major contributors to pollution cannot be identified. Such a fingerprinting capability enables the selective targeting of the specific fuel types primarily responsible for breaching PM limit values, even if disproportionate; the identification of the prime suspects contributing to PM pollution is effectively impossible using standard procedures. As demonstrated by the AEROSOURCE results, this could have significant benefits without incurring major costs, in that 70–90% of the problem could be resolved by introducing a measure to target only a small percentage of fuel consumed.

The findings from the AEROSOURCE network demonstrate the power of using a 24/7 operational national AMS network alongside the National Ambient Air Quality Monitoring Programme, and **it is strongly recommended that the operation of this pilot network continues and that it is further developed**. We have only skimmed the surface of what AEROSOURCE could potentially deliver, from providing data on the formation and evolution of the complex organic chemical species in OM to delivering health-impact research with highly advanced datasets that have been hitherto lacking and slowing down progress. Moreover, the continuation of these advanced measurements is essential to record changes in the dominant air pollutants and, thus, enable the quantification of the short- and long-term effects of environmental policies.

References

Ackermann, J.I., Hass, H., Memmesheimer, M., Ebel, A., Binkowski, F. and Shankar, U., 1998. Modal aerosol dynamics model for Europe: development and first applications. *Atmospheric Environment* 32: 2981–2999.

Akhtar, U.S., McWhinney, R.D., Rastogi, N., Abbatt, J.P.D., Evans, G.J. and Scott, J.A., 2010. Cytotoxic and proinflammatory effects of ambient and source-related particulate matter (PM) in relation to the production of reactive oxygen species (ROS) and cytokine adsorption by particles. *Inhalation Toxicology* 22: 37–47.

Alfarra, M.R., Prevot, A.S.H., Szidat, S., Sandradewi, J., Weimer, S., Lanz, V.A., Schreiber, D., Mohr, M. and Baltensperger, U., 2007. Identification of the mass spectral signature of organic aerosols from wood burning emissions. *Environmental Science & Technology* 41: 5770–5777.

Allan, J.D., Delia, A. E., Coe, H., *et al*., 2004. A generalised method for the extraction of chemically resolved mass spectra from Aerodyne aerosol mass spectrometer data. *Journal of Aerosol Science* 35: 909–922.

Archer-Nicholls, S., Lowe, D., Utembe, S., Allan, J., Zaveri, R.A., Fast, J.D., Hodnebrog, Ø., Denier van der Gon, H. and McFiggans, G., 2014. Gaseous chemistry and aerosol mechanism developments for version 3.5.1 of the online regional model, WRF-Chem. *Geoscientific Model Development* 7: 2557–2579.

Argyropoulos, G., Besis, A., Voutsa, D., Samara, C., Sowlat, M.H., Hasheminassab, S. and Sioutas, C., 2016. Source apportionment of the redox activity of urban quasi-ultrafine particles ($PM_{0.49}$) in Thessaloniki following the increased biomass burning due to the economic crisis in Greece. *Science of the Total Environment* 568: 124–136.

Atkinson, R.W., Kang, S., Anderson, H.R., Mills, I.C. and Walton, H.A., 2014. Epidemiological time series studies of $PM_{2.5}$ and daily mortality and hospital admissions: a systematic review and meta-analysis. *Thorax* 69: 660–665.

Ayres, J.G., Borm, P., Cassee, F.R., *et al*., 2008. Evaluating the toxicity of airborne particulate matter and nanoparticles by measuring oxidative stress potential – a workshop report and consensus statement. *Inhalation Toxicology* 20: 75–99.

Bates, J.T., Weber, R.J., Abrams, J., *et al*., 2015. Reactive oxygen species generation linked to sources of atmospheric particulate matter and cardiorespiratory effects. *Environmental Science & Technology* 49: 13605–13612.

Bi, X., Sheng, G., Peng, P.A., Chen, Y., Zhang, Z. and Fu, J., 2003. Distribution of particulate- and vapor-phase *n*-alkanes and polycyclic aromatic hydrocarbons in urban atmosphere of Guangzhou, China. *Atmospheric Environment* 37: 289–298.

Brunekreef, B., 1997. Air pollution and life expectancy: is there a relation? *Occupational and Environmental Medicine* 54: 781–784.

Brunekreef, B. and Holgate, S. T., 2002. Air pollution and health. *Lancet* 360: 1233–1242.

BSI (British Standards Institution), 1969. Standard No. 1747. Methods for the Measurement of Air Pollution. Determination of Concentration of Suspended Matter. BSI, London.

Buckley, P., 2020. Nature and origin of black carbon in Ireland. PhD Thesis. University College Cork, Cork, Ireland.

Burchiel, S.W., Lauer, F.T., Dunaway, S.L., Zawadzki, J., McDonald, J.D. and Reed, M.D., 2005. Hardwood smoke alters murine splenic T cell responses to mitogens following a 6-month whole body inhalation exposure. *Toxicology and Applied Pharmacology* 202: 229–236.

Canagaratna, M.R., Jayne, J.T., Ghertner, D.A., *et al*., 2004. Chase studies of particulate emissions from in-use New York City vehicles. *Aerosol Science and Technology* 38: 555–573.

Canagaratna, M.R., Jayne, J.T., Jimenez, J.L., *et al*., 2007. Chemical and microphysical characterisation of ambient aerosols with the Aerodyne aerosol mass spectrometer. *Mass Spectrometry Reviews* 26: 185–222.

Canonaco, F., Crippa, M., Slowik, J.G., Baltensperger, U. and Prévôt, A.S.H., 2013. SoFi, an IGOR-based interface for the efficient use of the generalized multilinear engine (ME-2) for the source apportionment: ME-2 application to aerosol mass spectrometer data. *Atmospheric Measurement Techniques* 6: 3649–3661.

Canonaco, F., Slowik, J.G., Baltensperger, U. and Prévôt, A.S.H., 2015. Seasonal differences in oxygenated organic aerosol composition: implications for emissions sources and factor analysis. *Atmospheric Chemistry and Physics* 15: 6993–7002.

Carslaw, D.C. and Ropkins, K., 2012. *openair* — An R package for air quality data analysis. *Environmental Modelling & Software* 27–28: 52–61.

Centre for Climate and Air Pollution Studies, undated. AEROSOURCE: Source apportionment of air borne pollutants transported to and across Ireland using aerosol mass spectrometry and positive matrix factorization techniques. Available online: http://macehead.org/index.php?option=com_content&view=article&id=189&Itemid=94 (accessed 25 June 2019).

Chakraborty, A., Gupta, T. and Tripathi, S.N., 2016. Chemical composition and characteristics of ambient aerosols and rainwater residues during Indian summer monsoon: insight from aerosol mass spectrometry. *Atmospheric Environment* 136: 144–155.

Charrier, J.G. and Anastasio, C., 2012. On dithiothreitol (DTT) as a measure of oxidative potential for ambient particles: evidence for the importance of soluble transition metals. *Atmospheric Chemistry and Physics* 12: 9321–9333.

Charrier, J.G., Richards-Henderson, N.K., Bein, K.J., McFall, A.S., Wexler, A.S. and Anastasio, C., 2015. Oxidant production from source-oriented particulate matter – Part 1: oxidative potential using the dithiothreitol (DTT) assay. *Atmospheric Chemistry and Physics* 15: 2327–2340.

Chin, M., Rood, R.B., Lin, S.-J., Müller, J.-F. and Thompson, A.M., 2000. Atmospheric sulfur cycle simulated in the global model GOCART: model description and global properties. *Journal of Geophysical Research: Atmospheres* 105: 24,671–24,687.

Cho, A.K., Sioutas, C., Miguel, A.H., Kumagai, Y., Schmitz, D.A., Singh, M., Eiguren-Fernandez, A. and Froines, J.R., 2005. Redox activity of airborne particulate matter at different sites in the Los Angeles Basin. *Environmental Research* 99: 40–47.

Chung, M.Y., Lazaro, R.A., Lim, D., Jackson, J., Lyon, J., Rendulic, D. and Hasson, A.S., 2006. Aerosol-borne quinones and reactive oxygen species generation by particulate matter extracts. *Environmental Science & Technology* 40: 4880–4886.

Clancy, L., Goodman, P., Sinclair, H. and Dockery, D.W., 2002. Effect of air-pollution control on death rates in Dublin, Ireland: an intervention study. *Lancet* 360: 1210–1214.

Crenn, V., Sciare, J., Croteau, P.L., *et al*., 2015. ACTRIS ACSM intercomparison – Part I: reproducibility of concentration and fragment results from 13 individual quadrupole aerosol chemical speciation monitors (Q-ACSM) and consistency with time-of-flight ACSM (ToF-ACSM), high resolution ToF aerosol mass spectrometer (HR-ToF-AMS) and other co-located instruments. *Atmospheric Measurement Techniques* 8: 7239–7302.

Crippa, M., Canonaco, F., Lanz, V.A., *et al*., 2014. Organic aerosol components derived from 25 AMS data sets across Europe using a consistent ME-2 based source apportionment approach. *Atmospheric Chemistry and Physics* 14: 6159–6176.

CSO (Central Statistics Office), 2011. Census 2011 – This is Ireland (Part 1). CDD41 – Private households in permanent housing units in the aggregate town and rural areas of each province, county or city, classified by type of central heating. CSO, Cork, Ireland.

Daher, N., Ning, Z., Cho, A.K., Shafer, M., Schauer, J.J. and Sioutas, C., 2011. Comparison of the chemical and oxidative characteristics of particulate matter (PM) collected by different methods: filters, impactors, and biosamplers. *Aerosol Science and Technology* 45: 1294–1304.

Dall'Osto, M., Ovadnevaite, J., Ceburnis, D., *et al*., 2013. Characterization of urban aerosol in Cork city (Ireland) using aerosol mass spectrometry. *Atmospheric Chemistry and Physics* 13: 4997–5015.

Delfino, R.J., Sioutas, C. and Malik, S., 2005. Potential role of ultrafine particles in associations between airborne particle mass and cardiovascular health. *Environmental Health Perspectives* 113: 934–946.

Delfino, R.J., Staimer, N. and Vaziri, N.D., 2011. Air pollution and circulating biomarkers of oxidative stress. *Air Quality, Atmosphere & Health* 4: 37–52.

Delfino, R.J., Staimer, N., Tjoa, T., Gillen, D.L., Schauer, J.J. and Shafer, M.M., 2013. Airway inflammation and oxidative potential of air pollutant particles in a pediatric asthma panel. *Journal of Exposure Science and Environmental Epidemiology* 23: 466–473.

DeWitt, H.L., Hellebust, S., Temime-Roussel, B., *et al*., 2015. Near-highway aerosol and gas-phase measurements in a high-diesel environment. *Atmospheric Chemistry and Physics* 15: 4373–4387.

Donaldson, K., Stone, V., Seaton, A. and MacNee, W., 2001. Ambient particle inhalation and the cardiovascular system: potential mechanisms. *Environmental Health Perspectives* 109: 523–527.

Drinovec, L., Močnik, G., Zotter, P., *et al*., 2015. The "dual-spot" Aethalometer: an improved measurement of aerosol black carbon with real-time loading compensation. *Atmospheric Measurement Techniques* 8: 1965–1979.

Duscio, D., Proietti, L., Giarrusso, S., Fantauzzo, R., Rapisarda, V. and Calandra, C., 2003. Health effects of diesel exhaust. *Air Pollution XI* 13: 387–399.

Elser, M., Huang, R.J., Wolf, R., *et al*., 2016. New insights into $PM_{2.5}$ chemical composition and sources in two major cities in China during extreme haze events using aerosol mass spectrometry. *Atmospheric Chemistry and Physics* 16: 3207–3225.

Fang, T., Verma, V., Guo, H., King, L.E., Edgerton, E.S. and Weber, R.J., 2015. A semi-automated system for quantifying the oxidative potential of ambient particles in aqueous extracts using the dithiothreitol (DTT) assay: results from the Southeastern Center for Air Pollution and Epidemiology (SCAPE). *Atmospheric Measurement Techniques* 8: 471–482.

Fang, T., Verma, V., Bates, J.T., *et al*., 2016. Oxidative potential of ambient water-soluble $PM_{2.5}$ in the southeastern United States: contrasts in sources and health associations between ascorbic acid (AA) and dithiothreitol (DTT) assays. *Atmospheric Chemistry and Physics* 16: 3865–3879.

Fröhlich, R., Crenn, V., Setyan, A., *et al*., 2015. ACTRIS ACSM intercomparison – Part 2: intercomparison of ME-2 organic source apportionment results from 15 individual, co-located aerosol mass spectrometers. *Atmospheric Measurement Techniques* 8: 1559–1613.

Fuller, G.W., Tremper, A.H., Baker, T.D., Yttri, K.E. and Butterfield, D., 2014. Contribution of wood burning to PM_{10} in London. *Atmospheric Environment* 87: 87–94.

Fushimi, A., Saitoh, K., Hayashi, K., Ono, K., Fujitani, Y., Villalobos, A.M., Shelton, B.R., Takami, A., Tanabe, K. and Schauer, J.J., 2017. Chemical characterization and oxidative potential of particles emitted from open burning of cereal straws and rice husk under flaming and smoldering conditions. *Atmospheric Environment* 163: 118–127.

Fuzzi, S., Baltensperger, U., Carslaw, K., *et al*., 2015. Particulate matter, air quality and climate: lessons learned and future needs. *Atmospheric Chemistry and Physics* 15: 8217–8299. https://doi.org/10.5194/acp-15-8217-2015

Gao, D., Fang, T., Verma, V., Zeng, L.G. and Weber, R.J., 2017. A method for measuring total aerosol oxidative potential (OP) with the dithiothreitol (DTT) assay and comparisons between an urban and roadside site of water-soluble and total OP. *Atmospheric Measurement Techniques* 10: 2821–2835.

Garshick, E., Laden, F., Hart, J.E., Smith, T.J. and Rosner, B., 2006. Smoking imputation and lung cancer in railway workers exposed to diesel exhaust. *American Journal of Industrial Medicine* 49: 709–718.

Gasser, M., Riediker, M., Mueller, L., Perrenoud, A., Blank, F., Gehr, P. and Rothen-Rutishauser, B., 2009. Toxic effects of brake wear particles on epithelial lung cells *in vitro. Particle and Fibre Toxicology* 6(30). https://doi.org/10.1186/1743-8977-6-30

Geng, F., Tie, X., Xu, J., Zhou, G., Peng, L., Gao, W., Tang, X. and Zhao, C., 2008. Characterizations of ozone, NO_x, and VOCs measured in Shanghai, China. *Atmospheric Environment* 42: 6873–6883.

Gentner, D.R., Jathar, S.H., Gordon, T.D., *et al*., 2017. Review of urban secondary organic aerosol formation from gasoline and diesel motor vehicle emissions. *Environmental Science & Technology* 51: 1074–1093.

Goodman, P.G., Rich, D.Q., Zeka, A., Clancy, L. and Dockery, D.W., 2009. Effect of air pollution controls on black smoke and sulfur dioxide concentrations across Ireland. *Journal of the Air & Waste Management Association* 59: 207–213.

Grigas, T., Ovadnevaite, J., Ceburnis, D., Moran, E., McGovern, F.M., Jennings, S.G. and O'Dowd, C., 2017. Sophisticated clean air strategies required to mitigate against particulate organic pollution. *Scientific Reports* 7: 44737. https://doi.org/10.1038/srep44737

Hallquist, M., Wenger, J.C., Baltensperger, U., *et al*., 2009. The formation, properties and impact of secondary organic aerosol: current and emerging issues. *Atmospheric Chemistry and Physics* 9: 5155–5236.

He, L.Y., Lin, Y., Huang, X.F., Guo, S., Xue, L., Su, Q., Hu, M., Luan, S.J. and Zhang, Y.H., 2010. Characterization of high-resolution aerosol mass spectra of primary organic aerosol emissions from Chinese cooking and biomass burning. *Atmospheric Chemistry and Physics* 10: 11,535–11,543.

Heal, M.R. and Quincey, P., 2012. The relationship between black carbon concentration and black smoke: a more general approach. *Atmospheric Environment* 54: 538–544.

Heal, M.R., Hibbs, L.R., Agius, R.M. and Beverland, I.J., 2005. Interpretation of variations in fine, coarse and black smoke particulate matter concentrations in a northern European city. *Atmospheric Environment* 39: 3711–3718.

Hedayat, F., Stevanovic, S., Miljevic, B., Bottle, S. and Ristovski, Z.D., 2015. Review – Evaluating the molecular assays for measuring the oxidative potential of particulate matter. *Chemical Industry & Chemical Engineering Quarterly* 21: 201–210.

Hu, S., Polidori, A., Arhami, M., Shafer, M., Schauer, J., Cho, A. and Sioutas, C., 2008. Redox activity and chemical speciation of size fractioned PM in the communities of the Los Angeles–Long Beach harbor. *Atmospheric Chemistry and Physics* 8: 6439–6451.

Hu, R.M., Coleman, L., Noone, C., Lin, C., Ovadnevaite, J., and O'Dowd, C., 2019. Regionally significant residential-heating source of organic aerosols. *International Journal of Earth & Environmental Science* 4: 170.

Huang, R.-J., Zhang, Y., Bozzetti, C., Ho, K.-F., Cao, J.-J., Han, Y., Daellenbach, K.R., Slowik, J.G., Platt, S.M. and Canonaco, F., 2014. High secondary aerosol contribution to particulate pollution during haze events in China. *Nature* 514: 218–222.

Hong, S.Y., 2010. A new stable boundary layer mixing scheme and its impact on the simulated East Asian summer monsoon. *Quarterly Journal of the Royal Meteorolgical Society* 136: 1481–1496.

Hong, S.Y., Noh, Y. and Dudhia, J., 2006. A new vertical diffusion package with an explicit treatment of entrainment processes. *Monthly Weather Review* 134: 2318–2341.

Ibarra, J., Muñoz, E. and Moliner, R., 1996. FTIR study of the evolution of coal structure during the coalification process. *Organic Geochemistry* 24: 725–735.

Janssen, N.A.H., Yang, A.L., Strak, M., *et al*., 2014. Oxidative potential of particulate matter collected at sites with different source characteristics. *Science of the Total Environment* 472: 572–581.

Janssen, N.A.H., Strak, M., Yang, A., *et al*., 2015. Associations between three specific a-cellular measures of the oxidative potential of particulate matter and markers of acute airway and nasal inflammation in healthy volunteers. *Occupational and Environmental Medicine* 72: 49–56.

Jayne, J.T., Leard, D.C., Zhang, X., Davidovits, P., Smith, K.A., Kolb, C.E. and Worsnop, D.R., 2000. Development of an aerosol mass spectrometer for size and composition analysis of submicron particles. *Aerosol Science and Technology* 33: 49–70.

Jenkin, M.E., Watson, L.A., Utembe, S.R. and Shallcross, D.E., 2008. A common representative intermediates (CRI) mechanism for VOC degradation. Part 1: gas phase mechanism development. *Atmospheric Environment* 47: 7185–7195.

Jiang, H.H. and Jang, M.S., 2018. Dynamic oxidative potential of atmospheric organic aerosol under ambient sunlight. *Environmental Science & Technology* 52: 7496–7504.

Jiang, H., Jang, M. and Yu, Z.C., 2017. Dithiothreitol activity by particulate oxidizers of SOA produced from photooxidation of hydrocarbons under varied NO_x levels. *Atmospheric Chemistry and Physics* 17: 9965–9977.

Jimenez, J.L., Canagaratna, M.R., Donahue, N.M., *et al*., 2009. Evolution of organic aerosols in the atmosphere. *Science* 326: 1525–1529.

Jung, H., Guo, B., Anastasio, C. and Kennedy, I.M., 2006. Quantitative measurements of the generation of hydroxyl radicals by soot particles in a surrogate lung fluid. *Atmospheric Environment* 40: 1043–1052.

Kagawa, J., 2001. Health effects of diesel exhaust emissions – A mixture of air pollutants of worldwide concern. *Toxicology* 164: 27–27.

Kamal, A., Cincinelli, A., Martellini, T. and Malik, R.N., 2015. A review of PAH exposure from the combustion of biomass fuel and their less surveyed effect on the blood parameters. *Environmental Science and Pollution Research* 22: 4076–4098.

Kelly, I. and Clancy, L., 1984. Mortality in a general hospital and urban air pollution. *Irish Medical Journal* 77: 322–324.

Kleinman, M.T., Sioutas, C., Froines, J.R., Fanning, E., Hamade, A., Mendez, L., Meacher, D. and Oldham, M., 2007. Inhalation of concentrated ambient particulate matter near a heavily trafficked road stimulates antigen-induced airway responses in mice. *Inhalation Toxicology* 19: 117–126.

Kodavanti, U.P., Schladweiler, M.C., Ledbetter, A.D., *et al*., 2005. Consistent pulmonary and systemic responses from inhalation of fine concentrated ambient particles: roles of rat strains used and physicochemical properties. *Environmental Health Perspectives* 113: 1561–1568.

Kourtchev, I., Hellebust, S., Bell, J.M., O'Connor, I.P., Healy, R.M., Allanic, A., Healy, D., Wenger, J.C. and Sodeau, J.R., 2011. The use of polar organic compounds to estimate the contribution of domestic solid fuel combustion and biogenic sources to ambient levels of organic carbon and $PM_{2.5}$ in Cork Harbour, Ireland. *Science of the Total Environment* 409: 2143–2155.

Kroll, J.H. and Seinfeld, J.H., 2008. Chemistry of secondary organic aerosol: Formation and evolution of low-volatility organics in the atmosphere. *Atmospheric Environment* 42: 3593–3624.

Kumagai, Y., Koide, S., Taguchi, K., Endo, A., Nakai, Y., Yoshikawa, T. and Shimojo, N., 2002. Oxidation of proximal protein sulfhydryls by phenanthraquinone, a component of diesel exhaust particles. *Chemical Research in Toxicology* 15: 483–489.

Lakey, P.S.J., Berkemeier, T., Tong, H.J., Arangio, A.M., Lucas, K., Poschl, U. and Shiraiwa, M., 2016. Chemical exposure–response relationship between air pollutants and reactive oxygen species in the human respiratory tract. *Scientific Reports* 6: 32916. https://doi.org/10.1038/srep32916

Lanz, V.A., Alfarra, M.R., Baltensperger, U., Buchmann, B., Hueglin, C. and Prevot, A.S.H., 2007. Source apportionment of submicron organic aerosols at an urban site by factor analytical modelling of aerosol mass spectra. *Atmospheric Chemistry and Physics* 7: 1503–1522.

Lanz, V.A., Alfarra, M.R., Baltensperger, U., *et al*., 2008. Source attribution of submicron organic aerosols during wintertime inversions by advanced factor analysis of aerosol mass spectra. *Environmental Science & Technolgy* 42: 214–220.

Lanz, V.A., Prêvot, A.S.H., Alfarra, M.R., *et al*., 2010. Characterization of aerosol chemical composition with aerosol mass spectrometry in Central Europe: an overview. *Atmospheric Chemistry and Physics* 10: 10,453–10,471.

Lee, S., Liu, W., Wang, Y., Russell, A.G. and Edgerton, E.S., 2008. Source apportionment of $PM_{2.5}$: comparing PMF and CMB results for four ambient monitoring sites in the southeastern United States. *Atmospheric Environment* 42: 4126–4137.

Lelieveld, J., Evans, J.S., Fnais, M., Giannadaki, D. and Pozzer, A., 2015. The contribution of outdoor air pollution sources to premature mortality on a global scale. *Nature* 525: 367–371.

Li, N., Sioutas, C., Cho, A., Schmitz, D., Misra, C., Sempf, J., Wang, M.Y., Oberley, T., Froines, J. and Nel, A., 2003. Ultrafine particulate pollutants induce oxidative stress and mitochondrial damage. *Environmental Health Perspectives* 111: 455–460.

Li, Q., Shang, J. and Zhu, T., 2013. Physicochemical characteristics and toxic effects of ozone-oxidized black carbon particles. *Atmospheric Environment* 81: 68–75.

Li, Y.J., Sun, Y., Zhang, Q., Li, X., Li, M., Zhou, Z. and Chan, C.K., 2017. Real-time chemical characterization of atmospheric particulate matter in China: a review. *Atmospheric Environment* 158: 270–304.

Lin, P. and Yu, J.Z., 2011. Generation of reactive oxygen species mediated by humic-like substances in atmospheric aerosols. *Environmental Science & Technology* 45: 10,362–10,368.

Lin, C.S., Ceburnis, D., Hellebust, S., Buckley, P., Wenger, J., Canonaco, F., Prevot, A.S.H., Huang, R.J., O'Dowd, C. and Ovadnevaite, J., 2017. Characterization of primary organic aerosol from domestic wood, peat, and coal burning in Ireland. *Environmental Science & Technology* 51: 10,624–10,632.

Lin, C., Huang, R.-J., Ceburnis, D., Buckley, P., Preissler, J., Wenger, J., Rinaldi, M., Facchini, M.C., O'Dowd, C. and Ovadnevaite, J., 2018. Extreme air pollution from residential solid fuel burning. *Nature Sustainability* 1: 512–517.

Lin, C., Ceburnis, D., Huang, R.-J., Canonaco, F., Prévôt, A.S.H., O'Dowd, C. and Ovadnevaite, J., 2019a. Summertime aerosol over the west of Ireland dominated by secondary aerosol during long-range transport. *Atmosphere* 10: 59. https://doi.org/10.3390/atmos10020059

Lin, C., Ceburnis, D., Huang, R.J., *et al*., 2019b. Wintertime aerosol dominated by solid-fuel-burning emissions across Ireland: insight into the spatial and chemical variation in submicron aerosol. *Atmospheric Chemistry and Physics* 19: 14,091–14,106.

Lin, C., Ceburnis, D., Xu, W., Heffernan, E., Hellebust, S., Gallagher, J., Huang, R.J., O'Dowd, C. and Ovadnevaite, J., 2020. The impact of traffic on air quality in Ireland: insights from simultaneous kerbside and sub-urban monitoring of submicron aerosols. *Atmospheric Chemistry and Physics* 20: 10,513–10,529.

Lin, Y.H., Arashiro, M., Martin, E., Chen, Y.Z., Zhang, Z.F., Sexton, K.G., Gold, A., Jaspers, I., Fry, R.C. and Surratt, J.D., 2016. Isoprene-derived secondary organic aerosol induces the expression of oxidative stress response genes in human lung cells. *Environmental Science & Technology Letters* 3: 250–254.

Liu, Q.Y., Baumgartner, J., Zhang, Y.X., Liu, Y.J., Sun, Y.J. and Zhang, M.G., 2014. Oxidative potential and inflammatory impacts of source apportioned ambient air pollution in Beijing. *Environmental Science & Technology* 48: 12,920–12,929.

Lundstedt, S., White, P.A., Lemieux, C.L., Lynes, K.D., Lambert, L.B., Oberg, L., Haglund, P. and Tysklind, M., 2007. Sources, fate, and toxic hazards of oxygenated polycyclic aromatic hydrocarbons (PAHs) at PAH-contaminated sites. *Ambio* 36: 475–485.

McCluskey, C.S., Ovadnevaite, J., Rinaldi, M., *et al*., 2018. Marine and terrestrial organic ice-nucleating particles in pristine marine to continentally influenced Northeast Atlantic air masses. *Journal of Geophysical Research: Atmospheres* 123: 6196–6212.

McWhinney, R.D., Zhou, S. and Abbatt, J.P.D., 2013a. Naphthalene SOA: redox activity and naphthoquinone gas-particle partitioning. *Atmospheric Chemistry and Physics* 13: 9731–9744.

McWhinney, R.D., Badali, K., Liggio, J., Li, S.M. and Abbatt, J.P.D., 2013b. Filterable redox cycling activity: a comparison between diesel exhaust particles and secondary organic aerosol constituents. *Environmental Science & Technology* 47: 3362–3369.

Mellor, G.L. and Yamada, T., 1982. Development of a turbulence closure model for geophysical fluid problems. *Reviews of Geophysics* 20: 851–875.

Minguillón, M.C., Ripoll, A., Pérez, N., Prévôt, A.S.H., Canonaco, F., Querol, X. and Alastuey, A., 2015. Chemical characterization of submicron regional background aerosols in the western Mediterranean using an aerosol chemical speciation monitor. *Atmospheric Chemistry and Physics* 15: 6379–6391.

Mohr, C., Decarlo, P.F., Heringa, M., *et al*., 2012. Identification and quantification of organic aerosol from cooking and other sources in Barcelona using aerosol mass spectrometer data. *Atmospheric Chemistry and Physics* 12: 1649–1665.

Nakanishi, M. and Niino, H., 2004. An improved Mellor–Yamada level-3 model with condensation physics: its design and verification. *Boundary-Layer Meteorology* 112: 1–31.

Nel, A., 2005. Air pollution-related illness: effects of particles. *Science* 308: 804–806.

Ng, N.L., Canagaratna, M.R., Zhang, Q., *et al*., 2010. Organic aerosol components observed in northern hemispheric datasets from aerosol mass spectrometry. *Atmospheric Chemistry and Physics* 10: 4625–4641.

Ng, N.L., Herndon, S.C., Trimborn, A., *et al*., 2011. An aerosol chemical speciation monitor (ACSM) for routine monitoring of the composition and mass concentrations of ambient aerosol. *Aerosol Science and Technology* 45: 780–794.

Ntziachristos, L., Froines, J.R., Cho, A.K. and Sioutas, C., 2007. Relationship between redox activity and chemical speciation of size-fractionated particulate matter. *Particle and Fibre Toxicology* 4: 5. https://doi.org/10.1186/1743-8977-4-5

O'Dowd, C.D. and de Leeuw, G., 2007. Marine aerosol production: a review of the current knowledge. *Philosophical Transactions of the Royal Society A: Mathematical, Physical and Engineering Sciences* 365: 1753–1774.

O'Dowd, C.D., Smith, M.H., Consterdine, I.E. and Lowe, J.A., 1997. Marine aerosol, sea-salt, and the marine sulphur cycle: a short review. *Atmospheric Environment* 31: 73–80.

O'Dowd, C.D., Facchini, M.C., Cavalli, F., Ceburnis, D., Mircea, M., Decesari, S., Fuzzi, S., Yoon, Y.J. and Putaud, J.-P., 2004. Biogenically driven organic contribution to marine aerosol. *Nature* 431: 676–680.

Ovadnevaite, J., Ceburnis, D., Leinert, S., Dall'Osto, M., Canagaratna, M., O'Doherty, S., Berresheim, H. and O'Dowd, C., 2014. Submicron NE Atlantic marine aerosol chemical composition and abundance: seasonal trends and air mass categorization. *Journal of Geophysical Research: Atmospheres* 119: 11,850–11,863.

Paatero, P., 1997. Least squares formulation of robust non-negative factor analysis. *Chemometrics and Intelligent Laboratory Systems* 37: 23–35.

Paatero, P. and Tapper, U., 1994. Positive matrix factorization: a non-negative factor model with optimal utilization of error estimates of data values. *Environmetrics* 5: 111–126.

Paatero, P., Eberly, S., Brown, S.G. and Norris, G.A., 2014. Methods for estimating uncertainty in factor analytic solutions. *Atmospheric Measurement Techniques* 7: 781–797.

Pandya, R.J., Solomon, G., Kinner, A. and Balmes, J.R., 2002. Diesel exhaust and asthma: hypotheses and molecular mechanisms of action. *Environmental Health Perspectives* 110: 103–112.

Patel, A. and Rastogi, N., 2018a. Seasonal variability in chemical composition and oxidative potential of ambient aerosol over a high altitude site in western India. *Science of the Total Environment* 644: 1268–1276.

Patel, A. and Rastogi, N., 2018b. Oxidative potential of ambient fine aerosol over a semi-urban site in the Indo-Gangetic Plain. *Atmospheric Environment* 175: 127–134.

Perrone, M.G., Zhou, J., Malandrino, M., Sangiorgi, G., Rizzi, C., Ferrero, L., Dommen, J. and Bolzacchini, E., 2016. PM chemical composition and oxidative potential of the soluble fraction of particles at two sites in the urban area of Milan, Northern Italy. *Atmospheric Environment* 128: 104–113.

Petit, J.E., Favez, O., Sciare, J., Crenn, V., Sarda-Estève, R., Bonnaire, N., Močnik, G., Dupont, J.C., Haeffelin, M. and Leoz-Garziandia, E., 2015. Two years of near real-time chemical composition of submicron aerosols in the region of Paris using an Aerosol Chemical Speciation Monitor (ACSM) and a multi-wavelength Aethalometer. *Atmospheric Chemistry and Physics* 15: 2985–3005.

Pope, C. and Dockery, D., 2006. Health effects of fine particulate air pollution: lines that connect. *Journal of the Air & Waste Management Association* 56: 709–742.

Pope, I.C., Burnett, R.T., Thun, M.J*., et al*., 2002. Lung cancer, cardiopulmonary mortality, and long-term exposure to fine particulate air pollution. *JAMA* 287: 1132–1141.

Pope, C., Burnett, R., Thurston, G., Thun, M., Calle, E., Krewski, D. and Godleski, J., 2004. Cardiovascular mortality and long-term exposure to particulate air pollution – Epidemiological evidence of general pathophysiological pathways of disease. *Circulation* 109: 71–77.

Pope, C.A., Ezzati, M. and Dockery, D.W., 2009. Fine-particulate air pollution and life expectancy in the United States. *New England Journal of Medicine* 360: 376–386.

Powers, J.G., Klemp, J.B., Skamarock, W.C., *et al*., 2017. The Weather Research and Forecasting model: overview, system efforts, and future directions. *Bulletin of the American Meteorological Society* 98: 1717–1737.

Quincey, P., 2007. A relationship between black smoke index and black carbon concentration. *Atmospheric Environment* 41: 7964–7968.

Quincey, P., Butterfield, D., Green, D. and Fuller, G.W., 2011. Black smoke and black carbon: further investigation of the relationship between these ambient air metrics. *Atmospheric Environment* 45: 3528–3534.

Ramanathan, V. and Carmichael, G., 2008. Global and regional climate changes due to black carbon. *Nature Geoscience* 1: 221.

Reyes-Villegas, E., Green, D.C., Priestman, M., Canonaco, F., Coe, H., Prévôt, A.S.H. and Allan, J.D., 2016. Organic aerosol source apportionment in London 2013 with ME-2: exploring the solution space with annual and seasonal analysis. *Atmospheric Chemistry and Physics* 16: 15545–15559.

Ripoll, A., Minguillón, M.C., Pey, J., Jimenez, J.L., Day, D.A., Sosedova, Y., Canonaco, F., Prévôt, A.S.H., Querol, X. and Alastuey, A., 2015. Long-term real-time chemical characterization of submicron aerosols at Montsec (southern Pyrenees, 1570 m a.s.l.). *Atmospheric Chemistry and Physics* 15: 2935–2951.

Samet, J.M., Dominici, F., Curriero, F.C., Coursac, I. and Zeger, S.L., 2000. Fine particulate air pollution and mortality in 20 US cities, 1987–1994. *New England Journal of Medicine* 343: 1742–1749.

Sandradewi, J., Prévôt, A.S.H., Szidat, S., Perron, N., Alfarra, M.R., Lanz, V.A., Weingartner, E. and Baltensperger, U., 2008. Using aerosol light absorption measurements for the quantitative determination of wood burning and traffic emission contributions to particulate matter. *Environmental Science & Technology* 42: 3316–3323.

Sbihi, H., Brook, J.R., Allen, R.W., *et al*., 2013. A new exposure metric for traffic-related air pollution? An analysis of determinants of hopanes in settled indoor house dust. *Environmental Health* 12: 48.

Schaumann, F., Borm, P.J.A., Herbrich, A., Knoch, J., Pitz, M., Schins, R.P.F., Luettig, B., Hohlfeld, J.M., Heinrich, J. and Krug, N., 2004. Metal-rich ambient particles (particulate matter 2.5) cause airway inflammation in healthy subjects. *American Journal of Respiratory and Critical Care Medicine* 170: 898–903.

Schell, B., Ackermann, I.J., Hass, H., Binkowski, F.S. and Ebel, A., 2001. Modeling the formation of secondary organic aerosol within a comprehensive air quality model system. *Journal of Geophysical Research: Atmospheres* 106: 28,275–28,293.

Schlag, P., Kiendler-Scharr, A., Johannes Blom, M., Canonaco, F., Sebastiaan Henzing, J., Moerman, M., Prévôt, A.S.H. and Holzinger, R., 2016. Aerosol source apportionment from 1-year measurements at the CESAR tower in Cabauw, the Netherlands. *Atmospheric Chemistry and Physics* 16: 8831–8847.

Schneider, J., Weimer, S., Drewnick, F., Borrmann, S., Helas, G., Gwaze, P., Schmid, O., Andreae, M.O. and Kirchner, U., 2006. Mass spectrometric analysis and aerodynamic properties of various types of combustion-related aerosol particles. *International Journal of Mass Spectrometry* 258: 37–49.

Sciare, J., D'Argouges, O., Sarda-Estève, R., Gaimoz, C., Dolgorouky, C., Bonnaire, N., Favez, O., Bonsang, B. and Gros, V., 2011. Large contribution of water-insoluble secondary organic aerosols in the region of Paris (France) during wintertime. *Journal of Geophysical Research: Atmospheres* 116: D22203. https://doi.org/10.1029/2011JD015756

Shafer, M.M., Hemming, J.D.C., Antkiewicz, D.S. and Schauer, J.J., 2016. Oxidative potential of size-fractionated atmospheric aerosol in urban and rural sites across Europe. *Faraday Discussions* 189: 381–405.

Sprenger, M. and Wernli, H., 2015. The LAGRANTO Lagrangian analysis tool – Version 2.0. *Geoscientific Model Development* 8: 2569–2586.

Stockwell, W.R., Middleton, P., Chang, J.S. and Tang, X., 1990. The second generation regional acid deposition model chemical mechanism for regional air quality modeling. *Journal of Geophysical Research: Atmospheres* 95: 16,343–16,367.

Sukoriansky, S., Galperin, B. and Perov, A.V., 2005. Application of a new spectral theory of stably stratified turbulence to the atmospheric boundary layer over sea ice. *Boundary-Layer Meteorology* 117: 231–257.

Sullivan, A.P., Hodas, N., Turpin, B.J., *et al*., 2016. Evidence for ambient dark aqueous SOA formation in the Po Valley, Italy. *Atmospheric Chemistry and Physics* 16: 8095–8108.

Sun, Y., Wang, Z., Dong, H., Yang, T., Li, J., Pan, X., Chen, P. and Jayne, J.T., 2012. Characterization of summer organic and inorganic aerosols in Beijing, China with an Aerosol Chemical Speciation Monitor. *Atmospheric Environment* 51: 250–259.

Sun, Y.L., Wang, Z.F., Fu, P.Q., Yang, T., Jiang, Q., Dong, H.B., Li, J. and Jia, J.J., 2013. Aerosol composition, sources and processes during wintertime in Beijing, China. *Atmospheric Chemistry and Physics* 13: 4577–4592.

Sun, Y., Xu, W., Zhang, Q., Jiang, Q., Canonaco, F., Prévôt, A.S.H., Fu, P., Li, J., Jayne, J., Worsnop, D.R. and Wang, Z., 2018. Source apportionment of organic aerosol from two-year highly time-resolved measurements by an aerosol chemical speciation monitor in Beijing, China. *Atmospheric Chemistry and Physics* 18: 8469–8498.

Szajdak, L., Brandyk, T. and Szatylowicz, J., 2007. Chemical properties of different peat-moorsh soils from the Biebrza River Valley. *Agronomy Research* 5: 165–174.

Ulbrich, I., Canagaratna, M., Zhang, Q., Worsnop, D. and Jimenez, J., 2009. Interpretation of organic components from Positive Matrix Factorization of aerosol mass spectrometric data. *Atmospheric Chemistry and Physics* 9: 2891–2918.

Uski, O., Jalava, P.I., Happo, M.S., Leskinen, J., Sippula, O., Tissari, J., Mäki-Paakkanen, J., Jokiniemi, J. and Hirvonen, M.R., 2014. Different toxic mechanisms are activated by emission PM depending on combustion efficiency. *Atmospheric Environment* 89: 623–632.

Vejerano, E.P., Ma, Y.J., Holder, A.L., Pruden, A., Elankumaran, S. and Marr, L.C., 2015. Toxicity of particulate matter from incineration of nanowaste. *Environmental Science: Nano* 2: 143–154.

Venkatachari, P., Hopke, P.K., Grover, B.D. and Eatough, D.J., 2005. Measurement of particle-bound reactive oxygen species in Rubidoux aerosols. *Journal of Atmospheric Chemistry* 50: 49–58.

Verma, V., Ning, Z., Cho, A., Schauer, J., Shafer, M. and Sioutas, C., 2009a. Redox activity of urban quasi-ultrafine particles from primary and secondary sources. *Atmospheric Environment* 43: 6360–6368.

Verma, V., Polidori, A., Schauer, J.J., Shafer, M.M., Cassee, F.R. and Sioutas, C., 2009b. Physicochemical and toxicological profiles of particulate matter in Los Angeles during the October 2007 Southern California wildfires. *Environmental Science & Technology* 43: 954–960.

Verma, V., Rico-Martinez, R., Kotra, N., King, L., Liu, J., Snell, T.W. and Weber, R.J., 2012. Contribution of water-soluble and insoluble components and their hydrophobic/hydrophilic subfractions to the reactive oxygen species-generating potential of fine ambient aerosols. *Environmental Science & Technology* 46: 11384–11392.

Verma, V., Fang, T., Guo, H., King, L., Bates, J.T., Peltier, R.E., Edgerton, E., Russell, A.G. and Weber, R.J., 2014. Reactive oxygen species associated with water-soluble $PM_{2.5}$ in the southeastern United States: spatiotemporal trends and source apportionment. *Atmospheric Chemistry and Physics* 14: 12,915–12,930.

Verma, V., Wang, Y., El-Afifi, R., Fang, T., Rowland, J., Russell, A.G. and Weber, R.J., 2015a. Fractionating ambient humic-like substances (HULIS) for their reactive oxygen species activity – Assessing the importance of quinones and atmospheric aging. *Atmospheric Environment* 120: 351–359.

Verma, V., Fang, T., Xu, L., Peltier, R.E., Russell, A.G., Ng, N.L. and Weber, R.J., 2015b. Organic aerosols associated with the generation of reactive oxygen species (ROS) by water-soluble $PM_{2.5}$. *Environmental Science & Technology* 49: 4646–4656.

Wenger, J., Arndt, J., Buckley, P., Hellebust, S., McGillicuddy, E., O'Connor, I., Sodeau J. and Wilson, E., 2020. *Source Apportionment of Particulate Matter in Urban and Rural Residential Areas of Ireland (SAPPHIRE)*. Environmental Protection Agency, Johnstown Castle, Ireland.

Yang, A., Janssen, N.A.H., Brunekreef, B., Cassee, F.R., Hoek, G. and Gehring, U., 2016. Children's respiratory health and oxidative potential of $PM_{2.5}$: the PIAMA birth cohort study. *Occupational and Environmental Medicine* 73: 154–160.

Zanobetti, A., Austin, E., Coull, B.A., Schwartz, J. and Koutrakis, P., 2014. Health effects of multi-pollutant profiles. *Environment International* 71: 13–19.

Zhang, Q., Jimenez, J.L., Canagaratna, M.R., Ulbrich, I.M., Ng, N.L., Worsnop, D.R. and Sun, Y., 2011. Understanding atmospheric organic aerosols via factor analysis of aerosol mass spectrometry: a review. *Analytical and Bioanalytical Chemistry* 401: 3045–3067.

Zhang, X., van Geffen, J., Liao, H., Zhang, P. and Lou, S., 2012. Spatiotemporal variations of tropospheric SO_2 over China by SCIAMACHY observations during 2004–2009. *Atmospheric Environment* 60: 238–246.

Zhang, Y.J., Tang, L.L., Wang, Z., Yu, H.X., Sun, Y.L., Liu, D., Qin, W., Canonaco, F., Prévôt, A.S.H., Zhang, H.L. and Zhou, H.C., 2015. Insights into characteristics, sources, and evolution of submicron aerosols during harvest seasons in the Yangtze River Delta region, China. *Atmospheric Chemistry and Physics* 15: 1331–1349.

Zhou, J., Zotter, P., Bruns, E.A., *et al*., 2018. Particle-bound reactive oxygen species (PB-ROS) emissions and formation pathways in residential wood smoke under different combustion and aging conditions. *Atmospheric Chemistry and Physics* 18: 6985–7000.

Zidek, J.V., Shaddick, G. and Taylor, C.G., 2014. Reducing estimation bias in adaptively changing monitoring networks with preferential site selection. *Annals of Applied Statistics* 8: 1640–1670.

Zomer, B., Colle, L., Jedynska, A., Pasterkamp, G., Kooter, I. and Bloemen, H., 2011. Chemiluminescent reductive acridinium triggering (CRAT)-mechanism and applications. *Analytical and Bioanalytical Chemistry* 401: 2945–2954.

Zotter, P., Herich, H., Gysel, M., El-Haddad, I., Zhang, Y., Močnik, G., Hüglin, C., Baltensperger, U., Szidat, S. and Prévôt, A.S.H., 2017. Evaluation of the absorption Ångström exponents for traffic and wood burning in the Aethalometer-based source apportionment using radiocarbon measurements of ambient aerosol. *Atmospheric Chemistry and Physics* 17: 4229–4249.

Abbreviations

α	Ångström exponent
ACSM	Aerosol chemical speciation monitor
AE	Aethalometer
AMS	Aerosol mass spectrometry
BBOA	Biomass burning organic aerosol
BC	Black carbon
BS	Black smoke
CMB	Chemical mass balance
COA	Cooking-related organic aerosol
CP–Dub	Carnsore Point to Dublin
DTT	Dithiothreitol
eBC	Equivalent black carbon
eBC_{BB}	Equivalent black carbon biomass burning component
eBC_{FF}	Equivalent black carbon fossil fuel component
eBC_{SF}	Equivalent black carbon solid fuel component
eBC_{TR}	Equivalent black carbon traffic component
ECMWF	European Centre for Medium-Range Weather Forecasts
HOA	Hydrocarbon-like organic aerosol
HR-ToF-AMS	High-resolution time-of-flight aerosol mass spectrometry
Lidar	Light detection and ranging
LV-OOA	Low-volatile oxygenated organic aerosol
ME-2	Multilinear engine 2
MH–CP	Mace Head to Carnsore Point
MH–Dub	Mace Head to Dublin
m*/*z	Mass-to-charge ratio
NH_4^+	Ammonium ion
NO_3^-	Nitrate ion
NR-PM_1	Non-refractory PM_1
OA	Organic aerosol
OM	Organic matter
OOA	Oxygenated organic aerosol
OP	Oxidative potential
OP_DTT	Oxidative potential measured using a dithiothreitol assay
OP_DTTm	Oxidative potential measured using a dithiothreitol assay normalised by particulate mass
OP_DTTv	Oxidative potential measured using a dithiothreitol assay normalised by volume of sampled air
PAH	Polycyclic aromatic hydrocarbon
PBL	Planetary boundary layer
PM	Particulate matter
PM_1	Particulate matter particles with a diameter of less than 1 µm
$PM_{2.5}$	Particulate matter particles with a diameter of less than 2.5 µm
PMF	Positive matrix factorisation
POA	Primary organic aerosol
R	Correlation coefficient
R^2	Coefficient of determination
RADM2	Second-generation Regional Acid Deposition Model

ROS	Reactive oxygen species
RSD	Relative standard deviation
SO_2	Sulfur dioxide
SO_4^{2-}	Sulfate ion
SOA	Secondary organic aerosol
SV-OAA	Semi-volatile oxygenated organic aerosol
TCD	Trinity College Dublin
TNO	Netherlands Organisation for Applied Scientific Research
UCD	University College Dublin
UMR	Unit mass resolution
VOC	Volatile organic compound
WHO	World Health Organization
WRF-Chem	Weather Research and Forecasting model coupled with Chemistry

Appendix 1 Publications Arising from This Research

Lin, C., Ceburnis, D., Hellebust, S., Buckley, P., Wenger, J., Canonaco, F., Prévôt, A.S.H., Huang, R.-J., O'Dowd, C. and Ovadnevaite, J., 2017. Characterization of primary organic aerosol from domestic wood, peat and coal burning in Ireland. *Environmental Science & Technology* 51: 10624–10632. https://doi.org/10.1021/acs.est.7b01926

Lin, C., Huang, R.-J., Ceburnis, D., Buckley, P., Preissler, J., Wenger, J., Rinaldi, M., Facchini, M.C., O'Dowd, C. and Ovadnevaite, J., 2018. Extreme air pollution from residential solid fuel burning. *Nature Sustainability* 1: 512–517. https://doi.org/10.1038/s41893-018-0125-x

Lin, C., Ceburnis, D., Huang, R.-J., Canonaco, F., Prévôt, A.S.H., Dowd, C. and Ovadnevaite, J., 2019. Summertime aerosol over the west of Ireland dominated by secondary aerosol during long-range transport. *Atmosphere* 10: 59. https://doi.org/10.3390/atmos10020059

Lin, C., Ceburnis, D., Huang, R.J., Xu, W., Spohn, T., Martin, D. and Ovadnevaite, J., 2019. Wintertime aerosol dominated by solid-fuel-burning emissions across Ireland: insight into the spatial and chemical variation in submicron aerosol. *Atmospheric Chemistry and Physics* 19: 14091–14106. https://doi.org/10.5194/acp-19-14091-2019

Hu, R.M., Coleman, L., Noone, C., Lin, C., Ovadnevaite, J. and O'Dowd, C., 2019. Regionally significant residential-heating source of organic aerosols. *International Journal of Earth & Environmental Science* 4: 170.

Lin, C., Ceburnis, D., Xu, W., Heffernan, E., Hellebust, S., Gallagher, J., Huang, R.J., O'Dowd, C. and Ovadnevaite, J., 2020. The impact of traffic on air quality in Ireland: insights from simultaneous kerbside and sub-urban monitoring of submicron aerosols. *Atmospheric Chemistry and Physics Discussions* 1–2. https://doi.org/10.5194/acp-2019-1178

Lin, C., Huang, R.J., Ceburnis, D., Buckley, P., Wenger, J., O'Dowd, C. and Ovadnevaite, J., in preparation. Long-term real-time characterization of submicron aerosol chemical composition and source apportionment of organic fraction in Dublin, Ireland.

Coleman, L. *et al*., in preparation. Simulating heavy pollution events in Dublin: accounting for residential solid fuel burning.

Rinaldi, M., *et al*., in preparation. Oxidative aerosol potential arising from solid fuel burning in Ireland.

AN GHNÍOMHAIREACHT UM CHAOMHNÚ COMHSHAOIL
Tá an Ghníomhaireacht um Chaomhnú Comhshaoil (GCC) freagrach as an gcomhshaol a chaomhnú agus a fheabhsú mar shócmhainn luachmhar do mhuintir na hÉireann. Táimid tiomanta do dhaoine agus don chomhshaol a chosaint ó éifeachtaí díobhálacha na radaíochta agus an truaillithe.

Is féidir obair na Gníomhaireachta a roinnt ina trí phríomhréimse:

Rialú: *Déanaimid córais éifeachtacha rialaithe agus comhlíonta comhshaoil a chur i bhfeidhm chun torthaí maithe comhshaoil a sholáthar agus chun díriú orthu siúd nach gcloíonn leis na córais sin.*

Eolas: *Soláthraímid sonraí, faisnéis agus measúnú comhshaoil atá ar ardchaighdeán, spriocdhírithe agus tráthúil chun bonn eolais a chur faoin gcinnteoireacht ar gach leibhéal.*

Tacaíocht: *Bímid ag saothrú i gcomhar le grúpaí eile chun tacú le comhshaol atá glan, táirgiúil agus cosanta go maith, agus le hiompar a chuirfidh le comhshaol inbhuanaithe.*

Ár bhFreagrachtaí

Ceadúnú
Déanaimid na gníomhaíochtaí seo a leanas a rialú ionas nach ndéanann siad dochar do shláinte an phobail ná don chomhshaol:
- saoráidí dramhaíola *(m.sh. láithreáin líonta talún, loisceoirí, stáisiúin aistrithe dramhaíola)*;
- gníomhaíochtaí tionsclaíocha ar scála mór *(m.sh. déantúsaíocht cógaisíochta, déantúsaíocht stroighne, stáisiúin chumhachta)*;
- an diantalmhaíocht *(m.sh. muca, éanlaith)*;
- úsáid shrianta agus scaoileadh rialaithe Orgánach Géinmhodhnaithe *(OGM)*;
- foinsí radaíochta ianúcháin *(m.sh. trealamh x-gha agus radaiteiripe, foinsí tionsclaíocha)*;
- áiseanna móra stórála peitril;
- scardadh dramhuisce;
- gníomhaíochtaí dumpála ar farraige.

Forfheidhmiú Náisiúnta i leith Cúrsaí Comhshaoil
- Clár náisiúnta iniúchtaí agus cigireachtaí a dhéanamh gach bliain ar shaoráidí a bhfuil ceadúnas ón nGníomhaireacht acu.
- Maoirseacht a dhéanamh ar fhreagrachtaí cosanta comhshaoil na n-údarás áitiúil.
- Caighdeán an uisce óil, arna sholáthar ag soláthraithe uisce phoiblí, a mhaoirsiú.
- Obair le húdaráis áitiúla agus le gníomhaireachtaí eile chun dul i ngleic le coireanna comhshaoil trí chomhordú a dhéanamh ar líonra forfheidhmiúcháin náisiúnta, trí dhíriú ar chiontóirí, agus trí mhaoirsiú a dhéanamh ar leasúchán.
- Cur i bhfeidhm rialachán ar nós na Rialachán um Dhramhthrealamh Leictreach agus Leictreonach (DTLL), um Shrian ar Shubstaintí Guaiseacha agus na Rialachán um rialú ar shubstaintí a ídíonn an ciseal ózóin.
- An dlí a chur orthu siúd a bhriseann dlí an chomhshaoil agus a dhéanann dochar don chomhshaol.

Bainistíocht Uisce
- Monatóireacht agus tuairisciú a dhéanamh ar cháilíocht aibhneacha, lochanna, uiscí idirchriosacha agus cósta na hÉireann, agus screamhuiscí; leibhéil uisce agus sruthanna aibhneacha a thomhas.
- Comhordú náisiúnta agus maoirsiú a dhéanamh ar an gCreat-Treoir Uisce.
- Monatóireacht agus tuairisciú a dhéanamh ar Cháilíocht an Uisce Snámha.

Monatóireacht, Anailís agus Tuairisciú ar an gComhshaol
- Monatóireacht a dhéanamh ar cháilíocht an aeir agus Treoir an AE maidir le hAer Glan don Eoraip (CAFÉ) a chur chun feidhme.
- Tuairisciú neamhspleách le cabhrú le cinnteoireacht an rialtais náisiúnta agus na n-údarás áitiúil *(m.sh. tuairisciú tréimhsiúil ar staid Chomhshaol na hÉireann agus Tuarascálacha ar Tháscairí)*.

Rialú Astaíochtaí na nGás Ceaptha Teasa in Éirinn
- Fardail agus réamh-mheastacháin na hÉireann maidir le gáis cheaptha teasa a ullmhú.
- An Treoir maidir le Trádáil Astaíochtaí a chur chun feidhme i gcomhair breis agus 100 de na táirgeoirí dé-ocsaíde carbóin is mó in Éirinn.

Taighde agus Forbairt Comhshaoil
- Taighde comhshaoil a chistiú chun brúnna a shainaithint, bonn eolais a chur faoi bheartais, agus réitigh a sholáthar i réimsí na haeráide, an uisce agus na hinbhuanaitheachta.

Measúnacht Straitéiseach Timpeallachta
- Measúnacht a dhéanamh ar thionchar pleananna agus clár beartaithe ar an gcomhshaol in Éirinn *(m.sh. mórphleananna forbartha)*.

Cosaint Raideolaíoch
- Monatóireacht a dhéanamh ar leibhéil radaíochta, measúnacht a dhéanamh ar nochtadh mhuintir na hÉireann don radaíocht ianúcháin.
- Cabhrú le pleananna náisiúnta a fhorbairt le haghaidh éigeandálaí ag eascairt as taismí núicléacha.
- Monatóireacht a dhéanamh ar fhorbairtí thar lear a bhaineann le saoráidí núicléacha agus leis an tsábháilteacht raideolaíochta.
- Sainseirbhísí cosanta ar an radaíocht a sholáthar, nó maoirsiú a dhéanamh ar sholáthar na seirbhísí sin.

Treoir, Faisnéis Inrochtana agus Oideachas
- Comhairle agus treoir a chur ar fáil d'earnáil na tionsclaíochta agus don phobal maidir le hábhair a bhaineann le caomhnú an chomhshaoil agus leis an gcosaint raideolaíoch.
- Faisnéis thráthúil ar an gcomhshaol ar a bhfuil fáil éasca a chur ar fáil chun rannpháirtíocht an phobail a spreagadh sa chinnteoireacht i ndáil leis an gcomhshaol *(m.sh. Timpeall an Tí, léarscáileanna radóin)*.
- Comhairle a chur ar fáil don Rialtas maidir le hábhair a bhaineann leis an tsábháilteacht raideolaíoch agus le cúrsaí práinnfhreagartha.
- Plean Náisiúnta Bainistíochta Dramhaíola Guaisí a fhorbairt chun dramhaíl ghuaiseach a chosc agus a bhainistiú.

Múscailt Feasachta agus Athrú Iompraíochta
- Feasacht chomhshaoil níos fearr a ghiniúint agus dul i bhfeidhm ar athrú iompraíochta dearfach trí thacú le gnóthais, le pobail agus le teaghlaigh a bheith níos éifeachtúla ar acmhainní.
- Tástáil le haghaidh radóin a chur chun cinn i dtithe agus in ionaid oibre, agus gníomhartha leasúcháin a spreagadh nuair is gá.

Bainistíocht agus struchtúr na Gníomhaireachta um Chaomhnú Comhshaoil
Tá an ghníomhaíocht á bainistiú ag Bord lánaimseartha, ar a bhfuil Ard-Stiúrthóir agus cúigear Stiúrthóirí. Déantar an obair ar fud cúig cinn d'Oifigí:
- An Oifig um Inmharthanacht Comhshaoil
- An Oifig Forfheidhmithe i leith cúrsaí Comhshaoil
- An Oifig um Fianaise is Measúnú
- Oifig um Chosaint Radaíochta agus Monatóireachta Comhshaoil
- An Oifig Cumarsáide agus Seirbhísí Corparáideacha

Tá Coiste Comhairleach ag an nGníomhaireacht le cabhrú léi. Tá dáréag comhaltaí air agus tagann siad le chéile go rialta le plé a dhéanamh ar ábhair imní agus le comhairle a chur ar an mBord.

EPA Research Report 385

Air Pollution Sources in Ireland

Authors: Jurgita Ovadnevaite, Chunshui Lin, Matteo Rinaldi, Darius Ceburnis, Paul Buckley, Liz Coleman, Maria Cristina Facchini, John Wenger and Colin O'Dowd

The project successfully established the AEROSOURCE network, comprising three sophisticated aerosol mass spectrometer nodes positioned in strategic locations: Carnsore Point (regional background), Dublin (urban environment) and Mace Head (marine background). It enhanced the National Transboundary Air Pollution Network with near real-time aerosol chemical speciation (including organic matter) and source apportionment capabilities.

Identifying Pressures

Air pollution is a major cause of health issues in Ireland and addressing it requires a better understanding of particulate matter (PM) sources. Despite generally good air quality, on account of prevailing oceanic air masses, AEROSOURCE revealed that extreme air pollution events, spanning conurbations across the entire country, occur frequently in wintertime. During these events, the PM limits recommended by World Health Organization are regularly breached (up to 1 in 5 days) during winter.

AEROSOURCE demonstrated that even though strict emission standards have resulted in downward trends of sulphate, these didnot necessarily translate into an equivalent reduction of overallPM levels. A deficiency of information on major PM sources,especially those of carbonaceous components (organic matterand black carbon), resulted in insufficient knowledge relating
to the cause of the pollution events and, in turn, prevented the development of informed air policy. Moreover, in some cases, policies promoting one environmental action but which was detrimental to another were found to exist; an example is the promotion of biomass as residential heating fuel as being "carbon neutral" and this reduces greenhouse gas emissions at the expense of clean air.

Informing Policy

The new National Ambient Air Quality Monitoring Programme marks an important advancement; however, it is not designed to provide chemical speciation or inform on sources without which adequate clean air policies cannot be developed.

The AEROSOURCE network revealed that carbonaceous aerosol prevails over historically dominant inorganic species, such as sulphate and nitrate, with the carbonaceous species contributingfrom 60% to 90% of PM1 mass (the mass of all particles ≤ 1 µmin aerodynamic diameter). Nevertheless, they are not routinelyclassified in regulatory air quality networks.

This study also highlighted the disproportionate effects of some sources. Peat and wood burning, in particular, are minor contributors to energy budgets, yet they are the major cause of extreme pollution events. Moreover, they were shown to be important in toxicity terms, as they possess a high oxidative potential and likely contribute substantially to the health effects alongside other expected culprits, such as coal and liquid fuel combustion.

AEROSOURCE demonstrated how critical it is to augment standard regulatory air quality networks with an aerosol mass spectrometry approach that can identify the main pollution contributors, which, in turn, can better inform policy measures and enable specifically targeted and sophisticated emission reduction strategies while minimising the risk of unintended consequences in other policy areas.

Developing Solutions

We have demonstrated that the AEROSOURCE "proof-of-concept" network can meet the challenges listed previously by enabling a better-informed and more sophisticated policy development. We thus recommend transforming the proof-of-concept network into a permanent national aerosol mass spectrometry network alongside the National Ambient Air Quality Monitoring Programme to provide a quantitative source apportionment and a continuous measurable assessment of policy implementation outcomes. Changes in emissions and their contributions and gathering up-to-date information on air pollution offenders in constantly changing environment are only possible with a permanent network rather than ad hoc facilities.

The AEROSOURCE approach underpins both the planned National Clean Air Strategy and the National Climate Mitigation Plan, as it identifies the real culprits of air pollution and climate forcers and, more importantly, allows synergetic, or co-beneficial solutions for air quality and climate change mitigation to be found.

EPA Research: McCumiskey House, Richiew, Clonskeagh, Dublin 14.

Phone: 01 268 0100
Twitter: @EPAResearchNews
Email: research@epa.ie